

Gwent College  
L11  
Allt-Yr-Yn Avenue

BOOK NO: 1838978



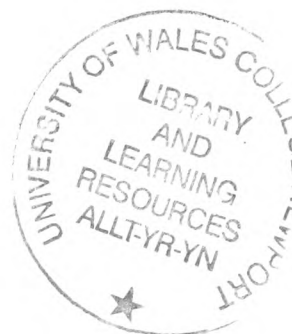
**NEWPORT AND MONMOUTHSHIRE**

Gwent College of Higher Education

**LIBRARY**

Allt-Yr-Yn Avenue, NEWPORT NPT 5XA.

**COLLEGE OF TECHNOLOGY**



**LIBRARY**

Gwent College of Higher Education

**LIBRARY**

Allt-Yr-Yn Avenue, NEWPORT NPT 5XA.

No. **25533**

Class.....

**NOT TO BE  
TAKEN AWAY**

Gwent College of Higher Education  
**LIBRARY**  
Allt-Yr-Yn Avenue, NEWPORT NPT 5XA.

FEASIBILITY STUDY OF HIGH CURRENT

TRANSISTOR D.C. CHOPPERS

by

B.Y.M. MAROGY

A dissertation submitted to the Council for National  
Academic Awards in support of an application for the  
degree of Master of Philosophy.

January 1975

## Memorandum

The accompanying dissertation is based on work carried out by the author at Gwent College of Technology between September 1972 and September 1974.

All work and ideas are original unless otherwise acknowledged in the text or by reference. This work has not been submitted for another C.N.A.A. Degree, nor for the award of a Degree or Diploma of any other institution.

This application for the degree of Master of Philosophy is based upon the following claims:

- (1) The design and construction of a transistor d.c. chopper capable of controlling 400 A d.c. at 72 volts.
- (2) A brief survey of power transistors to establish which transistors can offer an economic basis for the design.
- (3) The development of methods of voltage transient suppression.
- (4) The investigation of effects on chopper performance resulting from the replacement of Germanium transistors, used in the initial design, by Silicon power transistors: to date, Germanium power transistors have been preferred due to their comparatively low  $V_{CE(sat)}$ , and hence low power dissipation.

## Summary

This dissertation describes an investigation into the feasibility of high current transistor d.c. choppers.

Present d.c. choppers employ thyristors and are expensive due to the turn-off circuits required. The use of low cost power transistors in electric vehicle chopper controllers is investigated, and a brief survey of power transistors has been carried out to establish which transistors are most economical for use in choppers.

A transistor d.c. chopper employing Germanium transistors and capable of controlling 400 A at 72 V was designed and constructed: special design consideration was given to suppression of voltage transients and minimisation of power losses in the chopper during switching. Results of laboratory tests have shown the transistor chopper to be reliable and highly efficient. The replacement of the Germanium output transistors, used in the initial design, by Silicon power transistors resulted in the elimination of current sharing problems and a negligible effect on chopper efficiency.

The experimental chopper was costed and found to be cheap relative to a comparable thyristor chopper, thus offering the possibility of rapid industrial acceptance.



## LIST OF CONTENTS

### MEMORANDUM

### SUMMARY

### LIST OF FIGURES

### LIST OF SYMBOLS

(1.0)	INTRODUCTION	1
(1.1)	Current applications of battery electric vehicles	2
(1.2)	Current design and recent developments	3
(1.2.1)	The body and chassis	3
(1.2.2)	The battery	4
(1.2.3)	The motor	5
(1.3)	Propulsion systems incorporating series motors	7
(1.3.1)	Rheostatic controllers	7
(1.3.2)	Battery division	8
(1.3.3)	Battery scanning	11
(1.3.4)	Conclusions	13
(1.4)	Electrical braking	14
(1.4.1)	Rheostatic braking	14
(1.4.2)	Plug braking	15
(1.4.3)	Regenerative braking	18
(2.0)	CHOPPER CONTROLLERS	19
(2.1)	General	19
(2.2)	Thyristor choppers	20
(2.2.1)	Thyristor choppers with capacitive commutation	21
(2.2.1.1)	Advantages and disadvantages of capacitive commutation	24
(2.2.2)	Thyristor d.c. choppers employing resonant commutation	24
(2.2.2.1)	Advantages and disadvantages of resonant commutation	31

(3.0)	TRANSISTOR D.C. CHOPPER	32
(3.1)	General	32
(3.2)	Practical design considerations	37
(3.2.1)	Choice of power transistor	37
(3.2.2)	Secondary breakdown	42
(3.2.3)	Loadline tailoring circuit	44
(3.2.4)	Freewheeling diode	46
(3.2.5)	Reduction of switching losses	47
(3.2.6)	Saturated Darlington drive	48
(3.3)	Practical chopper circuit	53
(3.3.1)	The control oscillator	53
(3.3.2.1)	Variable pulse width oscillator	53
(3.3.1.2)	Current limiting circuit	60
(3.3.2)	Transistor chopper power circuit	61
(3.3.2.1)	Practical tests on circuit employing the MP 3731	67
(3.3.3)	Modified chopper power circuit	68
(3.3.3.1)	Practical tests on modified chopper circuit	69
(4.0)	CONCLUSIONS	78
(5.0)	SUGGESTIONS FOR FURTHER WORK	80
(6.0)	ACKNOWLEDGEMENTS	80a
(7.0)	REFERENCES	80b

APPENDIX (1)	CONTROL OSCILLATOR DESIGN CONSIDERATIONS	81
(1.1)	The square wave generator	81
(1.2)	The integrator	84
(1.3)	The regenerative comparator (Schmitt trigger)	84
(1.4)	Current limiting circuit	86
(1.4.1)	The comparator	86
(1.4.2)	The monostable multivibrator	87
APPENDIX (2)	CHOPPER CIRCUIT VOLTAGE AND CURRENT WAVEFORMS	90
APPENDIX (3)	CALCULATION OF CHOPPER EFFICIENCY	95

## List of Figures

<u>Figure No.</u>		<u>Page No.</u>
1.1	Series d.c. motor characteristics	6
1.2	Method of battery division	10
1.3	Modified method of battery division	12
1.4	Motoring and braking conditions	17
2.1	Circuit of a thyristor chopper employing capacitive commutation	22
2.2	Circuit waveforms in a thyristor d.c. chopper employing capacitive commutation	23
2.3	The conventional shunt-tuned chopper circuit	26
2.4	Modified circuits for d.c. chopper with resonant commutation	27
3.1	Inductive load line	33
3.2	Capacitive load line tailoring network	35
3.3	Inductive load line with capacitive shaping	36
3.4	Effects of emitter resistance on a parallel combination of transistors	38
3.5	Typical safe operating area for d.c. operation of a power transistor	39
3.6	Manifestation of second breakdown in a transistor	43
3.7	Typical safe operating area curves	45
3.8	Reduction of turn-on time with overdrive	49
3.9	Emitter follower drive	50
3.10	Saturated Darlington drive	51
3.11	Schematic diagram of a transistor d.c. chopper	54
3.12	Variable pulse width oscillator	55
	Component list for 3.12	56
3.13	Variation of comparator output waveform with d.c. reference voltage	59
3.14	Current limiting circuit	62
	Component list for 3.14	63
3.15	Transistor chopper power circuit	64
	Component list for 3.15	65
3.16	A single modified chopper output stage	70
3.17	Chassis of the modified transistor chopper	71
3.18	Variation of chopper efficiency with M-S-R	74

<u>Figure No.</u>		<u>Page No.</u>
3.19	Variation of chopper losses with mean motor current	75
3.20	Variation of efficiency with motor current for initial and modified chopper circuits	76
3.21	Variation of chopper efficiency with battery supply voltage	77
A1.1	Square wave generator output and capacitor voltage waveforms	82
A1.2	Typical integrator voltage waveforms	85
A1.3	Monostable multivibrator output and capacitor voltage waveforms	88
A2.1	Typical transistor chopper voltage waveforms	91
A2.2	Typical transistor chopper current waveforms	92
A2.3	Typical voltage transients occurring across chopper output transistors	93
A3.1	Schematic diagram of chopper efficiency test circuit	98

### List of Symbols

h	hour
Wh	Watt-hour
kg	kilo-gram
T	torque (Newton meters)
N	speed (radians/sec)
I	current (amperes)
$\phi$	flux (webers)
K	motor constant
R	resistance (ohms)
V	voltage (volts)
E	back-E.M.F. of motor (volts)
$\alpha$	conduction angle (radians)
TH	Thyristor
D	Diode
Q	Transistor
C	Capacitor (Farad)
L	inductance (Henry)
t	time
Ptot	Power dissipation (watts)
Tj	junction temperature
Tmb	mounting base temperature
Rth	thermal resistivity
j	junction area
mb	mounting base area
T	time constant
Ge	Germanium
Si	Silicon
f	frequency (Hz)
$\epsilon$	efficiency (%)

### Suffices

a = armature  
f = field  
B = battery  
L = load  
C = capacitor  
P = peak  
O = output  
i = input  
S = supply  
e = emitter  
m = motor

### Prefices

M mega-  
 $\mu$  micro-  
m milli -  
k kilo -

### Abbreviations

exp exponential  
LOGe natural logarithim  
M-S-R Mark to space ratio

## (1.0) INTRODUCTION

Conventional methods of controlling the speed of battery electric vehicles remain in wide use mainly due to their low initial cost and ease of maintenance. Such methods have either low efficiency (as in the case of rheostatic controllers) or impulsive starting characteristics (battery scanning). Electronic controllers, generally in the form of thyristor d.c. choppers, are becoming more popular even though the initial cost is higher compared to conventional controllers. The main advantages of electronic controllers are their high reliability, smooth control over a wide range of speeds, and high efficiency. The high efficiency of electronic controllers becomes extremely important when employed in battery electric vehicles, where stored energy is limited and maximum utilisation is essential.

The main part of this dissertation describes the design of a high current transistor d.c. chopper. The total cost of the chopper is made competitive with comparable thyristor chopper by the use of cheap, medium current transistors.

To date, most transistor controllers have been designed to operate from low supply voltages (usually 36 volts), and capable of handling currents of around 300 amperes. The design and construction of a transistor chopper capable of operating from a battery supply of 72 volts and able to handle currents of up to 400 amperes is described. Also included are details and results of reliability tests and efficiency measurements carried out on the chopper.

A preliminary survey examines the various types of controllers available and battery electric vehicle design in general.



It proceeds to consider the various methods of achieving electrical braking and the design and characteristics of d.c. choppers suitable for traction use.

#### (1.1.) Current applications for battery electric vehicles

Battery electric vehicles are, at present, mainly used for commercial applications and in the transportation of raw material and manufactured goods within the confines of industrial premises, and for local delivery of dairy and grocery products. The advantages in the use of this type of vehicle in such applications, over other forms of transport, such as the internal-combustion engined vehicle, are the electric vehicle's high reliability and low running cost. These advantages have resulted in a slow increase in the ratio of electric to internal-combustion engined trucks in most of the major industrial countries. In Britain, the number of industrial trucks and commercial road vehicles registered up to 1972 totalled over 120,000. With the present increasing demands for silent and pollution-free transport, the electric vehicle is being increasingly employed in hospitals and other situations where automatic goods handling is required (such as warehousing), and where the ease and flexibility of the control of the electric vehicle becomes distinctly advantageous.

The principal problem insofar as battery electric vehicles are concerned is energy storage; traction batteries currently available have low energy densities compared to fuel oil, and are expensive. This results in the battery electric vehicle having a poor power to weight ratio, low range, and high initial cost compared to the internal-combustion engined vehicle. Due to these factors, such vehicles have, almost exclusively, been used for industrial and short range/low speed applications and have no significant application at

present, to the long range haulage of freight, or to passenger transport, where energy requirements can only be met by internal-combustion engines running on fuel oil, or, by hybrid electric vehicles employing heat engines or fuel cells to generate energy.

Because of their relatively short range per charge (approximately 45 miles) battery powered motor cars are not popular, although a number of models are being tested in a number of countries. On the other hand a much more favourable view is taken of battery propelled urban buses, and vehicles of this type are being tested in the U.S.A., Japan, Germany and the U.K. These vehicles mainly employ a battery-electric motor-power train or a hybrid system with a motor generator set coupled to the battery-operated drive.

Currently, work is being done on methods by which battery energy density and power can be increased while keeping the cycling life above a tolerable minimum although, at present, the only advancements are in the form of constructional improvements of the lead-acid batteries. Even with improvements of this kind the range of the vehicle can only be extended by around 10 miles.

Although range and performance can be somewhat improved with better car construction design and more efficient speed control systems, it is clear that a major breakthrough in traction battery design must be made before the battery electric vehicle can be considered a serious challenger to the internal-combustion engined vehicle in the private transport and long range travel fields.

## (1.2) Current design and recent developments

### (1.2.1) The body and chassis

Since a full vehicle chassis is necessary to support the batteries and motor etc., it is possible to use very light unstressed

materials for body construction. Vehicle bodies are often constructed of glass fibre and/or aluminium to reduce weight and thus increase payload. Body shape is usually governed by the vehicle's intended use rather than aerodynamic considerations, but at speeds over 30 m.p.h., aerodynamic drag becomes significant and bodies are then designed for minimum drag. Tyre drag, which constitutes nearly 50% of total vehicle drag, can be reduced by the use of large radial tyres.

#### (1.2.2) The battery

The present position and limitations of the battery electric vehicle can be largely attributed to the characteristics of the batteries used (mainly lead-acid, although some nickel-iron batteries are also used: these are more expensive than lead-acid but have longer life). In the case of electric delivery vehicles, up to 25% of initial capital is due to the battery.

The use of lead-acid traction batteries in electric delivery vehicles result in a battery weight of about 25% of gross vehicle weight and a payload of 40% to 50% of gross vehicle weight. To date, the batteries for electric traction have followed conventional lines of flat, pasted plate or tubular positive plate assemblies, having energy densities of about 20-30 Wh/kg at a 3.5h rate of discharge. In their normal duty of daily use in industrial trucks or road vehicles, these units have a service life of about 6 years, equivalent to about 1800 discharge/charge cycles.

At present, improved energy and power densities can be achieved but only at the expense of shorter service life. Work is being carried out on methods by which the energy density can be increased while keeping the cycle life within an acceptable minimum (500 cycles). To this end, the lessons learned from recent battery developments

are being applied; namely thinner plates, through-partition inter-cell connectors, lightweight plastic cell containers and battery crates. Such improvements enable energy densities of about 40 Wh/kg to be reached at the 5h rate, although this would only extend the range of the vehicle to approximately 60-70 miles. Vast amounts of work have gone into developing new fuel cells using different types of chemical action, the most promising of these is the metal-air cell (zinc being one of the most favoured anodes). Rectangular batteries, having electrodes of this type have been made with energy densities in the region of 250 Wh/kg. If such a battery could be made in a rechargeable form with an adequate cycle life, it would meet most of the requirements for electric traction batteries already mentioned.

### (1.2.3) The motor

Traction motors in electric vehicles are almost exclusively d.c. machines, since they can be simply controlled from a d.c. power source. Solid-state chopper controllers are now extensively used with d.c. motors, and they are much cheaper than the sophisticated circuitry required to control a.c. motors.

Although, of the various types of d.c. machines available the series wound type is the most widely used in present day applications due to its high torques at low speeds as shown by the characteristics given in figure (1.1), the series motor has the distinct disadvantage of being unstable when used as a generator and of exhibiting very low torques at high speeds. These make the series machine difficult to use in vehicles employing regenerative braking and those which require adequate acceleration at high speeds; the separately excited machine is sometimes used as an alternative.

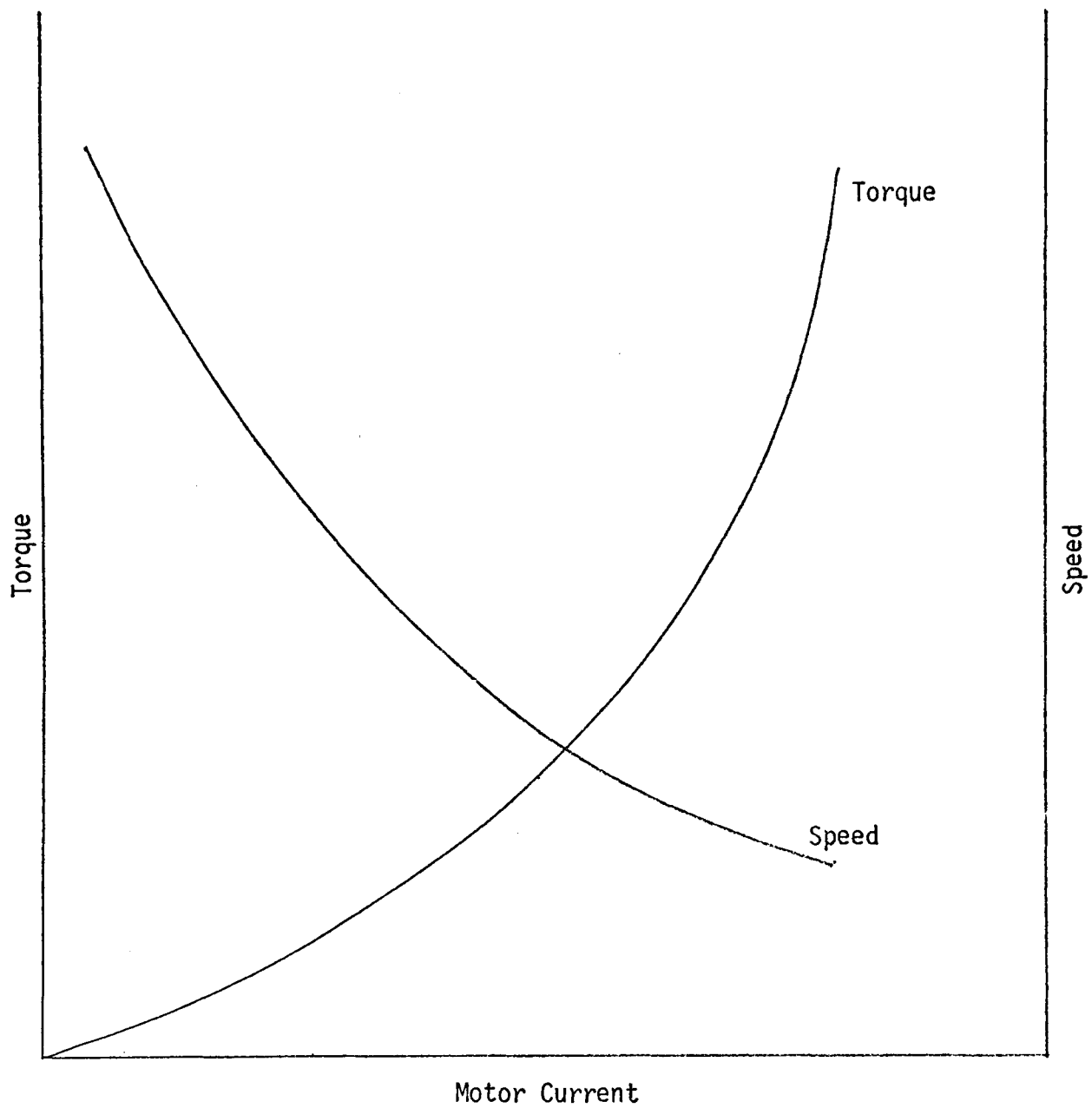


Figure 1.1 - Series d.c. motor characteristics.

The separately excited d.c. machine can be made to exhibit characteristics similar to that of the series machine through the choice of a suitable relationship ( $\delta$ ) between armature and field currents ( $\delta = I_a/I_f$ ). This relationship can also be used to vary the braking torques produced by the machine and this, coupled with the machine's stability during the generating mode, render it highly suitable for use in vehicles employing regenerative braking.

### (1.3) Propulsion systems incorporating series motors

The characteristics of several conventional methods of starting and controlling the speed of series traction motors will be described.

#### (1.3.1) Rheostatic controllers

The standstill torque available from a series motor, when supplied at the nominally correct voltage for the machine, is extremely large. The high motor current drawn under such conditions may be injurious to both the batteries and the commutator of the machine. A method commonly employed to overcome this problem is to insert a resistance in series with the motor: this limits the initial surge of motor current, and therefore the 'starting' torque, to an acceptable level. As the motor runs up, the resistance is gradually reduced, and finally removed altogether when the motor attains normal operating speed. The main function of this type of controller is to limit starting currents and it has only a limited value as a speed controller because of heat dissipation in the series resistors. All stepped controllers produce acceleration jerks at each step and as much as 50% of energy supplied to the system is dissipated in the series resistors.

Acceleration jerks can be eliminated by the use of a carbon pile rheostat, but approximately half the supplied energy will still be wasted through heat dissipation which limits its use as a speed controller to relatively short time ratings, and the only economical

running speed is at full voltage.

An improvement in efficiency is possible through the use of the series/parallel system, using several motors instead of a single unit. Consider two identical motors used to provide the tractive effort in a vehicle. These may be arranged in series for the first part of the starting period, and in parallel for the second part of this period and for subsequent 'normal' operation. If the current per motor is maintained at a constant value over the whole of the starting period, the torque output during this period will be constant and independent of the method of connection. When the motors are in series, their back-E.M.F.'s will also be in series: thus, for a given power consumption from the supply, the mechanical power output will be double that available from one motor. When the total voltage across the pair of motors, made up by the back-E.M.F. as the motors run up, reaches the supply voltage  $V_B$  the motors are connected in parallel.

The use of a series/parallel system results in a 67% average efficiency during the starting period. A considerable improvement compared to the 50% average efficiency when a single motor is used.

The use of a larger number of motors allow a further increase in efficiency during the starting period. If four motors were used, a 75% average efficiency can be obtained.

#### (1.3.2) Battery division

In order to provide a sufficiently low voltage to the static motor, the battery is divided into several equal sections, which are initially connected in parallel. As the motor runs up to speed, rearrangement of all connections allows a gradual increase in voltage applied to the motor, thus maintaining a uniform current during

the starting period.

It is essential to ensure that load current is drawn equally from all cells, in order to prevent premature discharge of any one cell. The voltage available by battery division is therefore limited to specific sub-multiples of the total voltage. Suppose that the total number of storage cells may be divided into  $2^n$  equal groups, where  $n$  is some convenient small number. If the cells in each group are connected in series, then the smallest battery voltage is obtained by the parallel connection of all the groups,  $V_1$ , say. This voltage is applied to the motor at standstill: as the motor runs up to speed, the battery is reconnected, with double the number of cells per group. There are consequently  $2^{n-1}$  parallel-connected groups, each of terminal voltage  $2V_1$ . This process may be repeated until the motor attains normal speed, when all the cells are in series and the terminal voltage is  $2^n V_1$ .

A typical system is shown diagrammatically in figure (1.2): the switching sequence is as follows,

- (1) The switches marked 'D', 'C' are closed to excite the motor.
- (2) Switches 'D' are opened, and switches 'B' closed to double the supply voltage.
- (3) Switches 'C' are opened, switch 'A' closed, thus placing all the cells in series.

This method of starting has several disadvantages: firstly, a large number of high-current switches is required; if there are  $n$  steps of applied voltage, the output voltage being doubled at each step, therefore,  $X$  switch contacts are required, where

$$X = 3 \sum_{r=0}^{n-2} 2^r$$



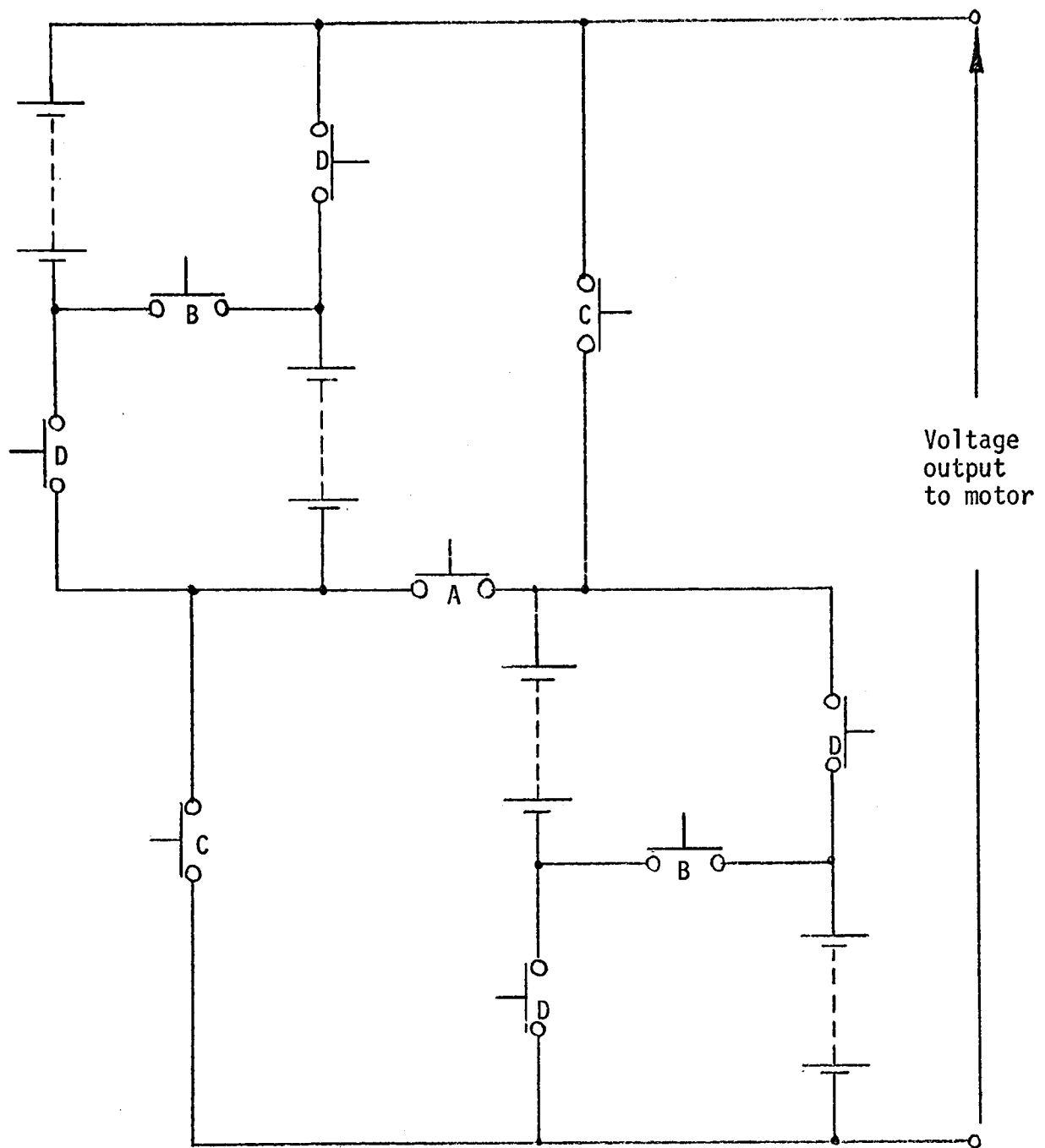


Figure 1.2 - Method of 'battery division'.

secondly, circulating currents may flow within the battery if one section fails in service.

Diodes may replace all switches marked C and D, as in figure (1.3), without affecting the starting procedure. The number of switch contacts may therefore be reduced to

$$X = \sum_{r=0}^{n-2} 2^r$$

whilst double this number of diodes are required. This modification has two disadvantages. Firstly, in the battery configuration of lowest output voltage, there are (n-1) diodes in series with the supply, which absorb a considerable proportion of the power delivered by the battery. The efficiency of this system is consequently little better than that obtained with rheostatic starting. Secondly, the presence of diodes in the circuit precludes the flow of current into the battery, except where all of the sections are in series. Regeneration for braking purposes may therefore only take place into full battery voltage, and so electrical braking may only be used at high speeds. Thus the introduction of diodes to simplify the switching apparatus is unacceptable if regeneration is to be employed.

#### (1.3.3) Battery scanning

The technique of battery scanning is very similar to that of battery division discussed above, but is only applicable where normal vehicle duty does not involve frequent halts.

The cells of the battery are connected permanently in series. Inter-cell connections are brought out so that the voltage applied to the motor may be increased progressively in a number of uniform steps. The starting characteristics are therefore considerably smoother than those obtained by battery division; where in the

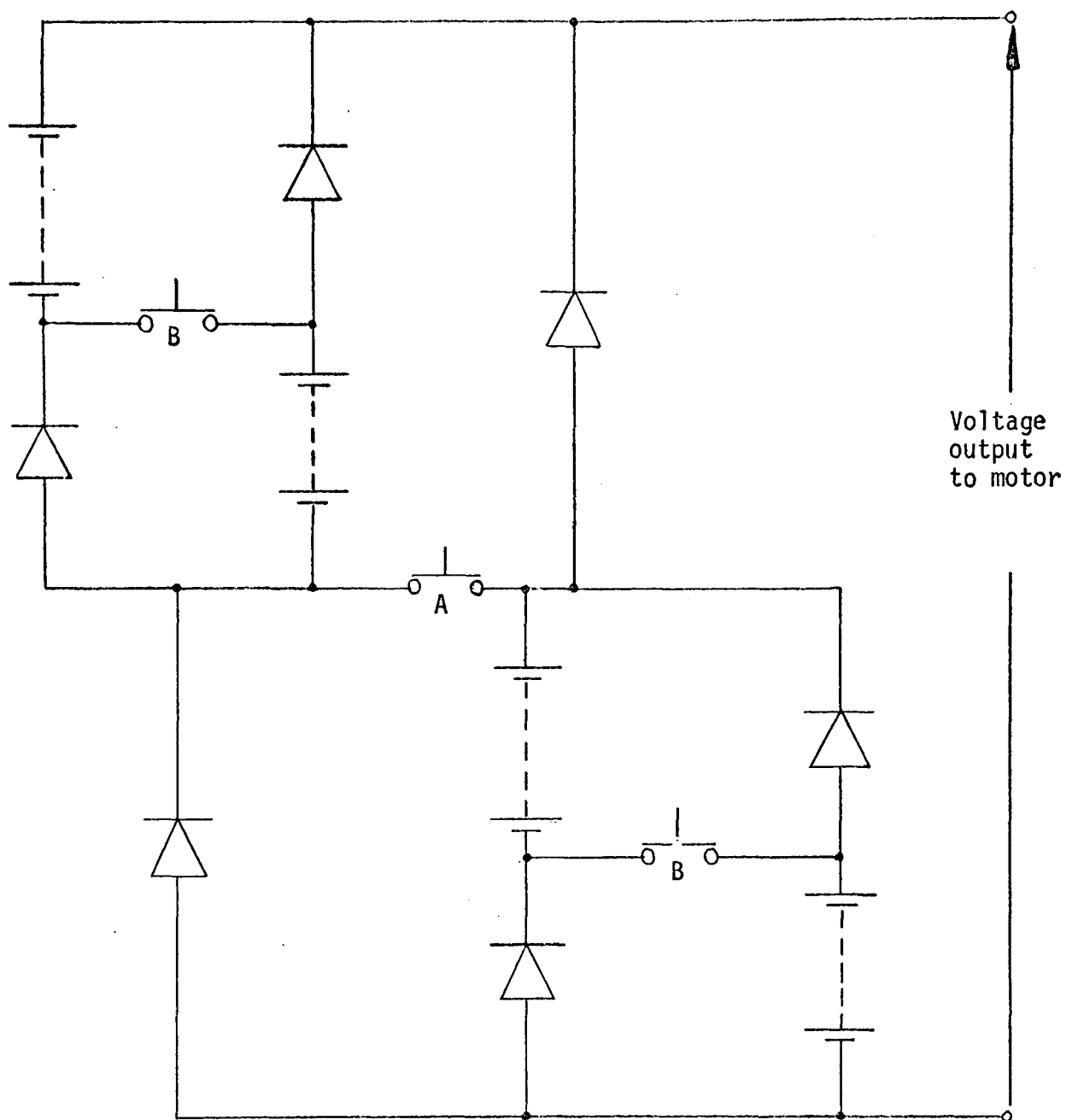


Figure 1.3 - Modified method of 'battery division'.

latter case the voltage increases in geometric progression, doubling in each step.

The obvious disadvantage of the use of battery scanning is that the cells discharge by unequal amounts during the starting period, hence the restriction on the number of halts permitted. If, however, regenerative braking is employed, then when the vehicle halts, a large proportion of the kinetic energy may be returned to the battery section of the lowest voltage. This compensates for the large drain upon the cells during the starting period. If a considerable number of starts are involved in the duty cycle, however, the intermediate cells may become prematurely discharged.

The premature discharge of intermediate cells may be avoided by the progressive indexing of 'start' cell; the reference connection from the battery to the motor (a permanent connection in battery scanning) is sequentially moved, with every start, to a different cell along the battery.

#### (1.3.4) Conclusions

It has been shown that in rheostatic starting, the energy losses in the rheostat are of the same order of magnitude as the kinetic energy imparted to the vehicle: in applications where repetitive starting is involved, or high cruising speeds are required, these losses may detract considerably from the operational range of the vehicle. Adoption of one of the remaining two methods mentioned above, on the other hand, results in impulsive starting characteristics. Use of the method of 'battery scanning' may provide smoother starting characteristics, but these are only achieved at the expense of differential discharge of the battery, which is undesirable.

It is therefore apparent that the conventional propulsion

systems used in electric vehicles would prove unacceptable in a passenger-carrying vehicle.

#### (1.4) Electrical braking

Electric vehicles can be conveniently provided with electrical braking to improve manoeuvrability and greatly extend the life of the mechanical braking system. Electrical braking of d.c. motors is, in the main, achieved by driving the motor as a generator, thus converting the kinetic energy of the moving vehicle to electrical energy and the product of voltage, current and time ( $I E t$ ) represents the braking energy absorbed.

The following sub-sections will deal with methods used in applying electrical braking to series-wound motors, and also methods of achieving regenerative braking.

##### (1.4.1) Rheostatic braking

When the conversion of vehicle kinetic energy to electrical energy is performed at low voltage, high current, and dissipated in a resistance it is known as rheostatic braking. This involves the disconnection of the motor from the supply, reversing the field connection relative to the armature and connecting a resistance across the motor, as shown in figure (1.4b). The motor then acts as a series generator supplying the resistance load: an expression for the braking torque produced can be obtained by referring to the general torque equation for d.c. machines,

$$T = K \Phi I_a \quad (1)$$

In the circuit shown in figure (4.b), assuming the winding resistance of the machine to be negligible compared to the load resistance  $R$ , the current through the circuit is given by

$$I = \frac{E}{R} = I_a \text{ (for a series wound machine)}$$

substituting for  $I_a$  in equation (1)

$$T = \frac{K\Phi E}{R}$$

but the back-E.M.F. of the machine,  $E$ , is proportional to  $N\Phi$ , thus

$$T \propto \frac{N\Phi^2}{R} \quad (2)$$

From equation (2) it can be clearly seen that the braking torque is proportional to  $N\Phi^2$  for any specific value of load resistance  $R$ .

It can also be noted that the braking torque can be controlled by the variable load resistance  $R$  and decreases as the motor slows down.

This method of braking is used extensively on battery locomotives and industrial trucks, and frequently the starting resistors are also used as braking or load resistors.

#### (1.4.2.) Plug Braking

In this form of braking the motor field connections are reversed as shown in figure (1.4c), so that the motor tends to run in the opposite direction to vehicle motion. The supply voltage and the back-E.M.F. are then acting in the same direction, and a resistance is included in the circuit to limit the current.

Referring to the circuit in figure (1.4c) and neglecting the winding resistances of the machine, the current ( $I$ ) flowing through the circuit is given by

$$I = \frac{V + E}{R}$$

Substituting for  $I$  in equation (1), an equation for the braking torque produced by plug braking is obtained:

$$T = \frac{K}{R} (V\Phi + E\Phi)$$

The back-E.M.F. of the machine  $E$ , is  $KN\Phi$ .

Therefore equation (3) can be rewritten

$$T = \frac{K}{R} (V\phi + KN\phi^2) \quad (4)$$

Since the supply voltage (V) is constant, for a specific value of series resistance R, the torque equation becomes

$$T = A\phi + B\phi^2 \quad (5)$$

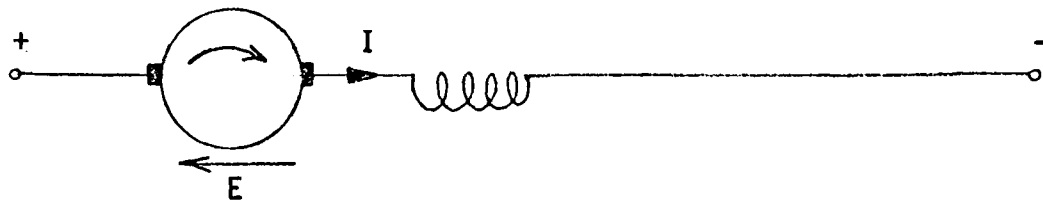
where A and B are constants.

The flux  $\phi$  in the machine is proportional to the current (I) flowing in the circuit, hence it can be clearly seen from equations (4) and (5) that unless the current is limited by the addition of the series resistor R, the braking torque produced at high speeds can be too excessive for use in braking vehicles. It can also be noted that the braking torque is available to standstill ( $t = A\phi$  from equation 5).

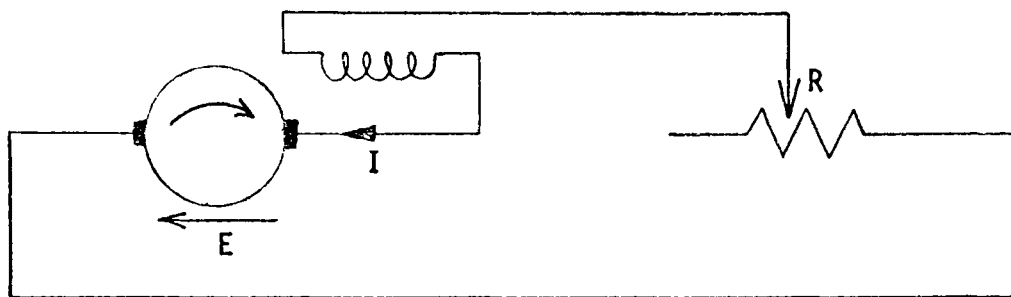
Although this method gives a greater braking torque than rheostatic braking, it has the disadvantage of drawing current from the battery during the braking period and this energy as well as the kinetic energy of the vehicle must be dissipated in the resistors. The braking resistors in this case require to be approximately twice the value of the starting resistors.

Figure (1.4d) shows a method of achieving dynamic braking which is a combination of rheostatic and plug braking. The armature current circulates through the diode D and the field current is controlled by the resistance R. At high speeds, the armature current is larger than the field current and the diode D is always forward biased. In this case the braking is rheostatic and the motor is operating as a generator.

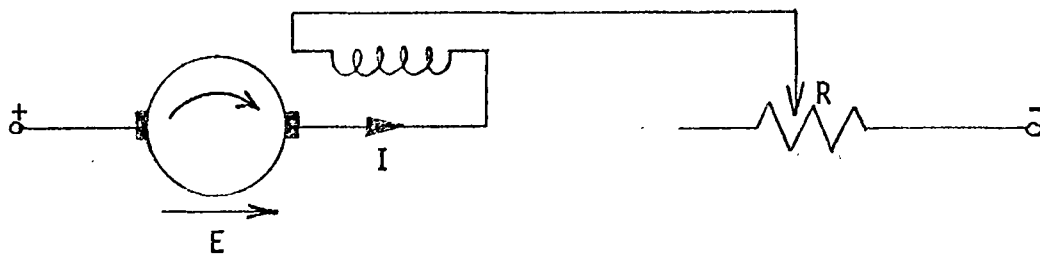
At low speeds, the current generated by the armature will fall until it is less than the field current and current will flow



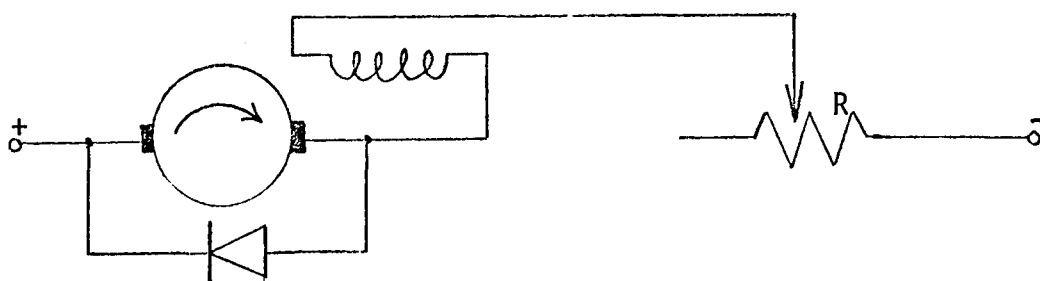
(a) Motoring



(b) Rheostatic braking



(c) Plug braking



(d) Dynamic braking

Figure 1.4 - Motoring and braking conditions.



from the battery through the armature and field and the machine will motor in reverse to the vehicle motion. This is the plug braking mode and will bring the vehicle to a standstill.

#### (1.4.3) Regenerative braking

It has been mentioned earlier that electrical braking of a d.c. motor can be achieved by driving the motor as a generator, thus converting the kinetic energy of the moving vehicle into electrical energy. When this conversion is performed at high voltage, low current and returned to the supply it is known as regenerative braking.

In bringing a moving vehicle to a halt on a level road the energy to be absorbed is relatively small and rheostatic braking is appropriate. On the otherhand, holding the vehicle to a specific speed down a long steep gradient represents a sustained output of a much higher order, then regenerative braking is most suitable.

To obtain regenerative braking, the voltage generated in the armature must exceed the supply voltage by an amount equal to the total voltage drop in the machine. Moreover, the generated voltage must be maintained at this value independent of the speed and braking torque. These conditions necessitate the use of either shunt - or separately - excited field windings, with the braking torque controlled by regulating the excitation.

## (2.0) Chopper Controllers

### (2.1) General

A d.c.chopper controls the voltage applied to a load by periodic switching of the supply. The load is alternately connected to the supply for a short period  $t_1$ , and subsequently disconnected for a further short period  $t_2$ , after which the cycle is repeated. The amount of energy delivered to the load may be controlled by the variation of the ratio  $t_1/t_2$ ; clearly, the mean load voltage  $\bar{V}_L$  may be expressed in terms of the battery voltage  $\bar{V}_B$  by the relation:

$$\bar{V}_L = \frac{t_1}{(t_1+t_2)} \bar{V}_B \quad (2.1)$$

It is both convenient and conventional to express the switching cycle in angular measure: the 'conduction angle', of the supply switch is then defined by the relation:

$$\alpha = \frac{2\pi t_1}{(t_1+t_2)} \quad \text{radians}$$

Inspection of equation (2.1) above, suggests two methods by which  $\alpha$  may be varied:

- (1)  $(t_1+t_2)$ , and hence the pulse- repetition-frequency (or PRF) is fixed, whilst  $t_1$  is varied. This is known as the 'fixed-frequency, variable Mark/space', or, 'pulse width modulation' system.
- (2)  $t_1$  is fixed and  $t_2$  varied; this is known as the 'variable-frequency, fixed Mark system'.

These two methods may be combined, such that  $t_1, t_2$  and  $(t_1+t_2)$  vary simultaneously. In this investigation, the pulse width modulation system will be used.

It must be emphasised at this point that where the load is inductive, a motor for example, a large transient will be induced when the supply is disconnected due to abrupt motor current change: some means of suppressing or absorbing the transient must be provided if semiconductor switches are to be used. In practice, a 'freewheeling' diode is placed across the motor, thus allowing utilisation of the inductive energy in the motor to aid the maintenance of load current whilst the supply is disconnected. The circulating current in the diode will cause, on average, more current to flow through the motor than is taken from the batteries, with a current equal to the circulating diode current flowing through the motor when the supply is disconnected. However, the power taken from the battery is approximately equal to the power delivered to the motor, indicating that energy is stored in the motor inductance at the battery voltage level and is delivered to the motor at the approximate current level when the battery is disconnected.

To provide quiet and smooth motor operation, the current variations in the motor must be kept to a minimum during the switching cycle. There are limitations on the amount of energy that can be stored in the motor inductance, which, in turn, limits the power delivered to the motor during the 'off' time; thus the 'off' time must be short. To operate the motor at low speeds, the 'on' time must be approximately 10% of the 'off' time and, therefore, a rapid switching rate is required that is generally beyond the capabilities of mechanical switches. This problem becomes more acute when high currents are to be switched, and semiconductors are therefore invariably used.

## (2.2) Thyristor Choppers

Thyristors are, at present, the most widely used switching element in electronic chopper controllers. They are readily available in a wide range of voltages and currents, and a single device is able to handle the power requirements of most traction controllers.

The basic characteristic of thyristors is well known: the device is made to conduct by the application of a current pulse of appropriate polarity between gate and cathode. To restore the device to the blocking state, on the other hand, the current through the device must be reduced to below the critical 'holding current' of the device, generally about 0.1% of rated forward current. Although turn-on time is rapid (3-4  $\mu$  sec.) turn-off time is slow (50-100  $\mu$  sec.) unless a reverse current is allowed to flow through the device during the commutation period. Thus any d.c. thyristor chopper requires an auxiliary circuit to enforce commutation of the load current.

There are two basic forms of thyristor chopper: those in which a subsidiary supply is developed by suitably charging a capacitor, and, those employing an under-damped resonant circuit to reverse the direction of current in the thyristor after a specific conduction period.

#### (2.2.1) Thyristor Choppers with Capacitive Commutation

The basic circuit of a thyristor chopper employing capacitive commutation is shown in figure (2.1). Suppose that both thyristors TH1 and TH2 are in the blocking 'off' state, so that any residual current in the load flows through the flywheeling diode  $D_1$ . The capacitor is consequently charged to the supply voltage  $V_B$ . If the load circuit thyristor TH1 is fired (at time  $t = \theta_1$  in figure 2.2), then the supply is connected across the load and a short-circuit placed across the resonant circuit C, TH1,  $D_2$ , L. A series of damped oscillations therefore commences in the circuit, but is truncated by diode  $D_2$  after the first half-wave of current has passed (at  $t = \theta_2$  in figure 2.2). The capacitor charge-polarity has thus been reversed, and the net voltage across C is negative. The charge is held, as both  $D_2$  and TH2 are non-conducting. If, at some later time ( $t = \theta_3$ ) TH2 is fired, then TH1 becomes reverse-biased and rapidly recovers to the blocking state.

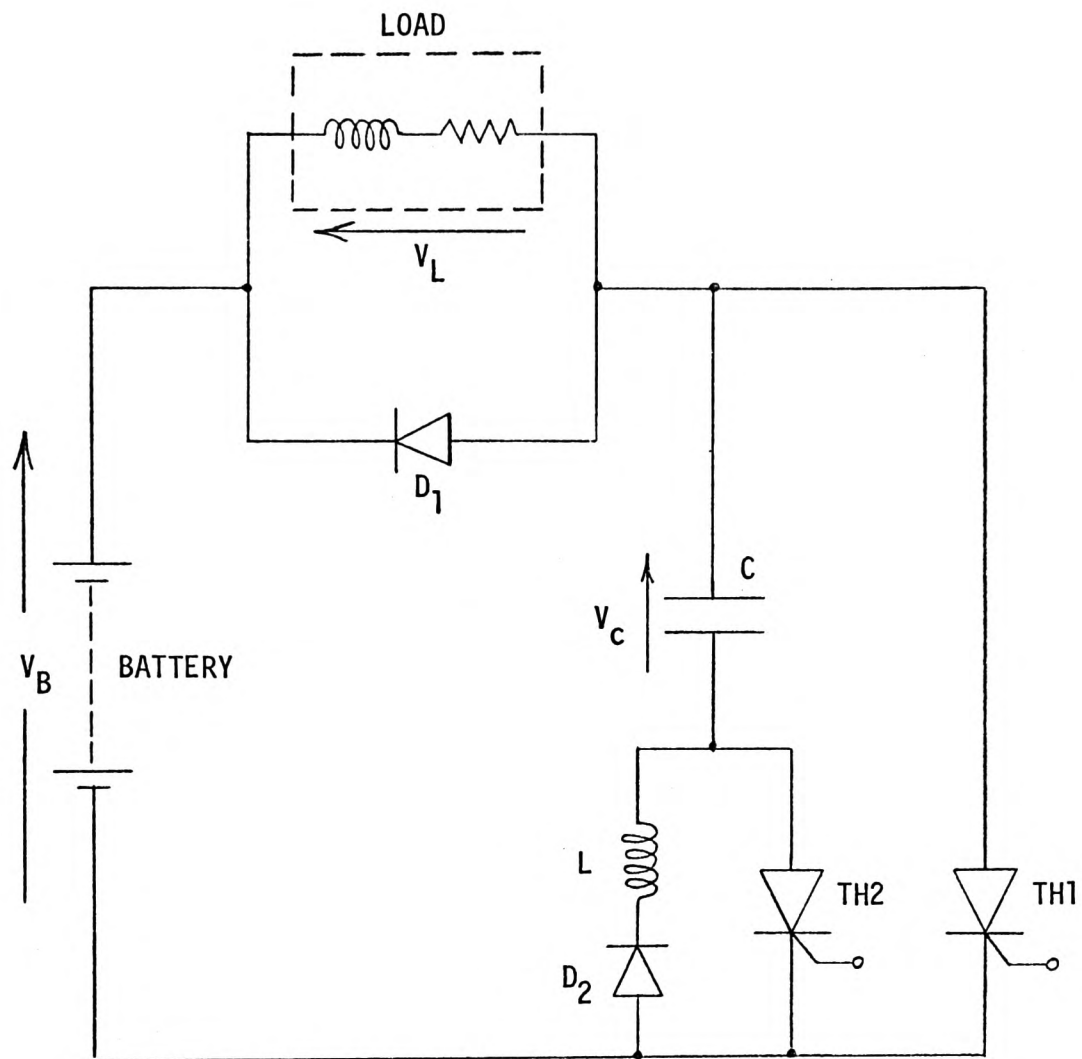


Figure 2.1 - Circuit of a thyristor chopper employing capacitive commutation.

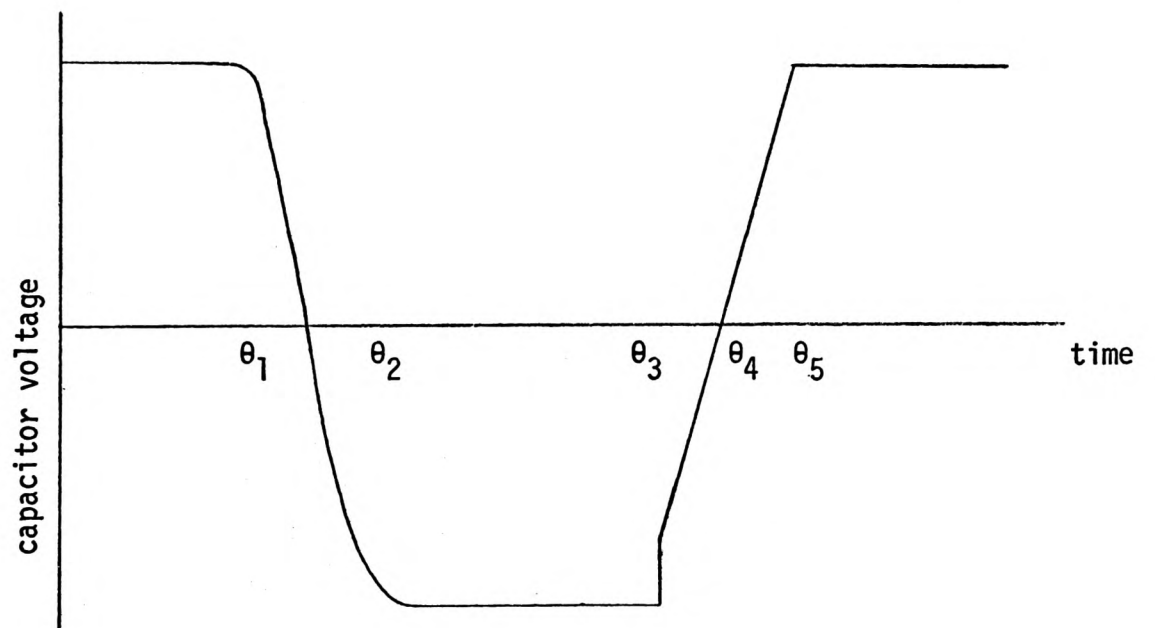
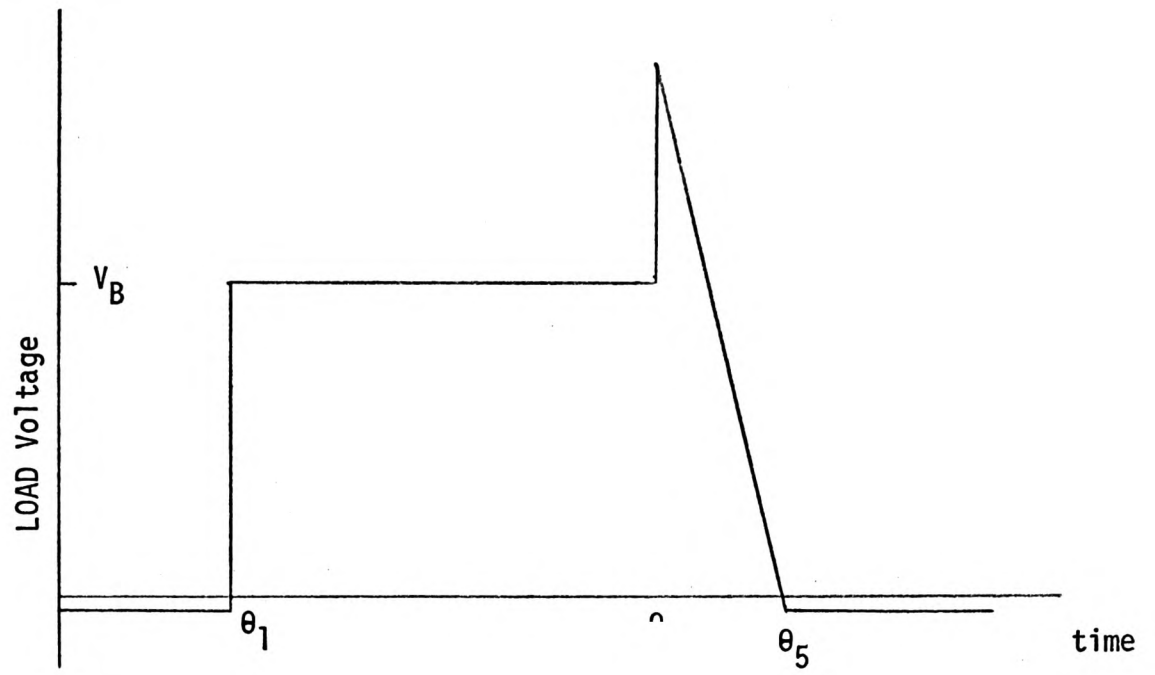


Figure 2.2 - Circuit waveforms in a thyristor d.c. chopper employing capacitive commutation.

The capacitor is then effectively in series with the battery and load: the residual capacitor voltage aids the battery in driving current through the load, and capacitor reverse voltage falls at a rate determined by load current. After a short period (at  $t=\theta_4$ ) the net capacitor voltage becomes positive, thus re-applying forward bias to TH1. After a further period (at  $t=\theta_5$ ) the net load voltage becomes negative, and the freewheeling diode conducts. There is subsequently no current through TH2, which recovers to the blocking state. The cycle is then complete.

Losses in the chopper circuit are made up of those occurring during the conduction of the load-circuit thyristor and freewheeling diode, and, in the capacitor during the commutation period.

#### (2.2.1.1.) Advantages and Disadvantages of Capacitive Commutation

The main advantage of any thyristor d.c. chopper employing capacitive commutation is that the conduction angle of the load-circuit thyristor may be varied independently of the pulse repetition frequency. The circuit has further advantages where some form of current limiting is to be used, as commutation may easily be initiated from some external current-sensor circuit. The most significant disadvantage of the circuit described is that separate gate-pulse generators are required for the load-circuit and commutation thyristors: furthermore, the circuit itself contains a relatively large number of components.

#### (2.2.2) Thyristor d.c. Choppers Employing Resonant Commutation

There are two distinct classes of thyristor d.c. choppers which employ resonant commutation. None of the conventional forms of these circuits is suitable for use with highly inductive loads. Other choppers of this type have been developed, employing a small number of components and requiring simple pulsing circuitry.

There are two systems conventionally employed to drive resistive loads: the series-tuned circuits, in which at least one of the resonating components is placed in series with the thyristor. The waveform of load current is largely determined by the characteristics of the resonant circuit, and the ripple component of load current is generally high; and, the shunt-tuned circuits, shown in figure (2.3).

Where the shunt-tuned circuit is employed, the waveform of load voltage is approximately rectangular, however, conduction of the freewheeling diode initiates a train of parasitic oscillations in the tuned circuit formed by L,C,D and the battery. The commutating capability of the circuit is thus influenced by the point in this cycle of oscillations at which the thyristor is refired. This circuit may be modified in one of two ways, in order to eliminate this undesirable effect: these modifications are shown in figures (2.4a) and (2.4b). Operating conditions in the two modified circuits are very similar to those in the original configuration, and the advantages of the new circuit may best be indicated by consideration of a single cycle of operation of the conventional circuit.

Suppose that the load is highly inductive, and the thyristor in figure (2.3) is 'off': the stored energy in the load inductance will aid the maintenance of load current, via diode D. The capacitor is assumed to be charged to steady voltage  $V_B$ . When the thyristor is fired, the supply is connected to the load, and a short-circuit placed across the resonant circuit LC. A train of damped oscillations commences in the loop formed by L,C and the thyristor, the initial direction of current flow being such that the net current in the loop initially rises to the approximate value  $V_B \sqrt{\frac{C}{L}}$ , and subsequently decreases with time.



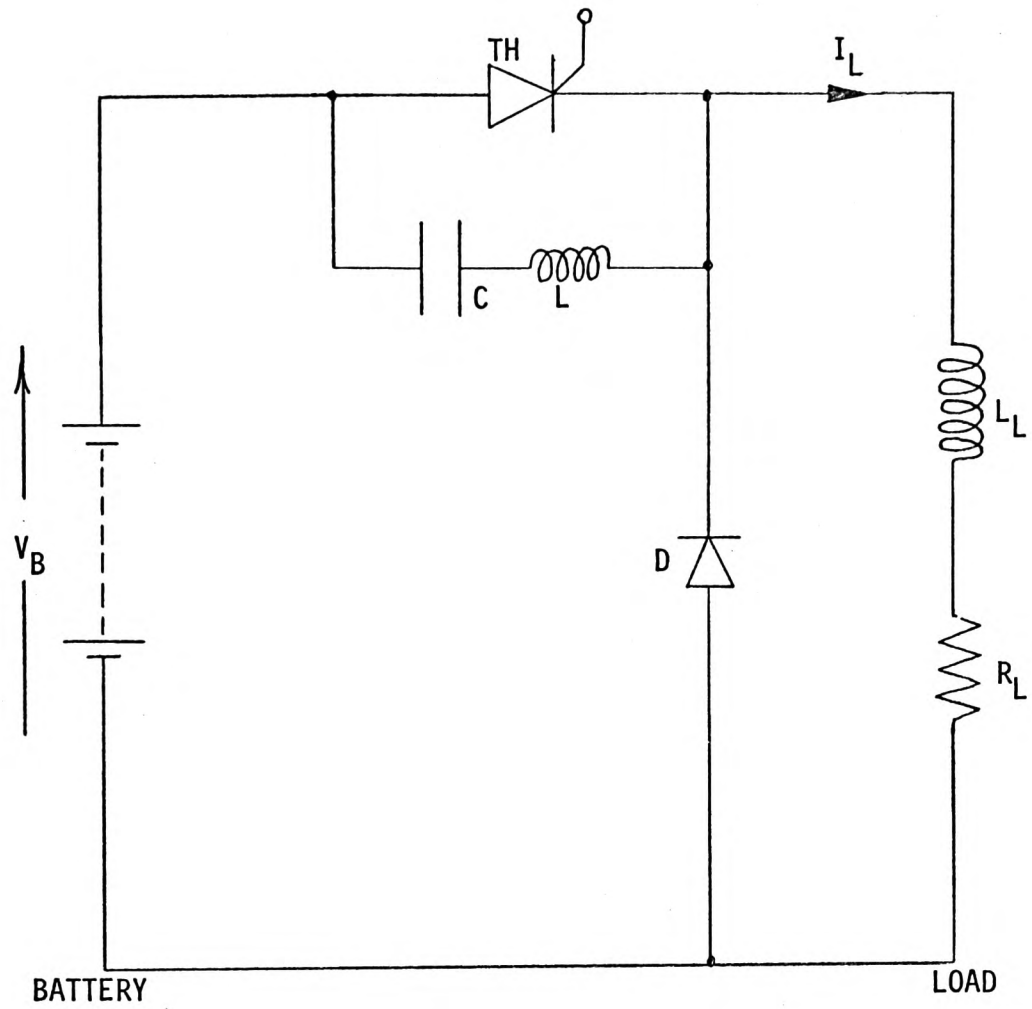
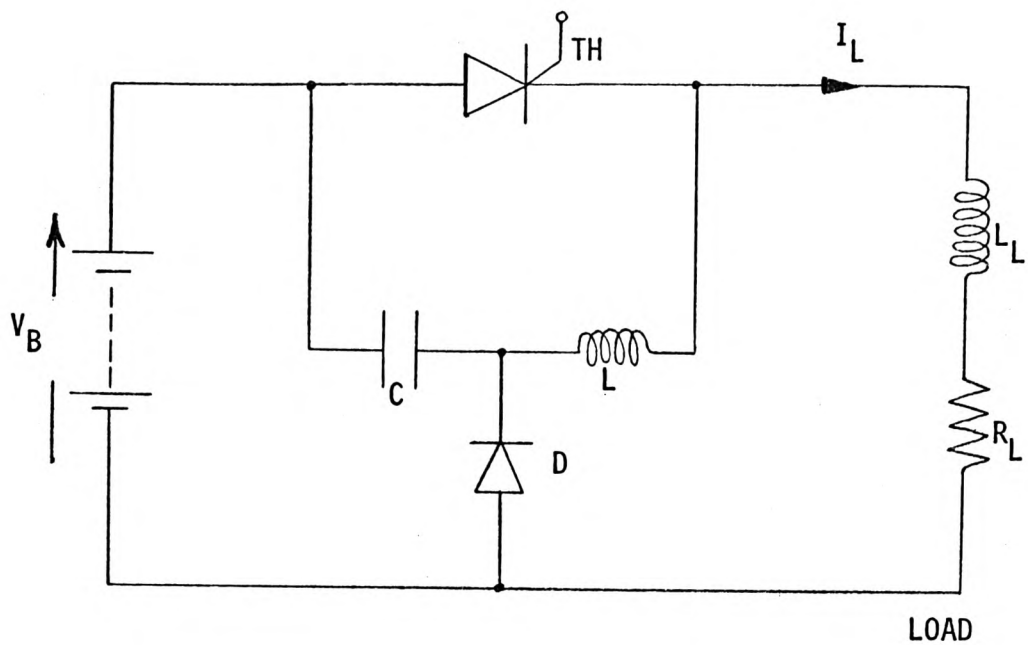
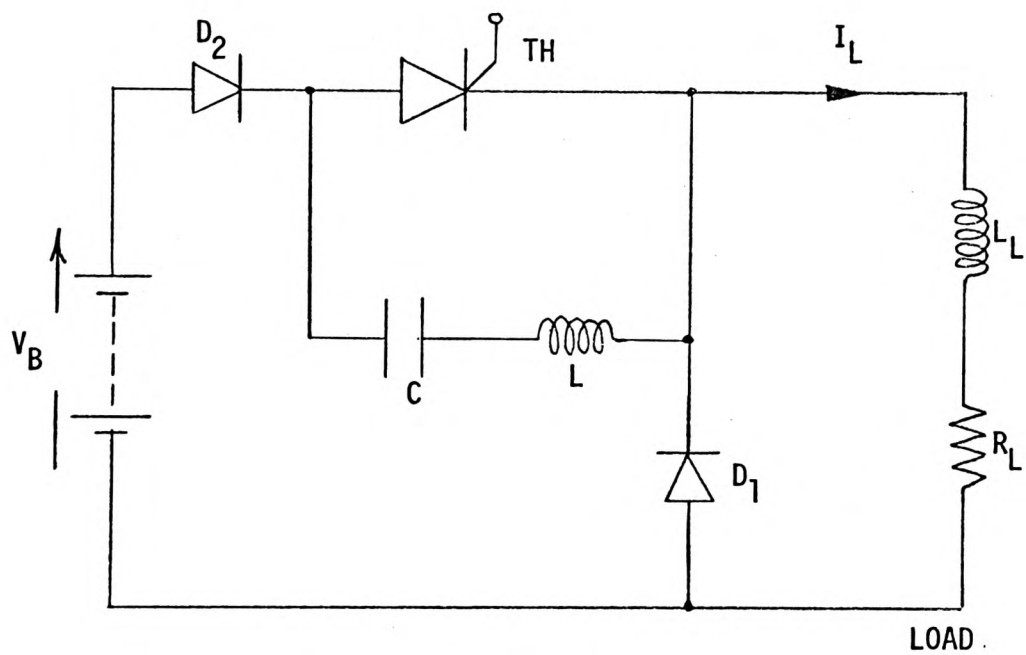


Figure 2.3 - The conventional shunt-tuned chopper circuit.



(a) Circuit modification 1



(b) Circuit modification 2

Figure 2.4 - Modified circuits for thyristor d.c. chopper with resonant commutation.

After a time  $\theta_1$ , where

$$\theta_1 = \pi \sqrt{LC} \text{ secs}$$

the direction of the circulating current is reversed, and net thyristor current diminishes rapidly. The device turns 'off' when the net current in it is zero. At the instant of turn-off, the polarity of the residual capacitor voltage is such that an increased voltage is applied to the load. Load current flows through the diode, however, and the net load voltage therefore decreases uniformly. The freewheeling diode conducts when the load voltage reaches zero. It is clear from the above description that thyristor turn-off may only be achieved if the circulating current in the resonant loop LC in figure (2.4) is greater than the load current

The conventional circuit is unsatisfactory in its subsequent behaviour: conduction of the freewheeling diode places a short-circuit, via the battery, across L and C. There is residual energy in this circuit due to the flow of load current in L. Furthermore, the current in the tuned circuit decreases from the initial value whereas the freewheeling load-current remains approximately constant: the freewheeling diode subsequently conducts continuously, so that oscillations in the tuned circuit are not interrupted. The sinusoidal variations in capacitor voltage profoundly affect the commutating capability in the following cycle: if the thyristor is fired when the capacitor voltage is greater than  $V_B$ , then commutation is facilitated, and vice-versa.

In practice, the circuit is designed so that the circulating current in the resonant loop is at least twice the maximum load current. Consequently, components are required to have current ratings of similar proportions. Owing to the high circulating current in the resonant loop, the power losses in this circuit will be high, and the overall efficiency of the system will therefore be low.

Consider now the suggested modifications to the conventional circuit.

The circuit of figure (2.4a)

In this circuit, the conduction of the freewheeling diode isolates both inductances in the load circuit, so that spurious resonance effects cannot occur. This circuit may therefore be designed such that, after allowing for losses, the circulating current in the commutating loop is slightly greater than the maximum load current. This circuit will allow more efficient utilisation of the circuit components employed: for a given set of components, the load-current rating is 50 to 100% greater than that obtainable using the conventional configuration.

Circuit of figure (2.4b)

With this circuit, the residual energy in the resonant circuit at the instant in which  $D_1$  conducts is stored in the capacitor, and utilised to facilitate commutation in the subsequent cycle. Consider circuit conditions at this instant: the net load voltage is zero, so that the induced voltage across the load inductance,  $V_{LL}$ , may be represented

$$V_{LL} = -I_L R_L = L_L \frac{dI_L}{dt}$$

The voltage at the junction of C and L is therefore negative by an amount  $V_1$ , where

$$V_1 = \frac{R_L I_L L}{L_L} \quad (2.2)$$

This contribution to the residual energy of the tuned circuit must be added to the inductive energy in L to determine the total residual energy:

$$\epsilon = \frac{1}{2} (C V_1^2 + L I_L^2)$$

thus, from equation (2.2) above,

$$\epsilon = \frac{1}{2} I_L^2 \frac{(L + CL^2 R_L^2)}{L_L^2}$$

The initial direction of oscillatory current in the loop L, D, supply, D<sub>2</sub> and C is such that D<sub>2</sub> in figure (2.4b) conducts. The train of oscillations is, however, truncated by diode D<sub>2</sub> after the first half-wave of current has passed. At this point, the residual energy in the tuned circuit has been stored in C, and the net capacitor voltage is greater than V<sub>B</sub>:

$$V_C = V_B + I_L \sqrt{\frac{L}{C} (1 + CL R_L^2)}$$

Thus, the final voltage across the capacitor is a linear function of load current. When the thyristor is re-fired the peak circulating current I<sub>p</sub> in the loop L, C, TH may be calculated:

$$I_p = V_B \sqrt{\frac{C}{L}} + I_L \sqrt{1 + \frac{LC R_L^2}{L_L^2}}$$

There is always a margin of safety between the actual load-current and the commutating capability of the circuit. If the load is highly inductive, then the margin is approximately constant, whereas if the load inductance is small, then the margin increases with load current.

The performance of any practical circuit will be affected by two factors: firstly, losses in the resonant circuit will reduce the magnitude of the circulating current, and thus reduce the load-current rating for the unit. Secondly, if the load inductance is low, load-current at the instant D<sub>1</sub> conducts will be considerably smaller than that flowing at the instant in which TH<sub>1</sub> turns 'off'. It is therefore to be expected that the 'commutation margin' will decrease as load-current increases.

The commutating capability of the resonant circuit for given component values, should nevertheless be greatly in excess of that obtainable with the two circuits previously described.

#### (2,2,2,1) Advantages and Disadvantages of Resonant Commutation

The main advantage of any thyristor d.c. chopper employing resonant commutation lies in the elimination of the commutating thyristor (TH2 in figure 2.1) and the resultant simplification of the gate-pulse unit required.

The disadvantages of the resonant commutation circuits described are firstly, the thyristor is required to have a peak-current rating of approximately double the peak prospective load-current and secondly, the power losses in such choppers are generally higher than in those employing capacitive commutation. The high power losses arise because

(1) the mean forward pulse-current in the thyristor when the maximum permissible load-current ( $I_L \text{ max.}$ ) flows, is generally 20 - 50% greater than  $I_L \text{ max.}$ , whereas in a chopper employing capacitive commutation the mean current in the load-circuit thyristor is only 10 - 30% greater than  $I_L \text{ max.}$

(2) the circulating current in the resonant loop in figures (2.3) and (2.4a) must be greater than the peak prospective load current. The circulating energy, and consequently the power loss in the circuit, is therefore high.

In this respect, the circuit shown in figure (2.4b) has an advantage in that the circulating current is only large if the load current is high.

### (3.0) Transistor d.c. Chopper

#### (3.1) General

The basic characteristics of the transistor clearly shows its suitability for use as a switch; it can be made to conduct by the application of a current signal of appropriate polarity between base and emitter, but unlike thyristors, the blocking state can be readily retrieved by the removal of the base signal and without the use of additional circuitry.

Present day traction motors often require high current levels. In small electric vehicles such as fork lifts and golf carts, a d.c. chopper controller may be required to handle current levels of between 300 and 500 amperes. This high current demand cannot be met by any single power transistor at the present time, and transistors must be operated in parallel to meet these high current requirements. The operating voltage of such controllers, typically less than 72 volts, poses no serious problems, since power transistors are available with peak voltage ratings of over 300 volts.

The maximum current level that any transistor can handle in any particular circuit is dependent upon the switching load line and the safe area of operation for the transistor. With the motor circuit as a load, the basic switching load line for a power transistor is shown in figure (3.1). It is clear that if the motor current (collector current in figure 3.1) has not reduced much during the "off" time, and if a fast recovery freewheeling diode is not used, the switching "on" load line can stress the transistor as much as the switching "off" load line. If there is no resistance or inductance in series with the supply, the initial part of the switching "on" load line would be practically perpendicular to the collector-emitter voltage axis.

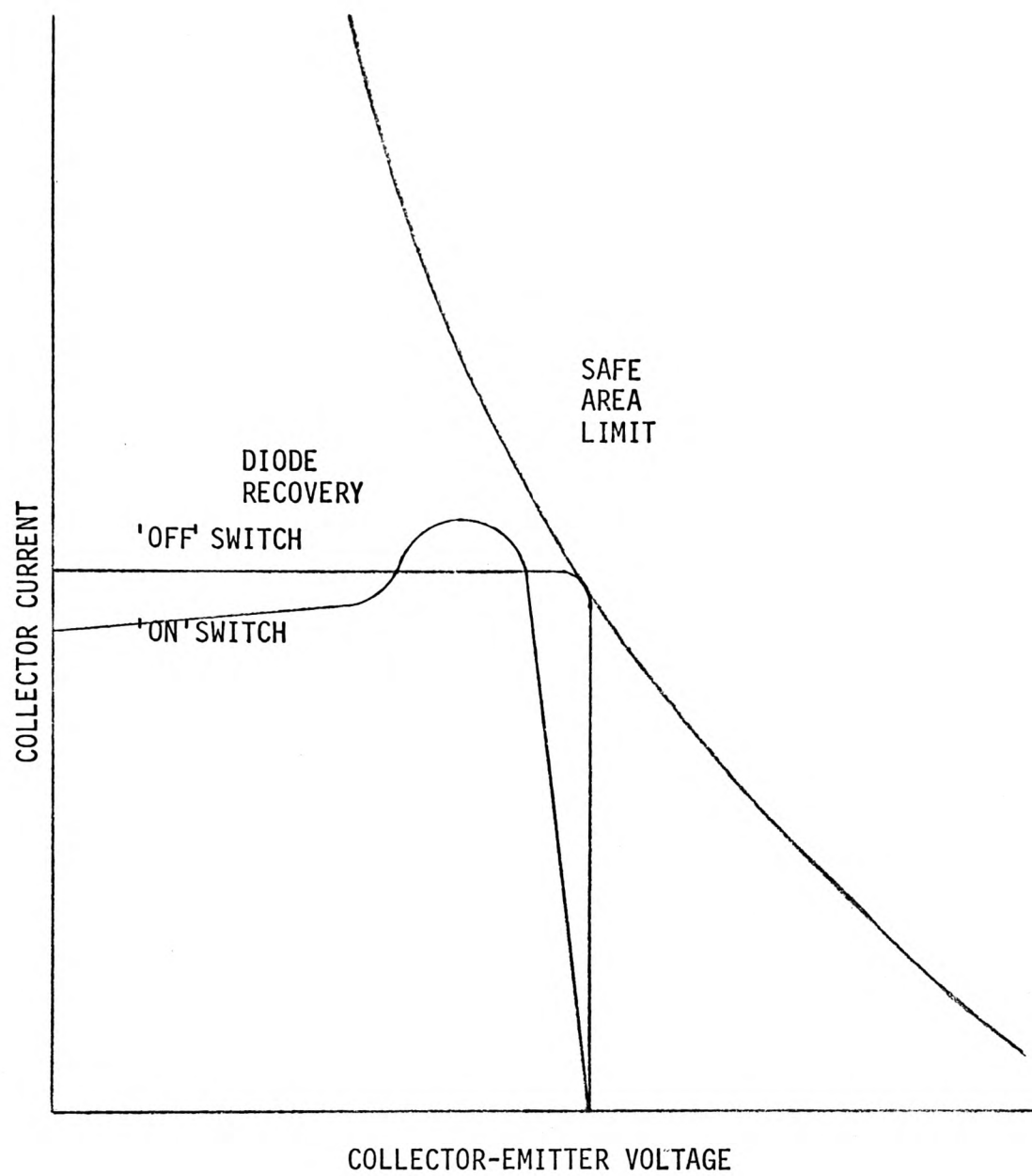


Figure 3.1 - INDUCTIVE LOAD LINE.



In many practical cases, the current through the motor would have substantially reduced before the transistor begins to turn "on". It is also impractical to assume that there is no impedance in series with the voltage supply and, therefore, the switching "off" load line becomes the limiting factor in load line stress for the transistor. Under such conditions, it is possible to tailor the switching "off" load line with a capacitive network and reduce load line stress on the transistor. This type of capacitor network together with a typical switching load line are shown in figures (3.2) and (3.3) respectively. The series diode provides a low impedance path for charging the capacitor and hence tailoring the switching "off" load line, while the resistor in parallel with the diode allows the capacitor to be discharged while preventing high peak currents flowing through the transistors while switching "on".

Because of the possible variation in the base to emitter saturation voltage,  $V_{BE}(\text{Sat})$  of each transistor, collector current levels of each individual transistor in a parallel combination can be quite different unless some precautions are taken to equalise the drive requirements. This is usually done by inserting a "sharing" resistance in series with each transistor emitter, resulting in smaller variation between collector current of individual transistors in a parallel combination as shown graphically in figure (3.4). The variation of collector current that is acceptable determines the value of the "sharing" resistance required. The "sharing" resistors can be reduced in value, and even eliminated, by pre-selecting  $V_{BE}(\text{Sat})$  to a close tolerance.

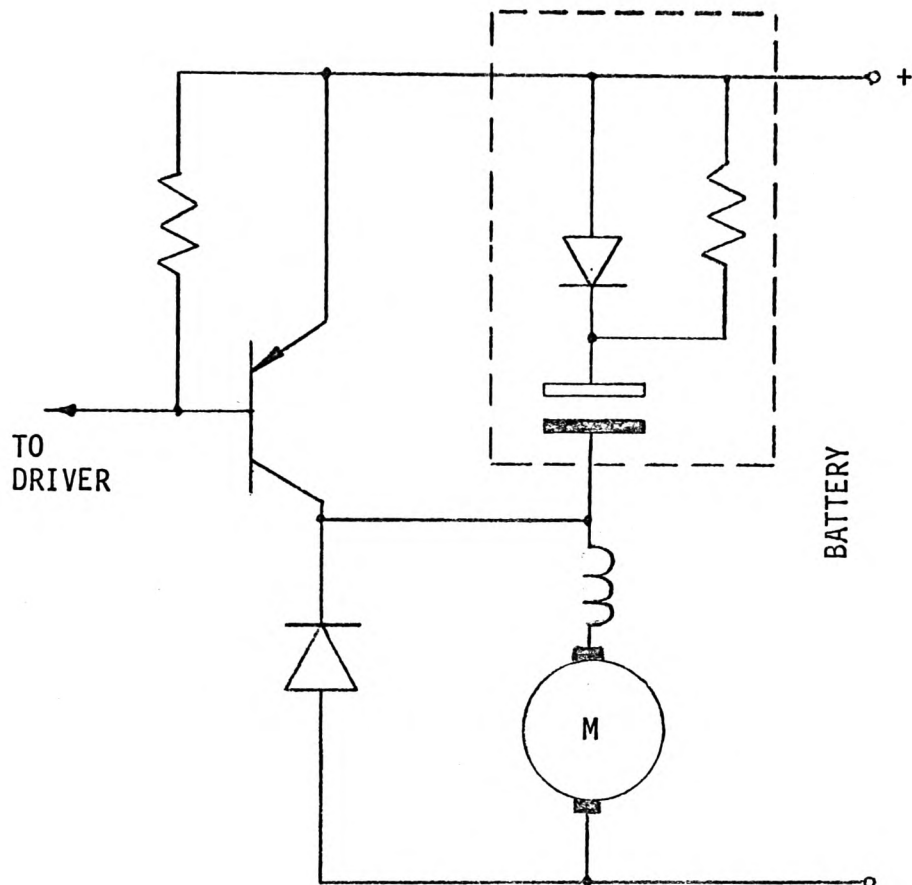


Figure 3.2 - CAPACITIVE LOAD LINE  
TAILORING NETWORK

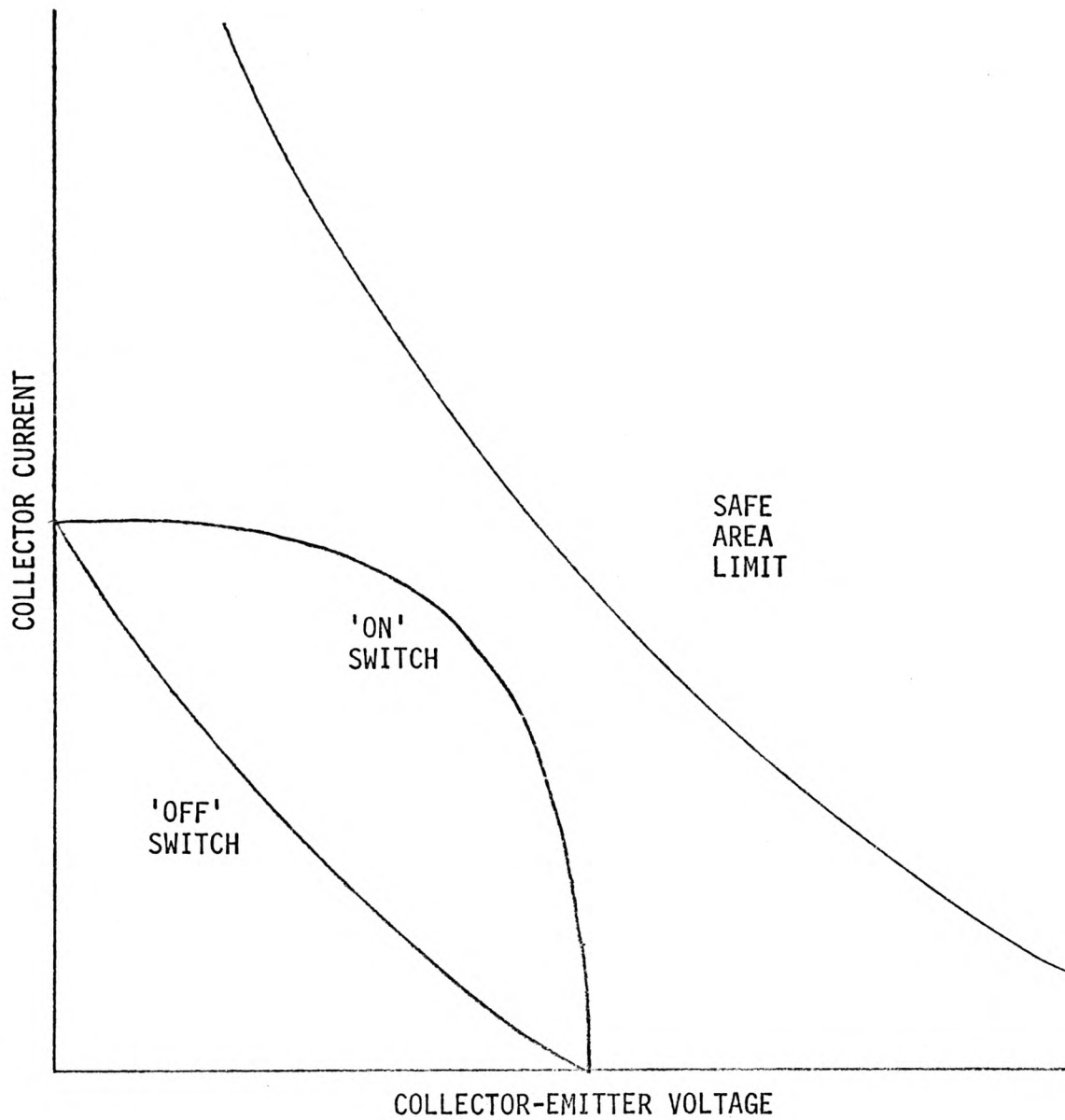


Figure 3.3 - INDUCTIVE LOAD LINE WITH  
CAPACITIVE SHAPING

Since most high current transistors have slow switching characteristics, variations in turn-on and turn-off times of such devices are made smaller than in faster switching transistors. Thus, mismatch in storage and switching times of individual transistors should pose no problems as long as low frequency devices are used.

### (3.2) Practical Design Considerations

When designing a commercially viable (by comparison with existing thyristor choppers) high current transistor d.c. chopper, a number of important points must be taken into consideration. These points include the operational requirements of the chopper and the various problems associated with the use of power transistors for switching highly inductive loads.

#### (3.2.1) Choice of Power Transistor

The choice of an appropriate transistor for use in power circuits must be made with a reference to the Safe Operating Area (SOA) curves of the device. The basis of any transistor SOA consists of electrical limitations under d.c. conditions; the SOA is enclosed by the  $V_{CE}$ ,  $I_C$ ,  $T_j(P_{tot})$ , and second breakdown limits. An example of a d.c. Safe operating Area curve is shown in figure (3.5).

In the case of the continuous d.c. collector current limit of the transistor,  $I_{C \text{ max.}}$  in figure (3.5), a maximum 'safe' operating current is chosen for the device. The value of this operating current is such that a safety margin exists between it and  $I_{C \text{ max.}}$ : the magnitude of this safety margin depends upon the conditions under which the device must operate. A safety margin of 20% of  $I_{C \text{ max.}}$  should be adequate, taking into account the fact that the circuit will be oil cooled and that a certain amount of inequality in current sharing between transistors, arranged in parallel, will exist even with the use of emitter 'sharing' resistors.

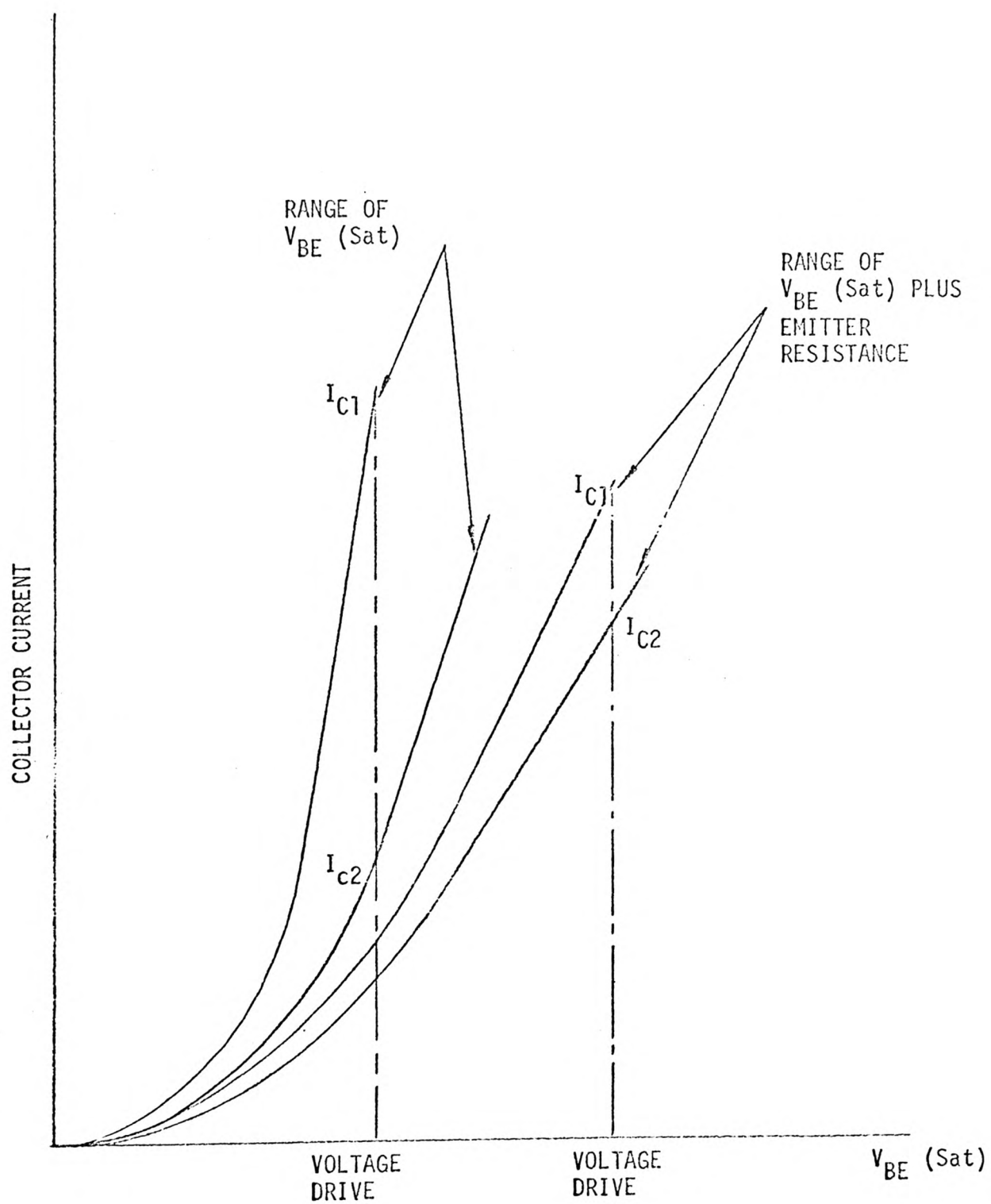


Figure 3.4 - Effects of emitter resistance on a parallel combination of transistors.

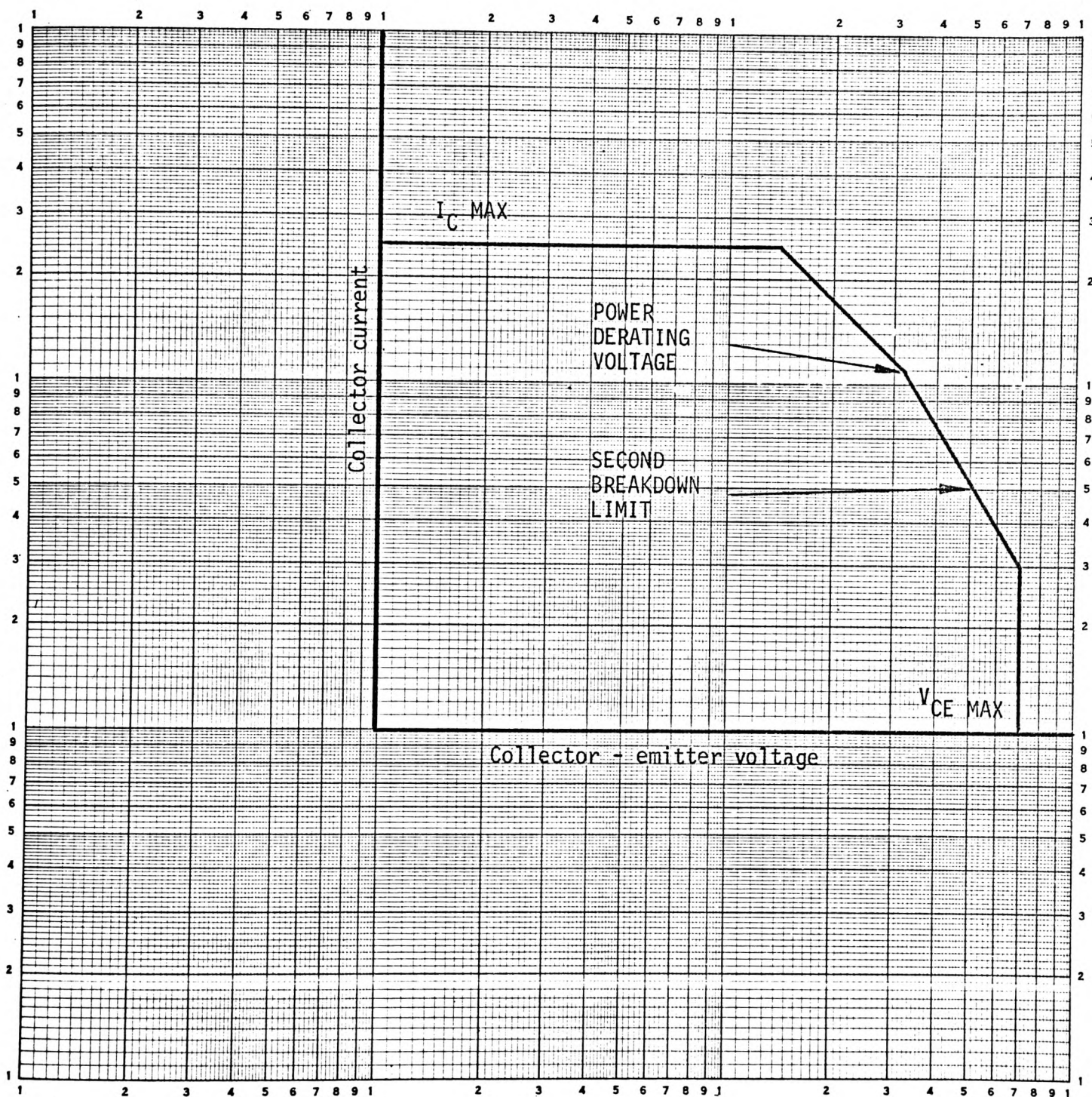


Figure 3.5 - Typical safe operating area for d.c. operation of a transistor

The collector-emitter voltage limit,  $V_{CE \text{ max.}}$  in figure (3.5), must not be exceeded even under pulse conditions. Since it is expected that voltage transients will occur in the chopper during operation in a vehicle, a wide safety margin must exist between  $V_{CE \text{ max.}}$  and the maximum intended chopper supply voltage. It is common practice to use a device with a  $V_{CEO}$  rating of at least twice the battery supply voltage.

In the case of the power dissipation limit,  $P_{tot \text{ max.}}$  in figure (3.5), the permissible steady state power dissipation in a transistor depends on its maximum permissible junction temperature and on the ability of the device to dissipate heat. The latter capability is, in itself, dependent on the thermal resistance from junction to mounting base and on the mounting base temperature. The equation for calculating the maximum permissible power dissipation is:

$$P_{tot \text{ max.}} = \frac{T_{j \text{ max.}} - T_{mb}}{R_{th(j - Mb)}}$$

It can be seen from the equation above that  $P_{tot \text{ max.}}$  can be increased by the reduction of mounting base temperature. The use of efficient heat sinks and forced cooling will ensure low mounting base temperature during sustained operation at high current levels.

The fourth SOA limit is due to secondary breakdown. No design of power circuits can be considered sufficiently reliable unless the circuit has been checked to ensure that the transistor will not undergo secondary breakdown. Secondary breakdown and the methods used to prevent its occurrence will be dealt with in more detail later in this section.



Since it was the intention to use cheap power transistors in the chopper, the d.c. current gain and transition frequency of the power transistor must be kept to a minimum, otherwise an unacceptable increase in cost of transistors will be incurred. The minimum forced d.c. current gain of the device depends upon the number of drive stages used in the chopper circuit, while a transition frequency of 1 - 2 MHz will be adequate to achieve the desired short period between the two switching states (and thus avoid excessive power dissipation in the device during switching). Adhering to the minimum acceptable values for d.c. current gain and transition frequency, the desired voltage and current ratings of the transistor become the two chief factors governing the cost of the device. At present, the price of high voltage transistors with comparable electrical characteristics vary little with variation in voltage ratings; hence, the remaining factor to be considered is the collector current rating of the device.

Transistors available on the market with collector current ratings of 10-35 amperes, have a minimum current to cost ratio of approximately 10A/\$1: this ratio falls rapidly as the current rating of the device increases above 35 amperes.

Little difference exists between the price of silicon(Si) and germanium(Ge) transistors with comparable characteristics, although germanium transistors are preferred due to their relatively low VCE(Sat), (0.2-0.75 volts compared with 1.0-2.0 volts for silicon transistors); this represents an important factor in minimising power losses in the chopper caused by dissipation in the transistors during saturation.



Taking into account the various points mentioned above, the transistor chosen for use in the drive and output stages of the chopper was the Motorola MP3731. This is a Ge, PNP transistor designed primarily for medium-power, horizontal deflection amplifier applications in television receivers. It is a 320 volt, 10 ampere, 56 watt device with an excellent safe operating area (SOA). The collector current rating of the MP3731 means that 48 transistors have to be used in parallel to handle the 480 ampere specified for the chopper.

### (3.2.2) Secondary Breakdown

One of the main restrictions in the operation of power transistors is the phenomenon known as 'second breakdown'. This is the name given to a transistor condition whereby the collector-emitter voltage abruptly switches from a high to a low voltage value with increased current. Figure (3.6) shows a sketch of the voltage-current characteristics of a transistor operating in the reverse breakdown mode. Note that at low collector currents, the voltage across the device exceeds the open base breakdown rating. The peak of the curve and the negative resistance region is termed the first breakdown, or the normal breakdown, and is the result of avalanche action in the transistor. However, as current in the avalanche mode is increased, a critical current,  $I_p$  in figure (3.6) is reached at which the voltage across the device drops to a very low level; this represents the 'second breakdown'.

Second breakdown in the transistors is triggered off when the temperature of some part of the semiconductor material achieves an extremely high value, causing the material to go

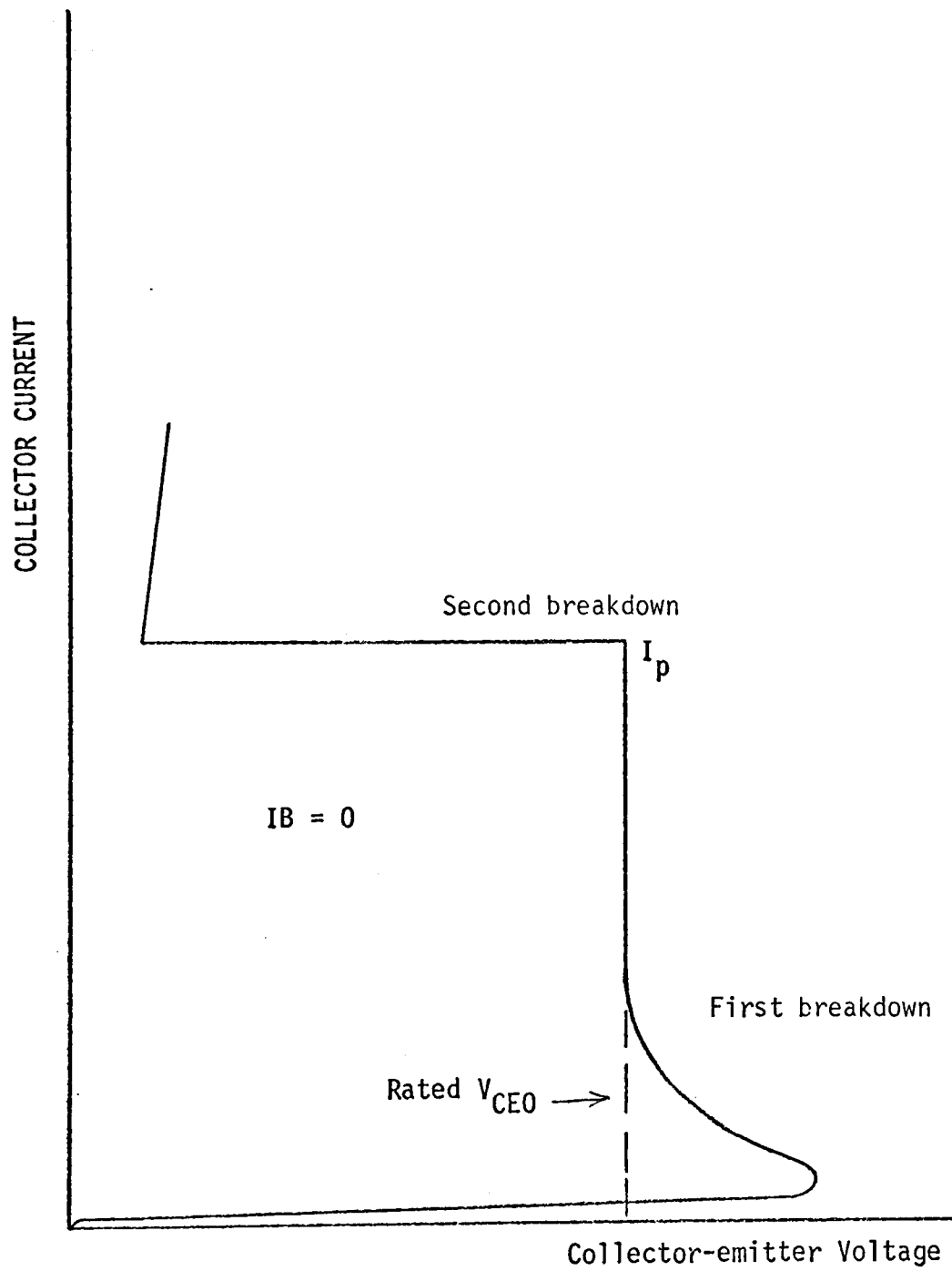


Figure 3.6 - Manifestation of second breakdown in a transistor.

into intrinsic conduction: that is, at sufficiently high temperatures, the semiconductor material undergoes a very rapid change in resistivity becoming essentially a conductor similar to a metal. While in second breakdown, if the current is removed or held to very low values, no damage is caused and the semiconductor will behave normally when it cools.

However, in most circuits, when the transistor enters second breakdown, a collector-emitter short results. The reason for this is that it is difficult to prevent the junction temperature from exceeding the melting point of the semiconductor material. If enough melting occurs in the region of high current path from collector to emitter, upon cooling, a low resistance path or short circuit from collector to emitter will exist.

Second breakdown is energy dependent; that is, it is a function of time, voltage, and current. Since transistors can be operated at an infinite number of time intervals, a family of SOA curves are given for pulse operation: each curve gives the SOA of the device for a specific pulse duration, as shown in figure (3.7). It can be noted from figure (3.7) that the SOA increases with shorter pulse durations, and under short pulse operation the power transistor is limited almost solely by second breakdown.

### (3.2.3) Loadline Tailoring Circuit

The maximum current level that any transistor can handle in any particular circuit is dependent upon the switching load line and the safe operating area of operation for the transistor. With a motor circuit as a load, the basic switching load line for a power transistor is as shown in figure (3.1).

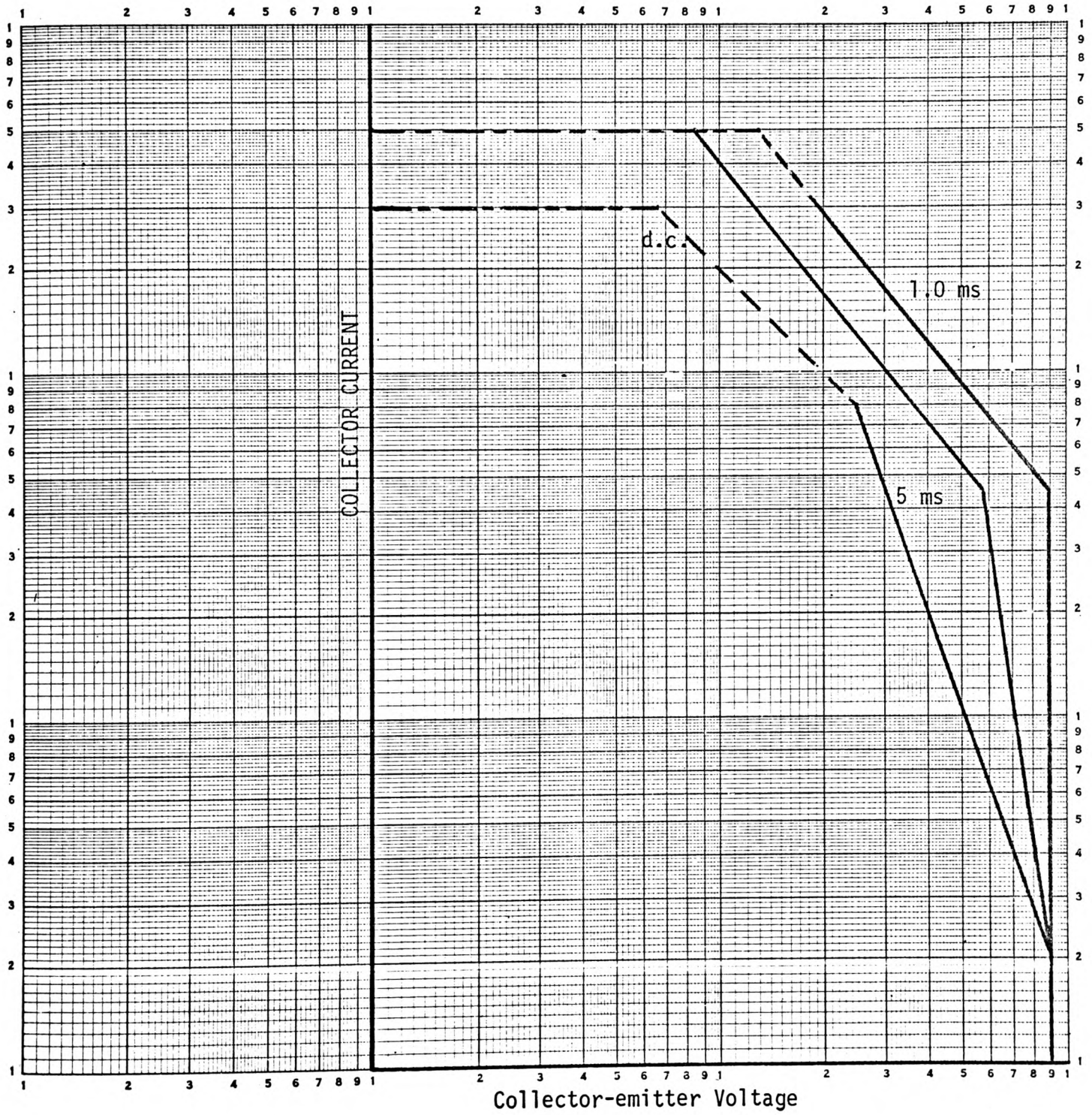


Figure 3.7 - Typical safe operating area curves of a transistor.

Under certain conditions, as explained previously in section (3.1). the switching 'on' load line may stress the transistor as much as the switching 'off' load line.

In many practical cases the current through the motor has substantially reduced before the transistor begins to switch 'on'. It is also impractical to assume that there is no impedance in series with the voltage supply and, therefore, the switching 'off' load line becomes the limiting factor in load line stress for the transistor. Under these conditions, it is possible to tailor the switching 'off' load line with a capacitive network to reduce load line stress on the transistor. This type of capacitor network is shown in figure (3.2), and a representative tailored switching load line is shown in figure (3.3).

The series diode, D in figure (3.2), provides a low impedance path for capacitive tailoring the switching 'off' load line; the capacitor value is chosen such that the rise of the collector voltage is slowed down to allow the transistor to cut-off properly before the collector voltage reaches  $V_{CEM}$ , otherwise excessive power dissipation may destroy the transistor. The resistor R, in parallel with the diode, allows the capacitor to be discharged through the transistor when switched 'on', the resistor value being high enough to limit the discharge current and avoid excessive current spike in the transistor.

#### (3.2.4) Freewheeling Diode

When a d.c. chopper is used to drive a motor, a large amount of energy is stored in the inductance during the 'on' period and, if allowed to do so, the motor current would continue to flow

through the transistors after the base currents have been interrupted, which would almost certainly destroy the transistor.

To prevent this action, a diode is connected in parallel with the motor in such a direction as to be reverse-biased when the battery voltage appears across the motor, when the transistors are turned 'off' this diode becomes forward-biased by the e.m.f. induced in the inductance, and the motor current continues to flow through the diode. The current then decreases exponentially until the chopper turns 'on' again, when the diode becomes again reverse-biased, and the cycle is repeated. Because of its mode of operation, a diode connected in this manner is known as a freewheeling diode.

By providing a circuit for the inductive motor current, the freewheeling diode prevents abrupt motor current changes which would otherwise cause high induced voltage across the switching device. The use of a fast-recovery freewheeling diode is essential; the use of an ordinary diode would cause peak transient voltages of 5 times the supply voltage to occur across the device, while the use of a fast-recovery rectifier would only produce a transient 20% increase on the supply voltage.

#### (3.2.5) Reduction of Switching Losses

Due to the slow switching characteristics of most high current transistors, switching power losses can be quite high. The switching losses are proportional to the peak load power, the switching rate (chopper frequency), and switching times of the transistor.

To minimise the switching losses, the chopper frequency and transistor switching times must be kept to a minimum. The chopper frequency was a matter of compromise between low power dissipation

at low frequency and smooth motor current wave form obtained at high frequency: the value decided upon was 100 Hz.

In the case of switching times, the overall turn-on time is reduced by the use of a large base current. An increased base drive results in higher prospective value of collector current, as shown in figure (3.8). In practical circuits the collector current cannot exceed  $\frac{V_{cc}}{R_c}$ . Any prospective current above this value, known as the overdrive current, must circulate through the internal base-collector diode of the transistor and does not appear in the collector circuit.

A method used for reducing turn-off time is to reverse bias the base-emitter junction of the transistor when the input voltage is zero. The function of the bias circuit, a resistance connecting base and emitter terminals, is to speed up the clearing of the base region from excess charges that tend to accumulate during the saturation period of the transistor.

#### (3.2.6) Saturated Darlington Drive

Power losses in the drive circuit of a transistor chopper can be quite high, and the saturated Darlington drive is used to reduce such losses as illustrated by the examples and figures (3.9) and (3.10).

The 36 volt, 200 ampere motor requirement determines a drive current of at least 10 amperes, assuming a forced d.c. current gain of 20. At this current level the emitter follower drive circuit would dissipate 350 watts ( $I^2R = 10^2 \times 3.5$ ). If the saturated Darlington circuit is used, the drive current contributes to the load current.

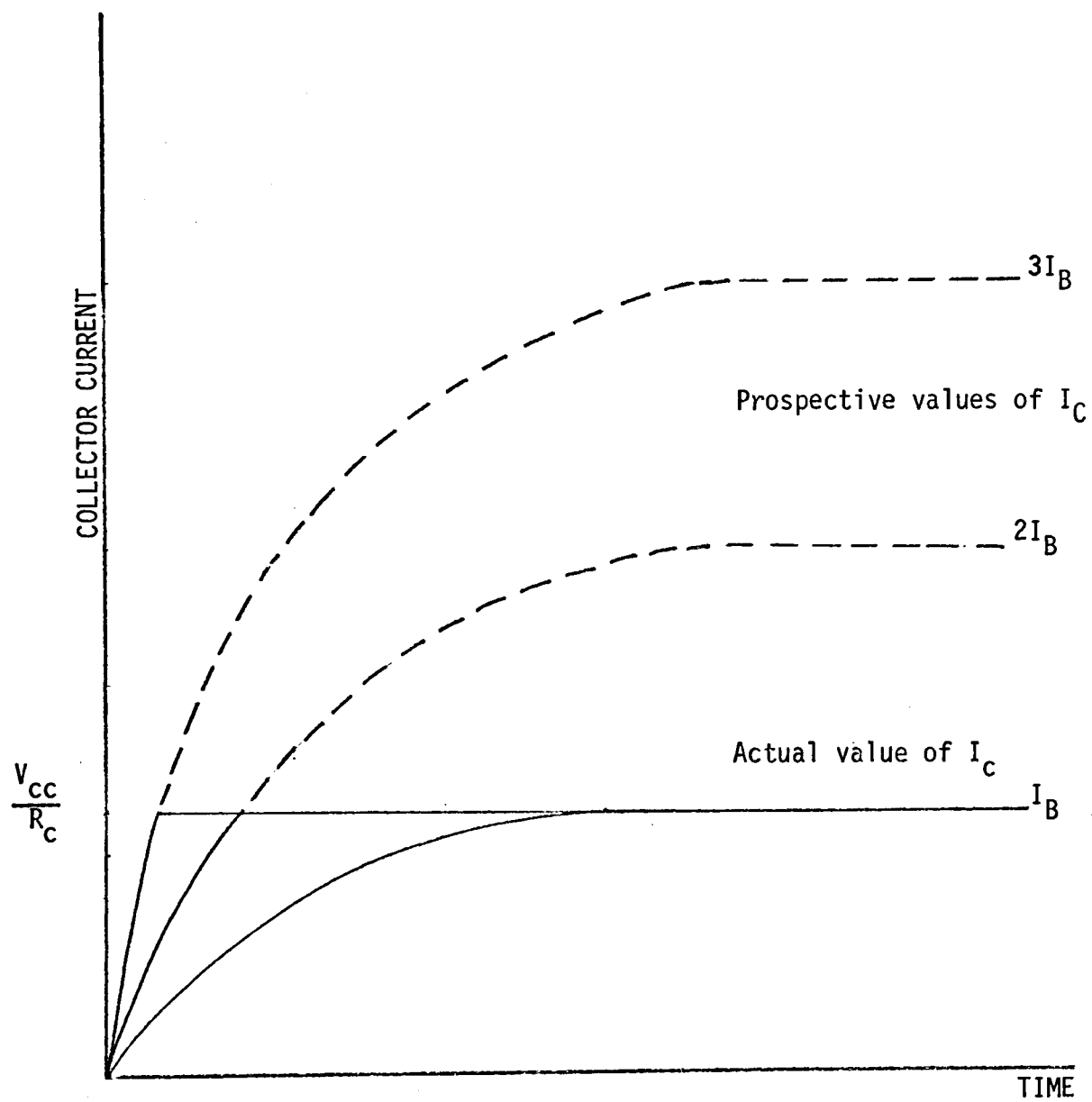


Figure 3.8 - Reduction of Turn-on time with overdrive.



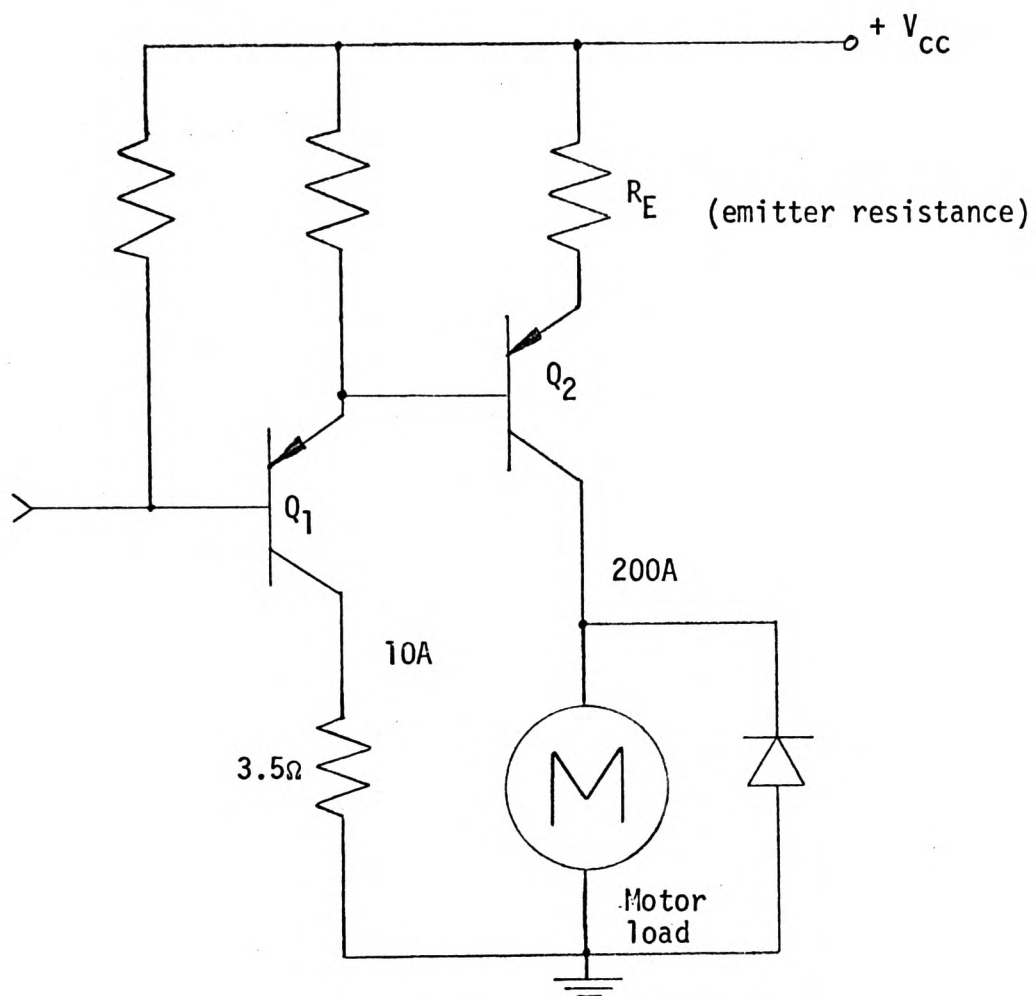


Figure 3.9 - Emitter follower drive.

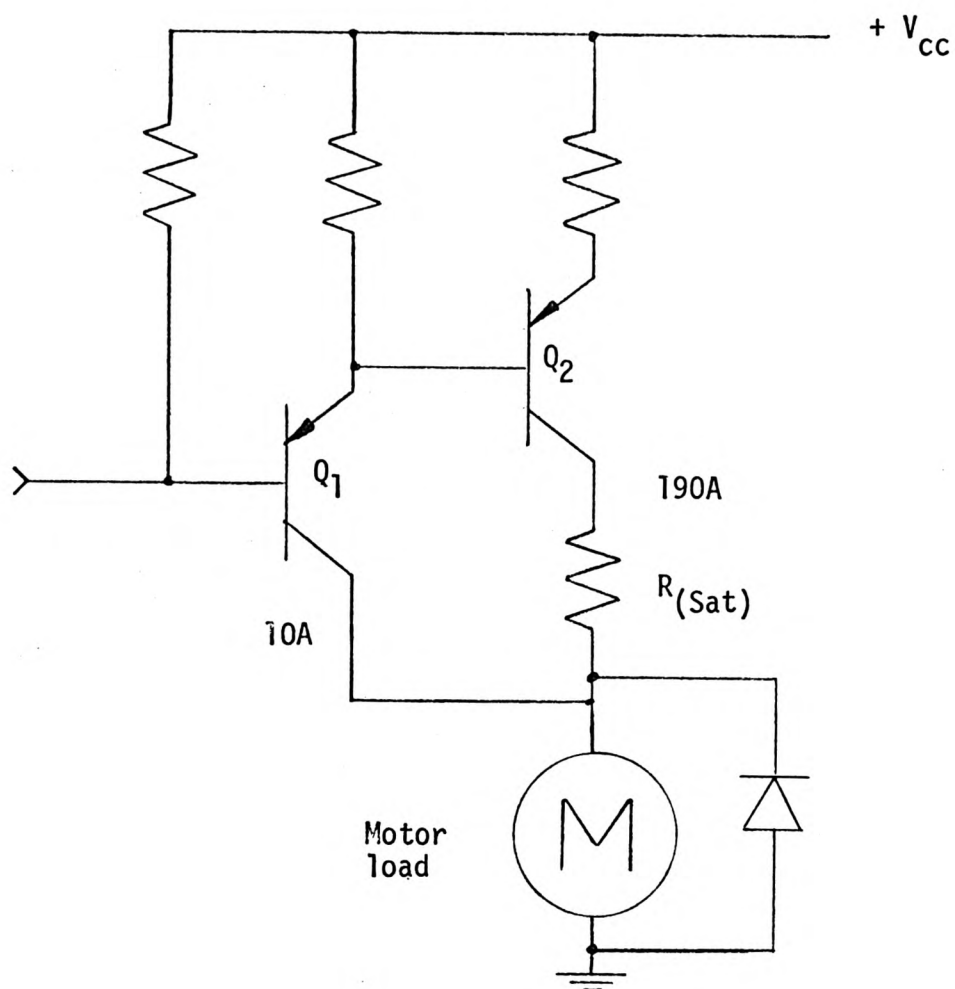


Figure 3.10 - Saturated Darlington Drive.

However, the 0.5 volt drop across the saturated resistor  $R(\text{sat})$  in series with the collector, assuming a  $V_{ce}(\text{sat})$  of 0.5 volt for transistor  $Q_1$ , can dissipate 95 watts ( $I \times V = 190 \times 0.5$ ) at the maximum current level of the motor. Of course, the power loss in this resistance will be in direct proportion to the peak motor current demand while the peak power dissipation in the emitter follower circuit will be constant, and independent of motor demand. The saturation resistor in the Darlington circuit is required to produce a low saturation voltage for the output transistors, and thus, reduce power dissipation. The value of this saturation resistor is determined from  $V_{BE}(\text{sat})$  and  $V_{CE}(\text{sat})$ , information obtained from the devices characteristics curves with the following relationship

$$R(\text{sat}) = \frac{V_{BE2}(\text{sat}) + V_{CE1}(\text{sat}) - V_{CE2}(\text{sat})}{I_L}$$

With reference to figure (3.10):-

$R(\text{sat})$  = Saturation resistor in series with the collector of  $Q_2$ .

$V_{BE2}(\text{sat})$  = Saturation emitter-base voltage of  $Q_2$ .

$V_{CE2}(\text{sat})$  = Saturation collector-emitter voltage of  $Q_2$ .

$V_{CE1}(\text{sat})$  = Saturation collector-emitter voltage of  $Q_1$ .

Because the drive transistor in the Darlington circuit will begin to turn'on' before the final transistor, it is apparent that unless the input to the driver is restricted, this transistor may switch a load line that is beyond it's safe area. A driver transistor must be selected with a safe operating area that extends to a collector current and battery voltage level that will not be reached by available inputs to the driver. As mentioned earlier, it is intended to use the MP 3731 power transistor in the drive as well as output stages of the chopper.

### (3.3) Practical Chopper Circuit

A schematic diagram of a transistor chopper circuit is shown in figure (3.11). The control oscillator produces a variable pulse width at constant repetition frequency (variable Mark-space-ratio rectangular signal) to drive the transistor chopper, and incorporates a current-limiting circuit to insure against exceeding the maximum current ratings of the output power transistors of the chopper. The chopper circuit contains a number of drive stages that provide adequate current amplification of the control oscillator output to ensure sufficient base current to saturate the output power transistors.

#### (3.3.1) The Control Oscillator

##### (3.3.1.1) Variable Pulse Width Oscillator

The oscillator is required to produce a variable M-S-R rectangular wave (variable pulse width) at a constant repetition frequency.

The repetition frequency decided upon was 100Hz; a compromise, as mentioned in the previous section, between the requirements of high frequency for smooth motor current and low frequency for low power losses in the chopper circuit. Although there is a wide choice of control oscillator circuits capable of meeting the requirements of this work, a design employing integrated circuit operational amplifiers was preferred because of its simplicity and reliability. The complete variable pulse width oscillator circuit is shown in figure (3.12).

The first stage of the oscillator is a constant frequency square wave generator, employing a 741 operational amplifier. A fraction  $\beta$  of the output (defined in appendix 1) is fed back to the non-inverting input terminal.

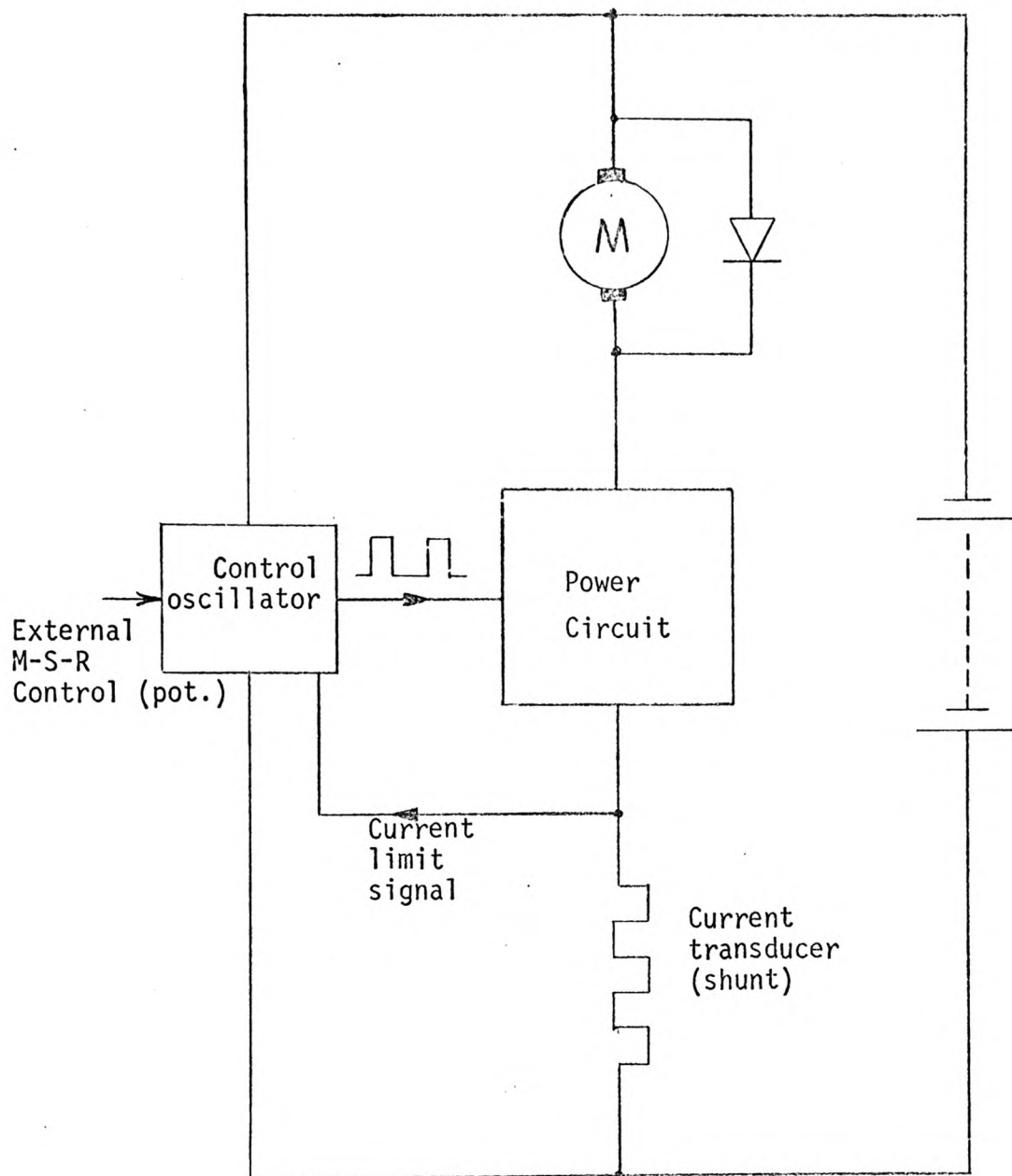


Figure 3.11 - Schematic diagram of a transistor d.c. chopper.

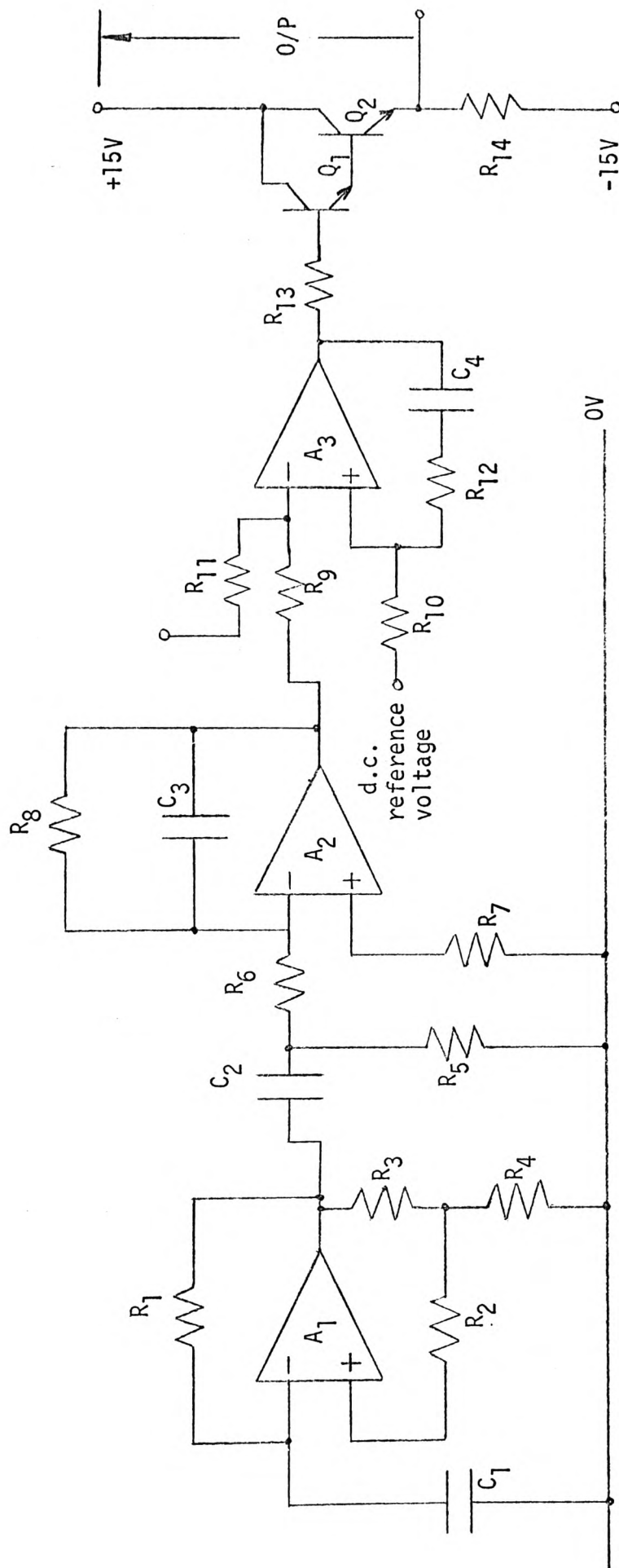


Figure 3.12 - Variable pulse width oscillator.

Component list for variable pulse width oscillator in figure 3.12

Resistors

$R_1$ :	330 k $\Omega$
$R_2$ :	10 k $\Omega$
$R_3, R_8$ :	1M $\Omega$
$R_4, R_{12}$ :	100 k $\Omega$
$R_5, R_9, R_{10}, R_{11}$ :	1 k $\Omega$
$R_6, R_7$ :	27 k $\Omega$
$R_{13}$ :	100 $\Omega$
$R_{14}$ :	5 k $\Omega$

Capacitors

$C_1, C_3$ :	0.1 $\mu$ F
$C_2$ :	10 $\mu$ F
$C_4$ :	0.001 $\mu$ F

Transistors and operational amplifiers

$Q_1$ :	BC 107
$Q_2$ :	BFY 51
$A_1, A_2$ :	741 I.C. operational amplifier
$A_3$ :	709 I.C. operational amplifier

The differential input voltage,  $V_i$ , is therefore

$$V_i = v_c - \beta V_o$$

Where  $V_c$  is the voltage across the capacitor  $C_1$ . The circuit will operate as a comparator with the output approximately equal to the negative supply voltage ( $-V_S$ ) of the operational amplifier when the differential input is positive, and approximately equal to the positive supply ( $+V_S$ ) when  $V_i$  is negative. The capacitor  $C_1$  charges exponentially through the integrating  $R_1C_1$  combination: when  $V_o$  is at  $-V_S$ , the capacitor charges towards  $-V_S$  and  $V_i$  becomes negative; at this instant,  $V_o$  changes to  $+V_S$  and the capacitor charges positively towards this voltage and  $V_i$  becomes positive with the consequent change in polarity of the output, and the cycle is repeated. The frequency of oscillation of the circuit depends upon the values of  $R_1, C_1, R_3$  and  $R_4$ : a derivation of the expression for frequency of oscillation is given in appendix 1. The frequency stability of the circuit depends mainly on the quality of the capacitor used for  $C_1$ , while waveform symmetry depends upon the matching of the negative and positive supply voltages to the operational amplifier.

The output from the square wave generator is fed into an integrator via the capacitor  $C_2$ , used to eliminate any drift in the output of the square wave generator. The integrator uses a 741 operational amplifier with  $C_3$  and  $R_6$  as the integrating combination; the resistors  $R_6$  and  $R_7$  are made equal to minimise the error due to the bias current. The integrator output was found to be too high, causing the overload of the 709 operational amplifier used in the subsequent modified comparator stage.



The output signal was reduced to a level within the specified maximum input limit for the 709 by increasing the time constant of the integrator, as explained in appendix 1. The integrator time constant ( $\tau = C_3 R_6$ ) is increased by increasing the value of capacitor  $C_3$ .

The triangular output waveform of the integrator is compared with a variable reference d.c. level to produce the required variable pulse width, as shown in figure (3.13): the variable d.c. reference is produced by a potentiometer connected across the chopper supply, with the high and low potentiometer arms connected to the supply through 1 k ohm resistors to avoid the appearance of damagingly high voltages at the input of the comparator when the variable arm is moved to either end of the potentiometer track.

The output signal of the initial comparator circuit, using a 741 operational amplifier, had relatively slow edges (15  $\mu$ sec front edge, 25  $\mu$  sec back edge) which, when applied to the chopper circuit caused repeated failure of output stage power transistors due to excessive power dissipation during switching. The modified comparator circuit eliminated this problem: a regenerative comparator (with positive feedback) employing a faster slew rate 709 comparator was used; the stability and switching periods of the output signal depended upon the value of frequency compensating capacitors of the 709 and the component values of the positive feedback loop, these values were highly critical and were obtained by trial and error. The output signal from the modified comparator circuit was highly stable and had the desired fast edges (1  $\mu$  sec front edge, 6  $\mu$  sec back edge).

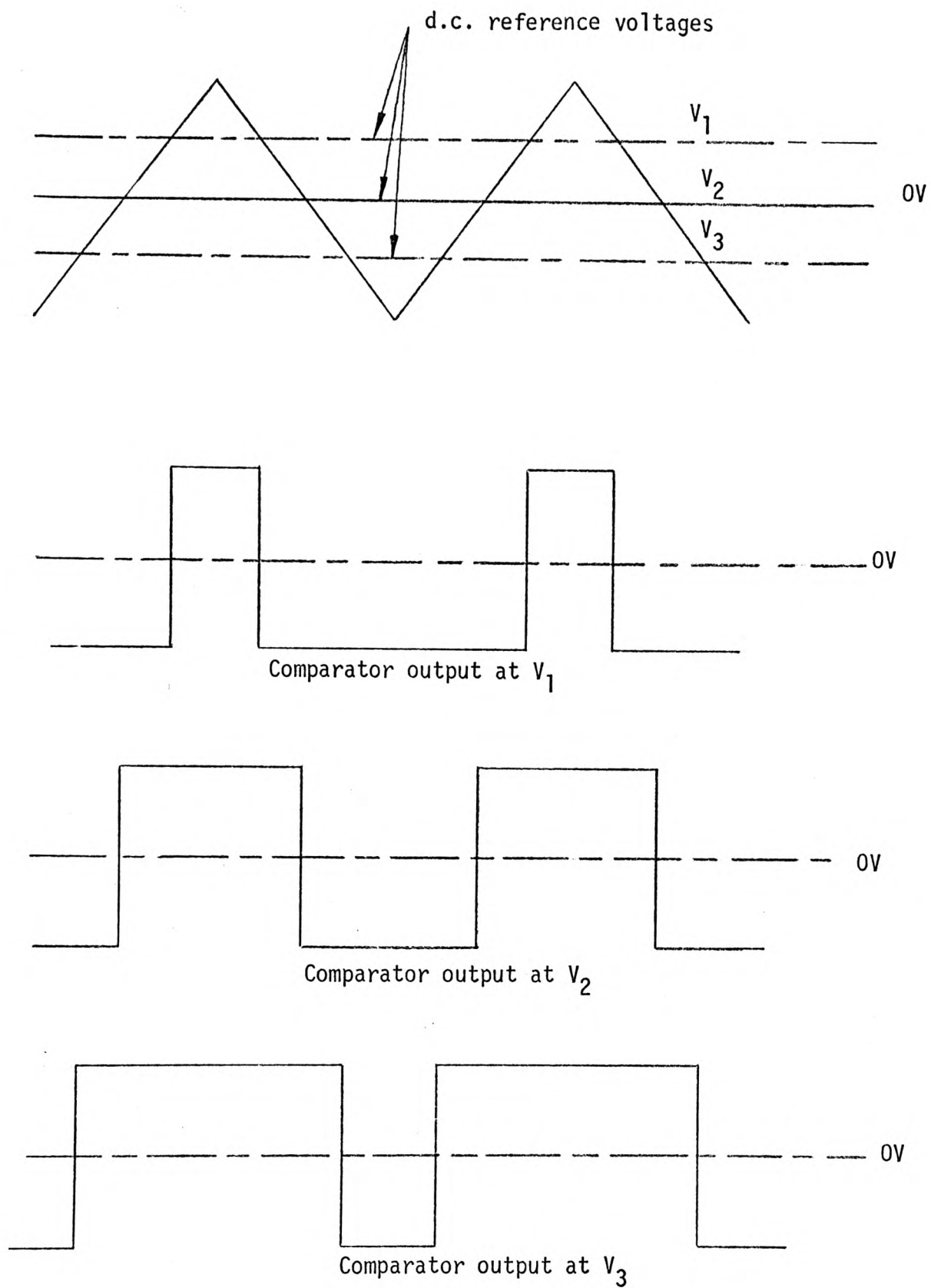


Figure 3.13 - Variation of comparator output waveform with d.c. reference voltage.

Having produced a 100 Hz rectangular wave with a M-S-R variable from zero to infinity, a drive circuit was essential to produce enough current from the control oscillator to enable the saturation of the input transistor of the chopper drive circuits. An emitter follower drive was initially used (using a BFY51 transistor), but the current signal from the comparator was found to be insufficient to saturate the driver. An important point since the control oscillator load, the chopper power circuit is connected across the driver and chopper 'switch-off' can only be achieved when the driver is fully saturated. Saturation of the driver was achieved by the use of a Darlington emitter-follower drive circuit: a high gain transistor (BC107) is used in the first stage to enable the output transistor (BFY51) to fully saturate. With this modification, the control oscillator output voltage of 5 volts peak-peak and current signal of 50 mA into a load of 100 ohms (simulating the input circuit of the chopper) should be sufficient to saturate the input power transistor of the chopper drive circuits.

#### (3.3.1.2) Current Limiting Circuit

Because of the high motor current levels that are encountered when operating under stall or starting conditions, a current limiting circuit becomes desirable. The current limiter would sense the total current through the chopper output transistors and when a preset current level is reached, the drive circuitry is turned 'off'. The current can be sensed across an individual transistor emitter sharing resistor in a well-matched parallel combination, or, across a shunt placed between the chopper's output stage common emitter rail and the appropriate battery supply

terminal. The limiting should be as instantaneous as possible and be repeatable at the preset limit under all conditions of operation.

The current limiting circuit of figure (3.14) is adequate for this application. It consists of a comparator whose output changes polarity as the voltage drops across the current sensing resistor exceeds the present current-limit reference d.c. level. The comparator output is differentiated and the pulses produced are used to trigger a monostable multivibrator. The monostable will produce a pulse of sufficient duration to allow the current level in the chopper to fall to a safe value before the drive circuitry, the control oscillator in this case, comes back into normal operation. A more detailed explanation of the operation of the current limiting circuit is given in appendix 1.

#### (3.3.2) Transistor Chopper Power Circuit

The chopper power circuit, shown in figure (3.15). is basically two saturated Darlington stages in cascade. The first Darlington stage consists of transistors  $Q_1$  and  $Q_2$ , the saturation resistor  $R_4$ , and resistor  $R_3$  (which determines the value of the collector saturation current of  $Q_2$ ). The resistors  $R_2$  and  $R_5$  are used to reverse bias the base-emitter junction of the transistors  $Q_1$  and  $Q_2$  respectively: the use of reverse bias reduces turn-off time of the transistors, and hence power dissipation in the stage.

The second Darlington stage, made up of four saturated Darlington circuits connected in parallel, consist of the four transistors  $Q_3$ - $Q_6$ , each driving a section containing a parallel combination of output transistors. The four saturation resistors of this stage (one for each output section),  $R_5$  in figure (3.15), are identical.

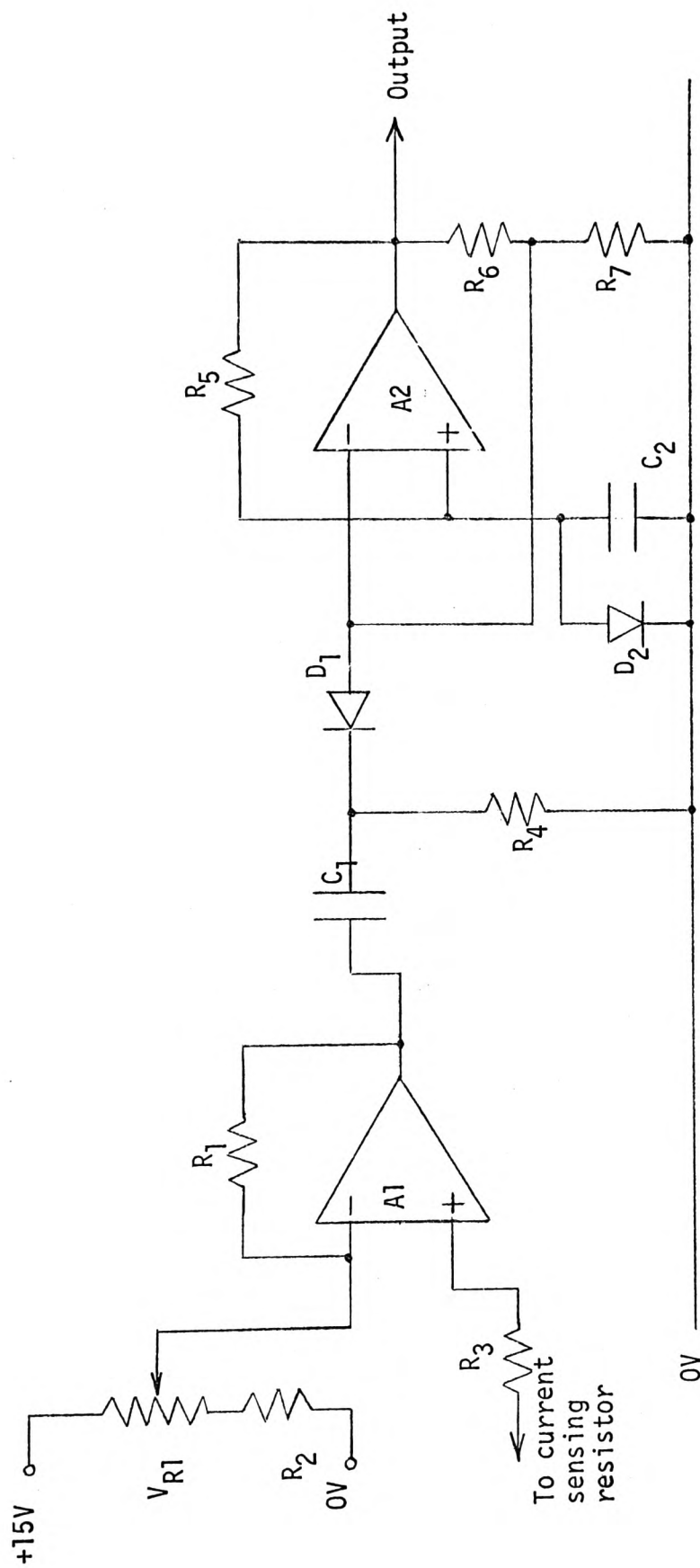


Figure 3.14 - Current limiting circuit.

Component List for Current Limiting Circuit in figure 3.14

Resistors

$R_1, R_5, R_6:$	1 M $\Omega$
$R_2, R_4:$	10k $\Omega$
$R_3:$	1k $\Omega$
$R_7:$	100k $\Omega$
Variable resistor VR1:	2.2k $\Omega$

Capacitors

$C_1$	0.001 $\mu$ F
$C_2$	0.15 $\mu$ F

Diodes

$D_1, D_2:$	BAX 13
-------------	--------

Operational amplifiers

$A_1, A_2:$	741 Integrated circuit
-------------	------------------------

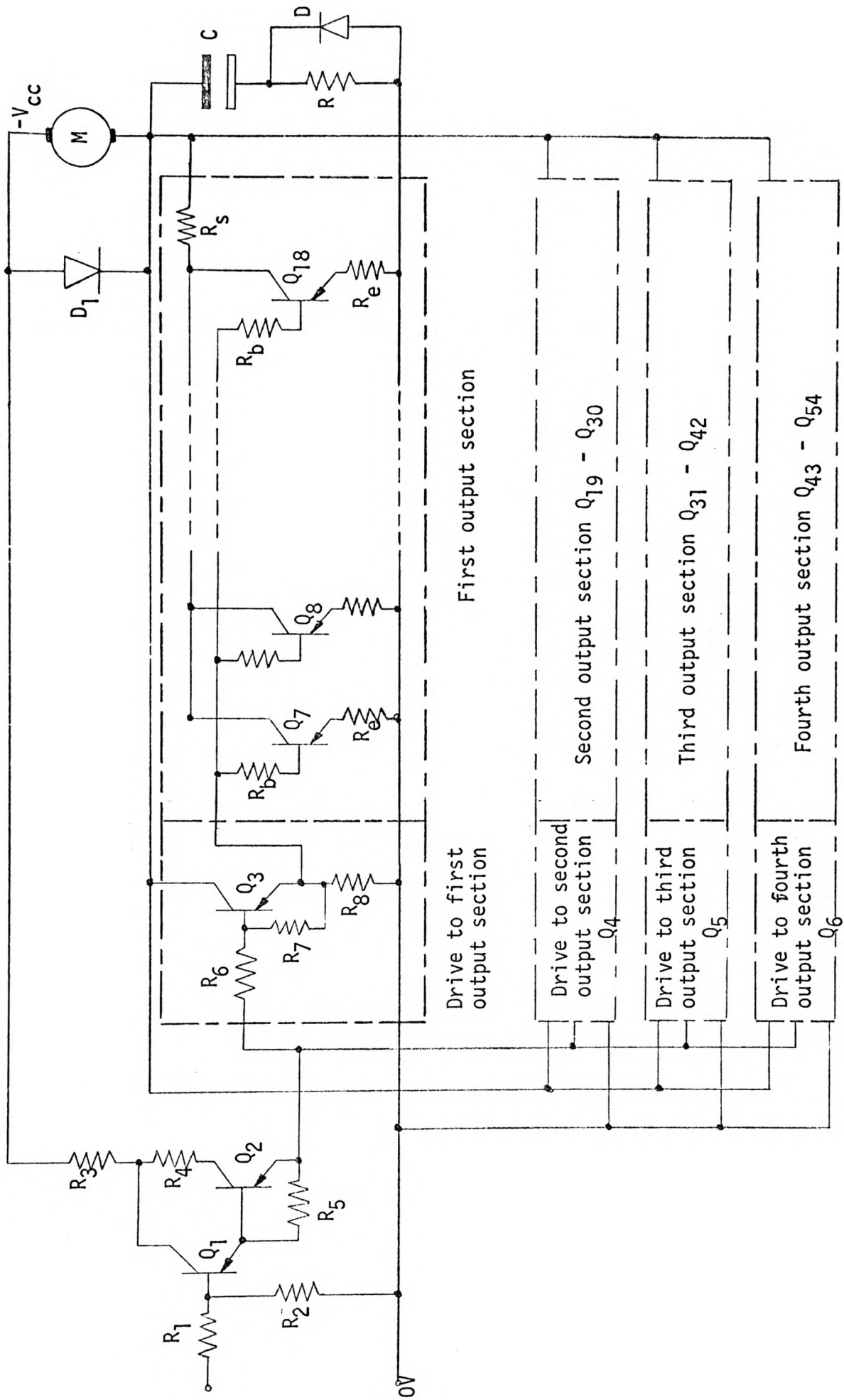


Figure 3.15 - Transistor chopper power circuit.

Component list for chopper circuit in figure 3.15

Resistors

$R_1, R_2, R_5, R_7, R_8:$	100 $\Omega$
$R_3:$	8 $\Omega$
$R_4:$	1 $\Omega$
$R_6, R_b:$	1 $\Omega$
$R_e:$	0.01 $\Omega$
$R_s:$	0.005 $\Omega$
$R:$	1 $\Omega$

Capacitor

C	1000 $\mu$ F, 100V, Electrolytic
---	----------------------------------

Semiconductors

$Q_1, Q_2, Q_3, Q_4, Q_5, Q_6:$	MP3731
$Q_7$ to $Q_{54}:$	MP3731
D:	BYY15 (Mullard)
$D_1:$	A396 (G.E.)



The value of the emitter-sharing resistors,  $R_e$  in figure (3.15), was a compromise between a high value for good current sharing between output transistors and a low value for low power dissipation: a value of 0.01 ohm was used.

The MP3731 Ge power transistor was initially used in all stages of the chopper circuit. Since this type of power transistor has a minimum fixed d.c. current gain of 10, the total base drive current required to fully saturate the output transistors at full load (400 A) is 40 amperes; this current is supplied by the four drive transistors  $Q_3$ - $Q_6$ . The maximum total base drive to  $Q_3$ - $Q_6$  is 4 amperes, if the pre-drive saturated Darlington stage ( $Q_1$  and  $Q_2$ ) has a total combined current gain of 100, then the maximum current required from the control oscillator to fully saturate the output transistors at full load (400 A) is 40 mA: a value within the capability of the control oscillator circuit.

The original rectifier used as a free-wheeling diode had a slow recovery time. During initial inductive load tests, failure of some output transistors was caused by the appearance of a high voltage transient across the output devices during 'switch off': a sketch of typical wave forms containing such transients are given in figure (A2.3). The slow diode was replaced by a fast recovery rectifier, G.E. type A396, having a reverse recovery time of  $2.5\mu$  sec at a mean forward current of 400 amperes. This eliminated the problem of voltage transients completely as shown by the plates in figure (A2.1).

In the case of the capacitive load line tailoring circuit, the resistance  $R$  was chosen to be 1 ohm: a high enough value to prevent the occurrence of capacitor discharge current spikes in

the output transistors. The value of capacitor C was initially chosen to be 500  $\mu\text{F}$ , but had to be raised to 1000  $\mu\text{F}$  to obtain reliable chopper operation at high currents.

All chopper circuit components were cooled by immersion in transformer oil; all power transistors and the free-wheeling diode were mounted on aluminium heat sinks to ensure maximum cooling efficiency. The chopper chassis was designed to be compact and accessible at the same time.

#### (3.3.2.1) Practical tests on circuit employing the MP3731

The chopper was connected to a 50 volt battery supply and operated with a resistive load consisting of a carbon pile regulator. Failure of chopper output transistors did occur at peak battery currents of around 100 amperes; these failures were due to the slow 'turn on' and 'turn off' of the control oscillator output signal, causing excessive power dissipation in the output transistors during switching. Satisfactory chopper operation at peak battery currents of up to 200 amperes was obtained after the reduction of switching times of the control oscillator output signal. The non-saturation of the original emitter-follower drive transistor used in the control oscillator circuit caused a current to flow through the load at zero M-S-R; this effect was eliminated by a modification made to the control oscillator drive circuit (through the use of a Darlington stage), and proper chopper 'switch off' was achieved.

Current sharing between the output stage transistors was examined by the connection of a single output section at a time (12 transistors in parallel): no device failure occurred at peak battery currents of up to 100 amperes.

Two sections at a time were connected in the output stage of the chopper and operated satisfactorily at a peak battery current of 200 A, indicating good current sharing between the four sections of the chopper output stage.

With a series d.c. motor connected as a load, high voltage transients appeared across the output devices and the motor caused by the slow recovery time of the original freewheeling diode. These transients were completely removed by the use of the fast recovery freewheeling diode.

Chopper operation at high motor currents resulted in output device failure due to the initially low value of load line tailoring circuit capacitor C (500  $\mu$ F): Satisfactory chopper operation was achieved at peak battery currents of more than 250 amperes when the value of capacitor C was increased to 1000  $\mu$ F.

#### (3.3.3) Modified Chopper Power Circuit

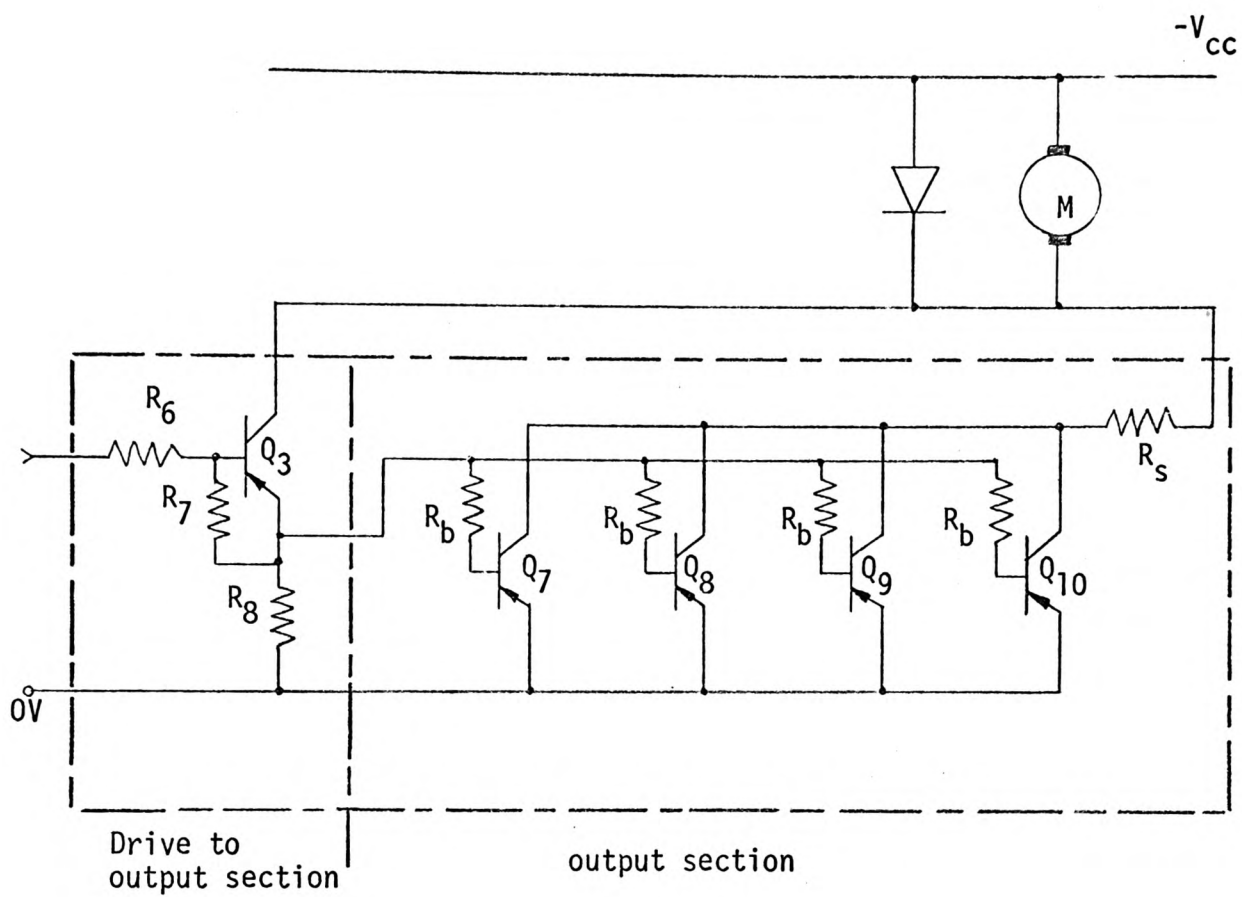
The high number of transistor failures encountered during tests carried out on the original chopper circuit employing the MP3731 power transistor, had resulted in the operation of the chopper with less than the required 48 transistors in the output stage. Attempts to obtain further stocks were unsuccessful due to the 'temporary' phasing out of production of most high voltage Germanium power transistors. It was therefore decided to replace the MP3731 in the chopper output stage by a silicon device of comparable characteristics and price. It was also decided to carry out efficiency tests on the original chopper circuit to enable a comparison with efficiency test results obtained from the modified circuit employing silicon transistors.

The silicon device chosen was the Motorola MJ4502; it has a maximum collector current rating of 30 amperes at a cost of £3 per unit. Although comparable to the MP3731 in cost and has a higher d.c. current gain and transition frequency, it has a comparatively low collector-emitter voltage of 100 volts. Even with such a relatively low voltage rating, it was felt that the MJ4502 would operate reliably from supplies of up to 50 volts. It is the intention to test the modified chopper circuit at a supply voltage of 72 volts.

The high d.c. current gain of the MJ4502 make changes in the drive circuits of the chopper unnecessary. The d.c. current gain and the  $V_{BE}(sat)$  of the 16 MJ4502's to be used in the chopper output stage (4 in each section) were compared and found to be very close, unlike the result of similar tests carried out on a selection of Ge MP3731 transistors. The closeness in the value of current gain and  $V_{BE}(sat)$  for individual silicon devices rendered the use of emitter sharing resistors unnecessary. An output stage of the modified chopper circuit is shown in figure (3.16). The absence of current sharing resistors makes it necessary to use a high current shunt between the common emitter rail of the output stage and the reference rail of the chopper (positive rail) to obtain a transistor current sensing signal for the current limiting circuit: this shunt is not shown in figure (3.16). Figure (3.17) shows the chassis of the modified chopper.

(3.3.3.1) Practical Tests on Modified Chopper Circuit

Even though the emitter sharing resistors were omitted from the circuit, current sharing between the silicon output power transistors was found to be excellent; each of the four sections of the chopper output stage was operated at a peak battery current of 105 amperes.



Q<sub>3</sub>:  
MP3731

Q<sub>7</sub>, Q<sub>8</sub>, Q<sub>9</sub>, Q<sub>10</sub>: MJ4502

Figure 3.16 - A single modified chopper output stage.

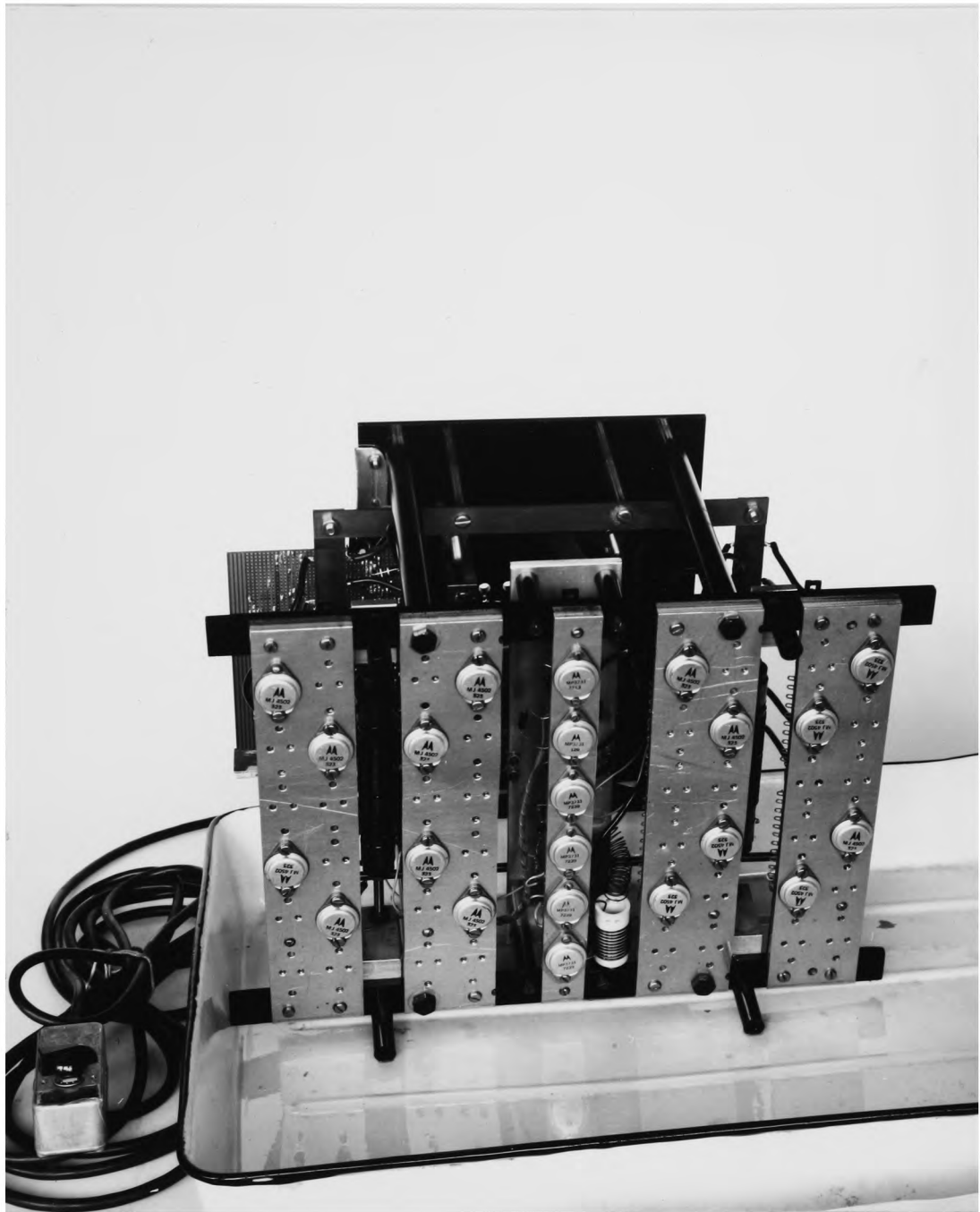


Figure 3.17 - Chassis of the modified transistor chopper.

Satisfactory chopper operation was obtained with a motor load at peak battery currents of up to 250 amperes from a battery supply of 50 volts. Operation at higher currents for appreciable periods was restricted by the overheating of the motor, although peak battery currents of over 300 amperes were reached under motor stall conditions.

Typical voltage and current wave forms in the transistor d.c. chopper are shown in figures (A2.1) and (A2.2) respectively. Detailed explanation of the shape of the waveforms is given in appendix 3.

The efficiency of the chopper was calculated as explained in appendix 4. Figure (3.18) shows the variation of chopper efficiency with M-S-R, while the curves in figure (3.19) show the variation of chopper power loss with mean motor current at infinite M-S-R. The curves given in figure (3.20) clearly show that chopper efficiency increases with motor current; in addition, the two curves in figure (3.20) allow a comparison between the efficiency of the modified chopper using silicon output transistors. At low motor currents, the  $V_{CE}(\text{sat})$  of the silicon transistors is comparable with that of the Germanium transistors; but the extra power dissipated in the emitter sharing resistors of the original chopper result in the original circuit having a relatively low efficiency at low motor currents. At higher motor currents, and hence higher transistor currents, the  $V_{CE}(\text{sat})$  of the silicon devices increases sharply (towards 2 volts) causing a large increase in the power dissipated in the output transistors, hence the relatively low efficiency of the modified chopper circuit at high motor currents.



Satisfactory operation of the modified chopper was achieved with a battery supply of 72 volts at peak battery currents of up to 250 amperes. Figure (3.21) shows the variation of chopper efficiency with battery supply voltage: at infinite M-S-R, the efficiency of the chopper remains constant at all supply voltages; whilst at unity M-S-R, the efficiency of the chopper increases linearly with supply voltage.



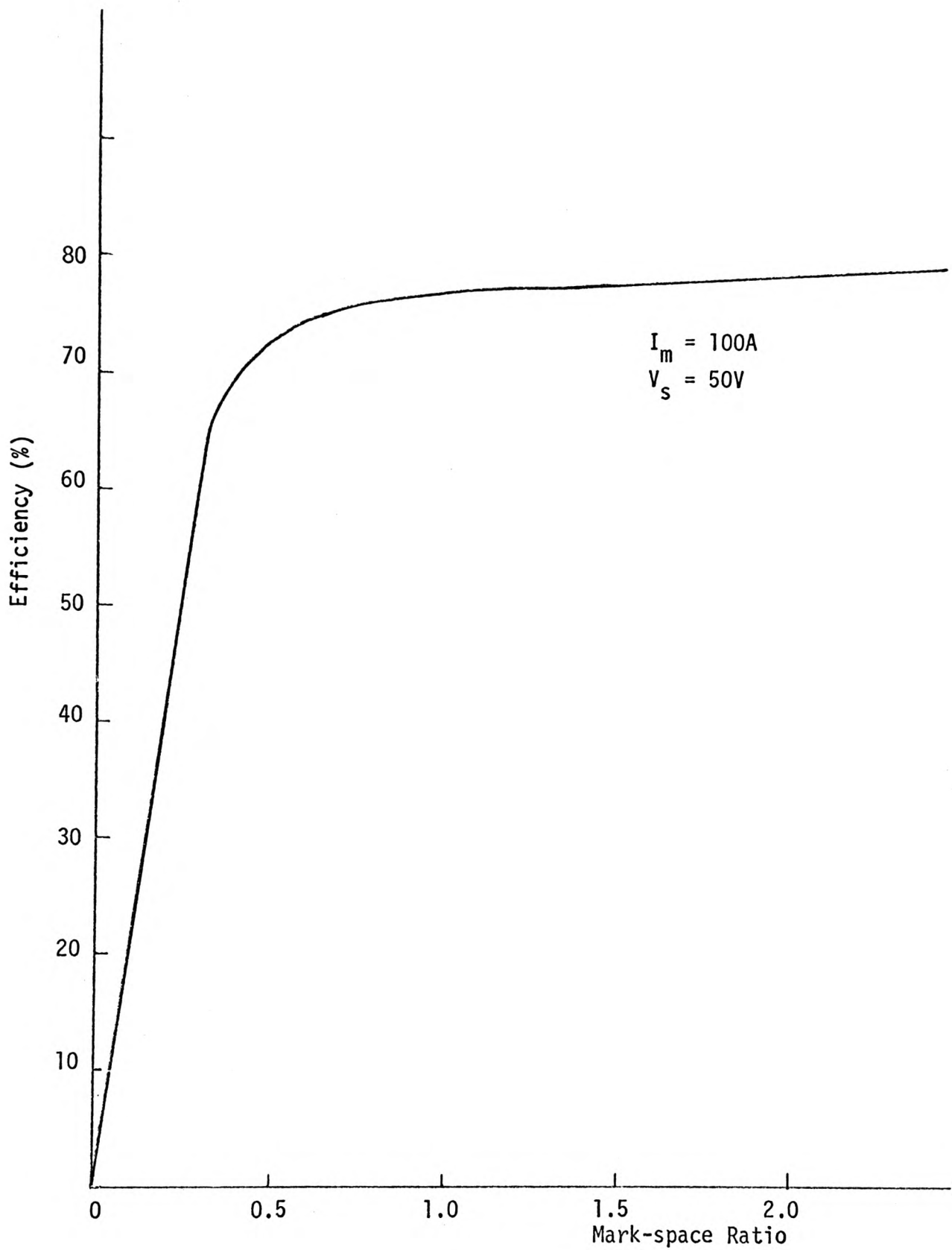


Figure 3.18 - Variation of chopper efficiency with M-S-R.

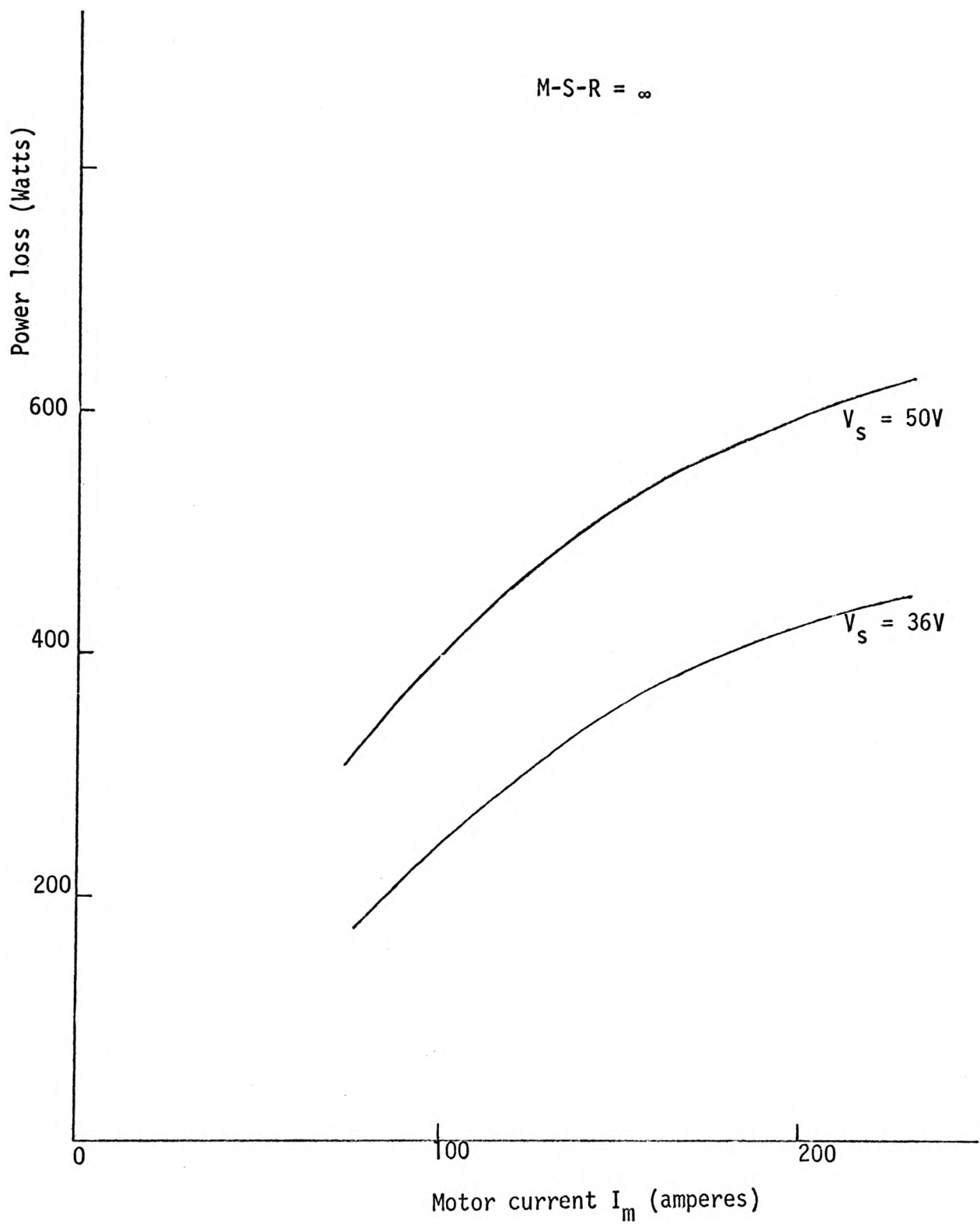


Figure 3.19 - Variation of chopper losses with mean motor current.

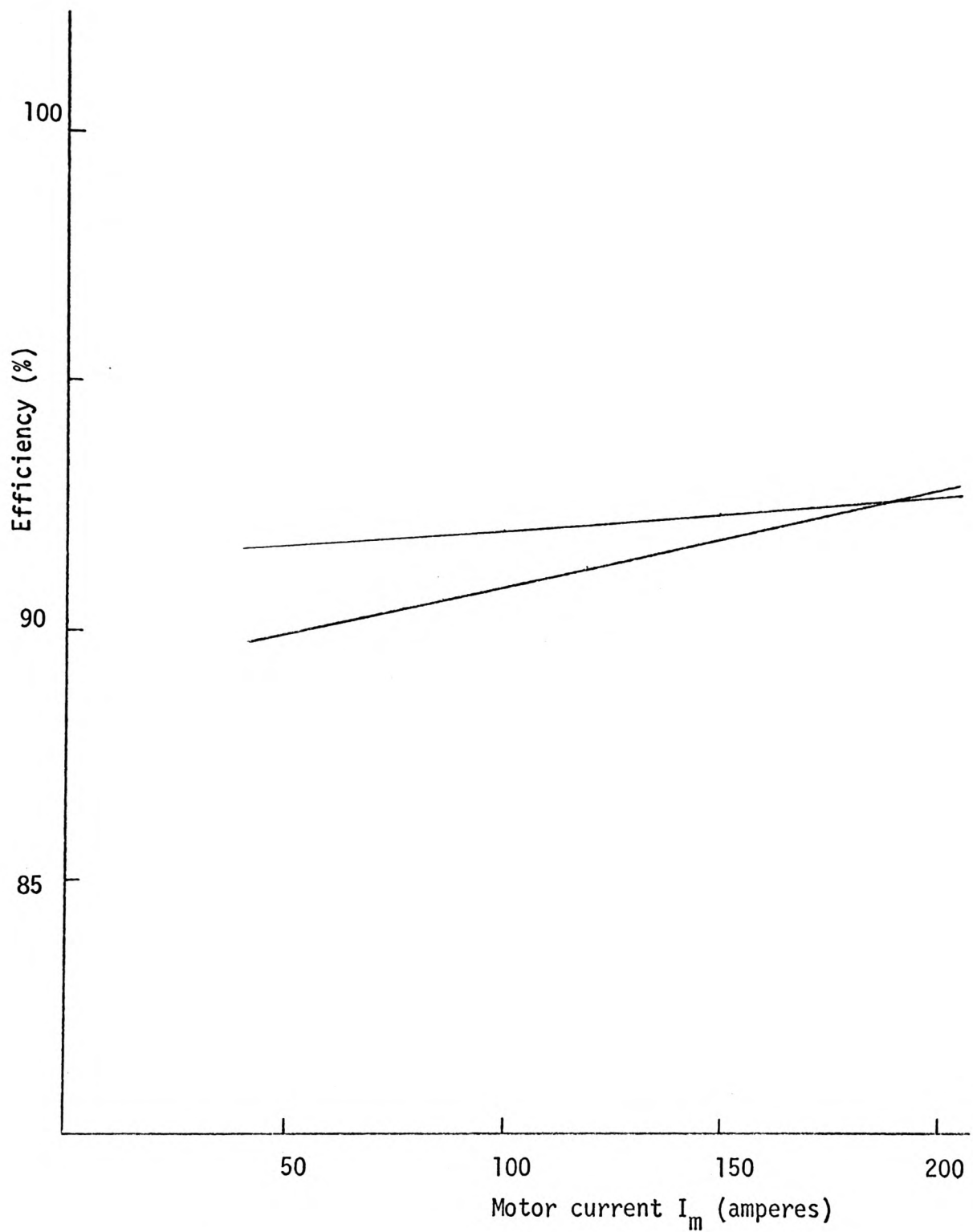


Figure 3.20 - Variation of efficiency with motor current for initial and modified chopper circuits.

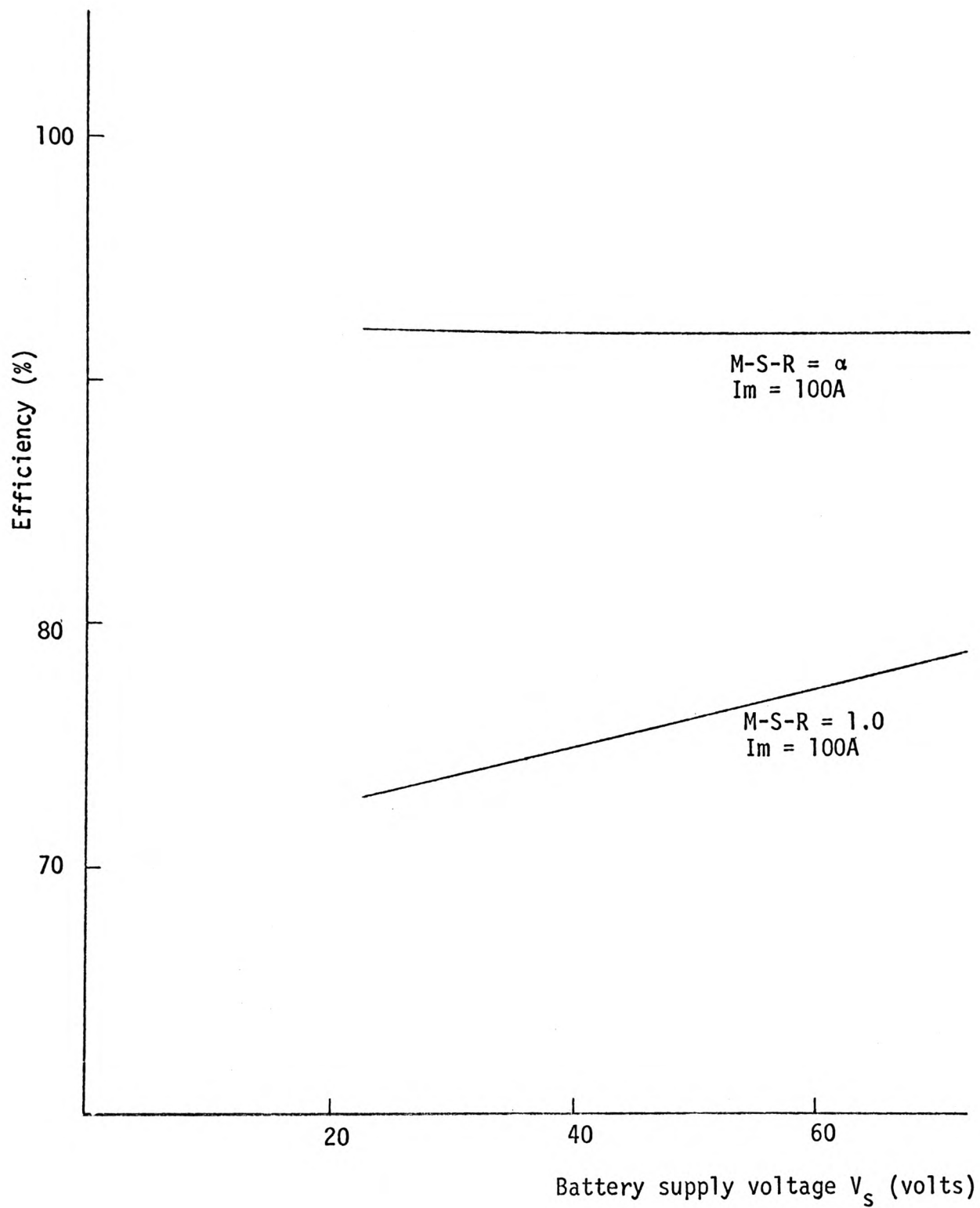


Figure 3.21 - Variation of chopper efficiency with battery supply voltage.

#### (4) Conclusions

A survey of power transistors was made to establish which transistors were the most economical for use in d.c. choppers: it was found that, at present, little difference exist between the cost of high voltage Ge and Si power transistors. It was also established that power transistors with maximum collector current ratings of greater than 35A would be uneconomical, whilst variations in maximum collector-emitter voltage ratings had little effect on the price of most high voltage power transistors comparable in other electrical characteristics.

Reliable operation of the chopper circuit was shown to depend upon the recovery speed of the freewheeling diode, the value of the load line tailoring circuit capacitance, and the switching times of the control oscillator output signal. In fact, the control oscillator was found to be one of the most critical parts of the chopper, where instability or slow switching times of the output signal would almost certainly cause failure of output transistors.

The modified chopper circuit, although using output transistors rated at 100 volts, operated reliably during laboratory tests at peak battery currents of over 300 amperes from a battery supply of 50 volts; the chopper was also found to operate satisfactorily from a battery supply voltage of 72 volts, although the voltage rating of the output devices (100 volts) is considered too low for operation of the chopper as an electric vehicle controller at such a high supply voltage where voltage transients (common in industrial vehicles) may cause the destruction of the power transistors through second breakdown.

The laboratory tests carried out on the chopper have shown the high efficiency of the circuit to be approximately the same whether Ge or Si devices are employed. Variations in electrical characteristics of individual silicon transistors, unlike Ge transistors, were found to be minimal, thus resulting in excellent current sharing between the parallel power transistors of the chopper output stages and makes the use of emitter sharing resistors unnecessary.

The total cost of the transistor chopper used in this investigation was approximately £ 76, this is appreciably lower than the cost of a comparable thyristor d.c. chopper (approximately £100).

This work has clearly shown that low cost power transistors can be successfully used in economically viable electric vehicle chopper controllers with a good possibility of rapid industrial acceptance.

#### (5) Suggestions for Further Work

The results of laboratory tests carried out on the experimental transistor d.c. chopper have shown the circuit to be reliable and highly efficient: The incorporation of the transistor chopper in a test vehicle is essential to ensure it's reliability as an electric vehicle controller under normal operating conditions.

The work described in this dissertation was performed on a d.c. chopper/series motor combination. Further work should be done on developing a transistor d.c. chopper/seperately-excited motor combination, with special emphasis placed on the suitability of the system for regenerative braking.

The main disadvantage with the use of transistors in switching applications has been their comparatively low maximum voltage and current ratings. The high current requirements of present day series tractive motors can only be met by the operation of a number of transistors in parallel. It would be of interest to investigate the feasibility of operating power transistors in series to enable the operation of transistor choppers from higher supply voltages than hitherto has been possible; although the operation of transistors in series involve a number of problems, namely, the rise in the total cost of the chopper and the difficulty of switching the series transistors simultaneously.

## (6) Acknowledgements

The author gratefully acknowledges the assistance and encouragement of Dr.B.M.Bird, reader in Electrical Engineering at the University of Bristol, who supervised the research to which this dissertation relates.

The encouragement of Mr.D.T.Rees, Head of Pure and Applied Science Department at Gwent College of Technology, is also warmly appreciated.

The author also wishes to express his thanks to Gwent College of Technology for the facilities provided and to the University of Bristol for financial support during this period of research.

Thanks are also due to the college technical staff for their assistance in the construction of the experimental equipment, and to the reprography and secretarial staff for the preparation of this volume.



## (7) References

1. Barak, M. 'Recent developments in batteries and voltaic cells', Electronics and power, August/September 1972, pp 290-296.
2. Morrison, J.J. 'Electronic Control of Battery Electric Vehicles', The Radio and Electronic Engineer, Vol. 42, No. 2, February 1972, pp 91-100.
3. Campbell, P. 'Current problems for electric cars', SQJ, September 1972, pp 80-82.
4. Mangan, M.F.  
Griffith, J.T. 'Motors and controllers for electric cars', The Electricity Council research centre, job No. 458, January 1970.
5. Weber, H.F. 'Solid-state d.c. motor control for traction drive vehicles', Motorola application note No. AN-189.
6. Jansson, L.E. 'A survey of converter circuits for switched-mode power supplies', Mullard Technical Communications No.119, July 1973, pp 271-278.
7. Bright, R.L. 'Junction transistors used as switches', AIEE, March 1955, pp 111-121.
8. Ebers, J.J.  
Moll, J.L. 'Large-Signal Behaviour of Junction Transistors', Proc. IRE, December 1954, pp 1761-1771.
9. Moll, J.L. 'Large-Signal Transient Response of Junction Transistors', Proc. IRE, December 1954, pp 1773-1782.
10. Newell, A.F. 'An introduction to the use of transistors in inductive circuits', Mullard Technical Communications, Vol. 4, No. 35, November 1958, pp 157-160.
11. Roehr, W.D. 'Avoiding Second Breakdown', Motorola application note AN-415A, April 1972.
12. Gates, T.W.  
Ballard, M.F. 'Safe Operating Area for Power Transistors', Mullard Technical Communications, No. 122, April 1974.
13. Lomas, R.A.  
Walker, A.V. 'High Power Planar Transistors', Electron, 18 July 1974, pp 24-26.

14. Martin,A.M. 'Defining and measuring reverse recovery in power rectifier diodes', Electronic Engineer, March 1971, pp 50-
15. 'Applications of Fast-Recovery Rectifiers', Motorola application note.
16. Morris,N.M. 'Logic Circuits',(book), published by McGraw-Hill.
17. Millman,J.  
Halkias,C.C. 'Integrated Electronics' (book), published by McGraw-Hill.
18. Davis,R.M. 'Power Diodes and Thyristor Circuits', (book), IEE Monograph series 7, published by Cambridge University Press.
19. 'Power Engineering using Thyristors', (book), Vol.1, Techniques of Thyristor power control, published by Mullard.
20. Greiner,R.A. 'Semiconductor Devices and applications' (book), published by McGraw-Hill.
21. Swayne,A.W.J.  
Oliver,M.J. 'High current transistorised d.c. chopper', internal report, University of Bristol, June 1970.
22. Hind,M.A. 'Battery Electric vehicle Performance Evaluation and Simulation', Ph.D. thesis, University of Bristol, September 1972.
23. Harlen,R.M. 'Novel Propulsion Schemes for Battery Electric Vehicles', Ph.D thesis, University of Bristol, March 1966.
24. Liversidge,M.H. 'Recent Developments in Battery-Electric Vehicle Drives', Ph.D. thesis, University of Bristol, March 1971.

(1) The Square Wave Generator

The operational amplifier used in the square wave generator described in section (3.3.1.1) compares the voltage across the capacitor,  $V_C$ , with a fraction of the output voltage,  $\beta V_o$ , fed back to the non-inverting input of the amplifier. The output voltage waveforms are shown in figure (A1.1). Assuming that the peak values of comparator output voltage are equal to the amplifier supply voltages ( $\pm V_s$ ), the comparator output will change from  $+V_s$  to  $-V_s$  as soon as the voltage across the capacitor  $C_1$  reaches  $+\beta V_s$ ; that is, the differential input of the operational amplifier becomes positive. When the generator output is at  $-V_s$  the capacitor will charge negatively towards  $-V_s$ , but as soon as the voltage across the capacitor reaches  $-\beta V_s$ , the differential input of the operational amplifier becomes negative and the generator output changes to  $+V_s$ , and the cycle is repeated.

The period of a complete cycle,  $T$ , can be expressed in terms of the generator external components. The expression for  $T$  is derived as follows:-

Assuming that  $V_C = -\beta V_s$  at  $t = 0$ , we have

$$V_C(t) = V_s \{1 - (1+\beta) \exp^{-\frac{t}{R_1 C_1}}\} \quad (1)$$

Since at  $t = \frac{T}{2}$   $V_C(t) = +\beta V_s$ , the period  $T$  for a complete cycle can be found by substituting for  $V_C(t)$  in equation (1) and solving

$$\text{at } t = \frac{T}{2},$$

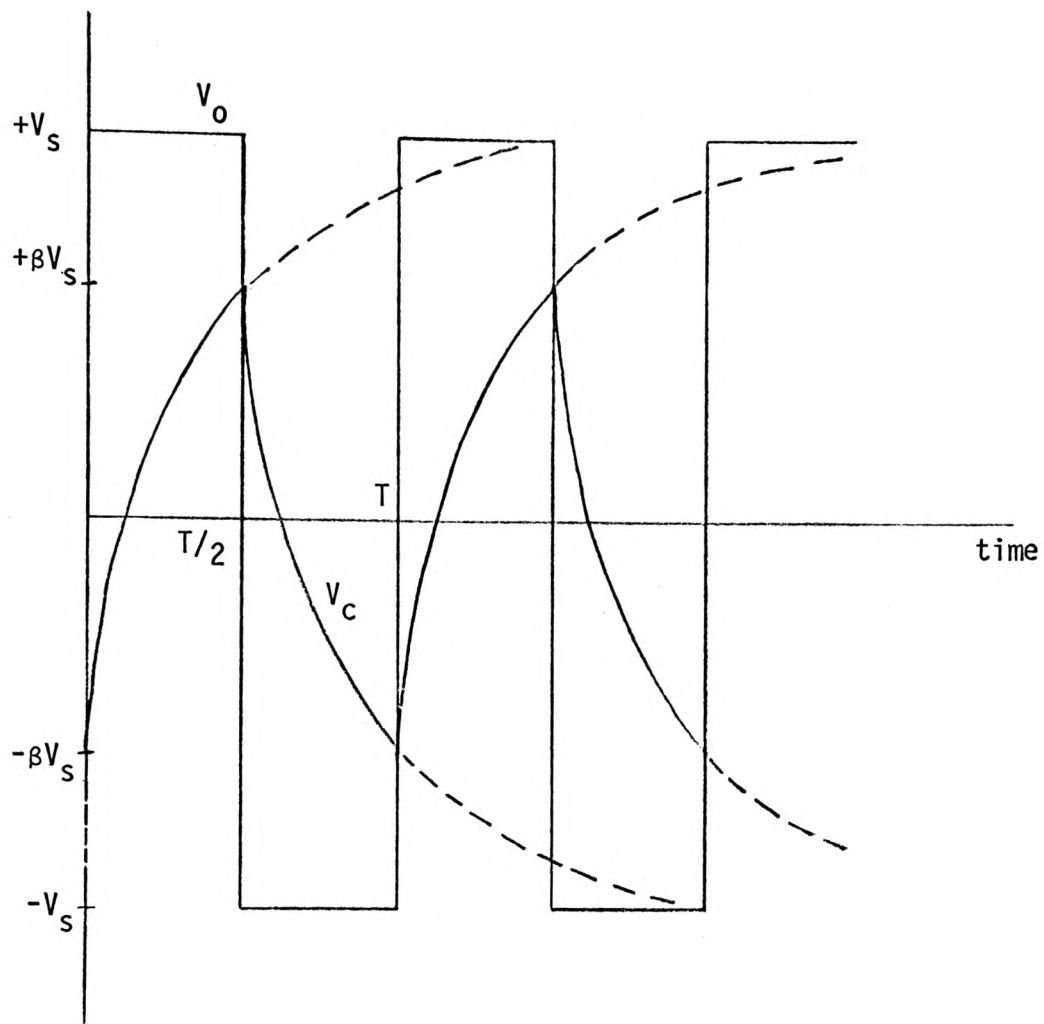


Figure A1.1 - Square wave generator output and capacitor voltage waveforms.

$$\beta V_S = V_S \left\{ 1 - (1 + \beta) \exp - \frac{T}{2R_1 C_1} \right\}$$

$$\beta = 1 - (1 + \beta) \exp - \frac{T}{R_1 C_1}$$

$$(1 + \beta) \exp - \frac{T}{R_1 C_1} = (1 - \beta)$$

$$\text{therefore, } \exp - \frac{T}{2R_1 C_1} = \frac{(1 - \beta)}{(1 + \beta)} \quad (2)$$

Using binomial expansion, and assuming a small time constant  $R_1 C_1$ ,  $\exp - \frac{T}{2R_1 C_1}$  is approximately equal to  $(1 - \frac{T}{2R_1 C_1})$

therefore equation (2) becomes

$$1 - \left( \frac{T}{2R_1 C_1} \right) = \frac{(1 - \beta)}{(1 + \beta)}$$

$$\frac{T}{2R_1 C_1} = 1 - \frac{(1 - \beta)}{(1 + \beta)}$$

$$\text{therefore, } T = 2R_1 C_1 \frac{2\beta}{1 + \beta}$$

oo where  $\beta = \frac{R_4}{R_3 + R_4}$  in figure (3.12).

Since  $R_3$  and  $R_4$  were chosen to be 1 M ohm and 1 k ohm respectively,

$$\text{then } T = \frac{R_1 C_1}{3}$$

Therefore by choosing a suitable value for capacitor  $C_1$ , 0.1  $\mu$ F in this case, the frequency of oscillation of the square wave generator ( $f = \frac{1}{T}$ ) will depend upon the value of resistor  $R_1$ .

### (1.2) The Integrator

As mentioned earlier in section (3.3.1.1), the amplitude of the output waveform of the integrator can be reduced by increasing the value of capacitance  $C_3$  in figure (3.12), thus increasing the time constant of the integrator  $C_3R_6$ . To explain why this is so, the operating of the integrating combination  $C_3R_6$  must be looked at in more detail: assuming that initially the capacitor  $C_3$  is negatively charged, when the input square wave becomes positive with respect to the reference level,  $+V_i$  in figure (A1.2), the capacitor will start to charge exponentially towards the peak voltage of the input signal with a time constant  $C_3R_6$ . Before the capacitor voltage reaches the peak input signal voltage, the input signal would have changed to a negative value,  $-V_s$  in figure (A1.2), and the capacitor will start charging exponentially with the same time constant towards  $-V_s$  until the input changes polarity again.

By increasing the time constant of the integrator, the time taken for the capacitor to charge to  $+V_s$  or  $-V_s$  is increased and therefore since the time available for the capacitor to charge positively or negatively is constant and determined by the period of half a cycle of the input signal, the capacitor would charge to a lower voltage in the available time and consequently the amplitude of the integrator output signal, as shown in figure (A1.2).

### (1.3) The Regenerative Comparator (Schmitt Trigger)

Regenerative comparators, used in the square wave generator, 709 comparator, and the current limiting circuit monostable multivibrator, use positive (regenerative) feedback to increase amplifier gain. The increased amplifier gain causes the total output

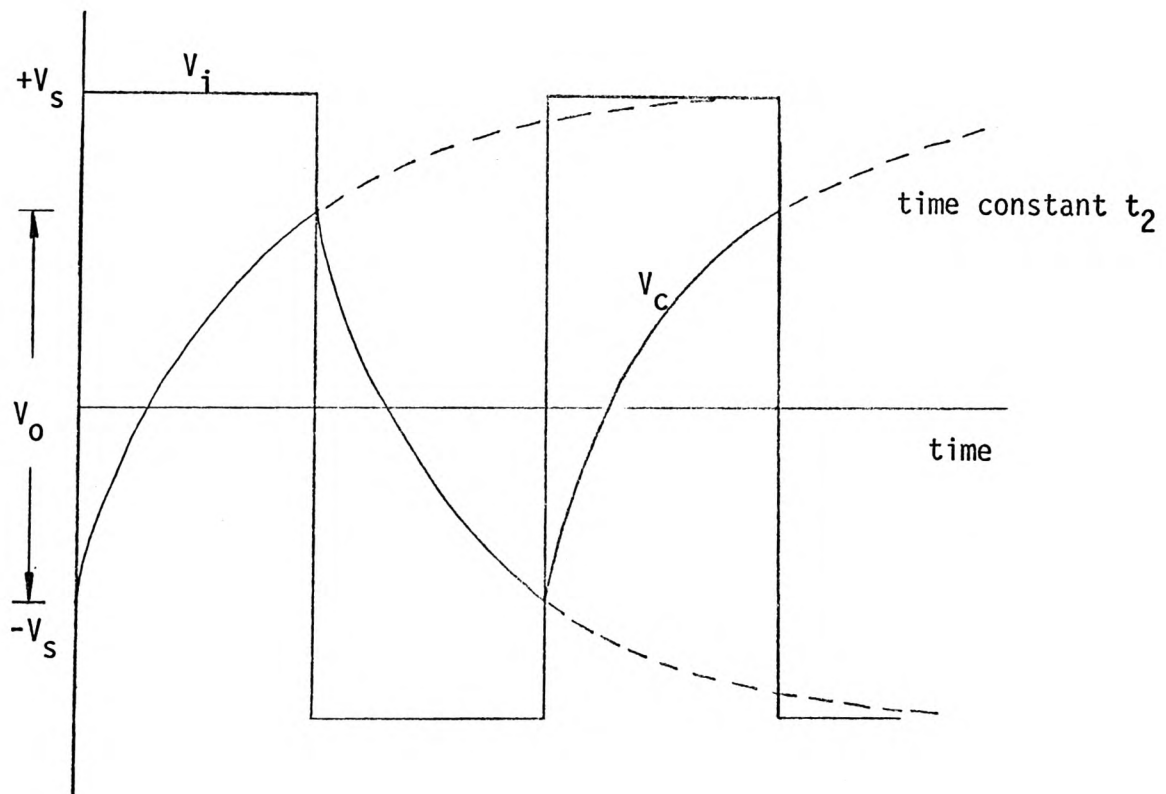
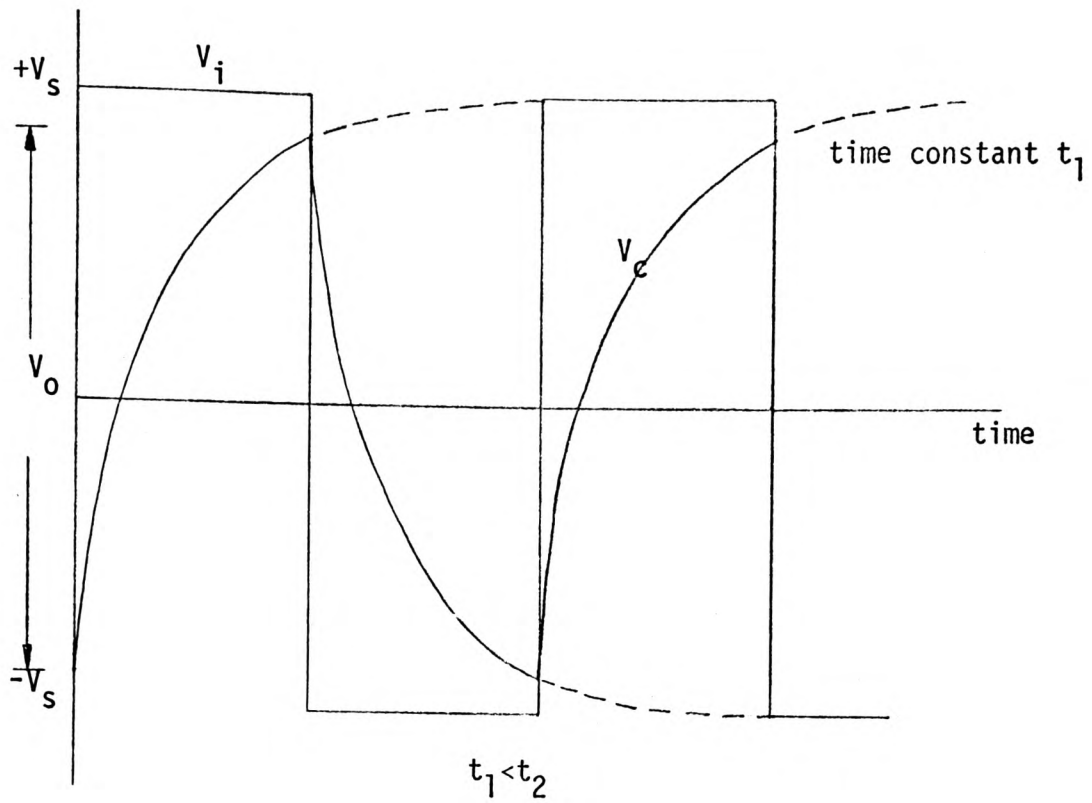


Figure A1.2 - Typical integrator voltage waveforms.

excursions to take place in a time interval during which the input is changing by much less than the required amount for a simple comparator circuit.

Consider a circuit using positive voltage series feedback; theoretically, if the loop gain  $-\beta A_v$  (where  $A_v$  is the large signal voltage gain of the amplifier) is adjusted to be unity, then the gain with feedback  $A_{vf}$  becomes infinite since

$$A_{vf} = \frac{A_v}{1 - \beta A_v}$$

Such an idealised situation results in an abrupt, zero rise time, transition between the extreme values of the output voltage. If a loop gain in excess of unity is chosen, the output waveform continues to be virtually discontinuous at the comparison voltage; however, the circuit now exhibits hysteresis or backlash. Hysteresis causes the circuit to trigger at a higher voltage for increasing than for decreasing input signals.

#### (1.4) Current Limiting Circuit

##### (1.4.1) The Comparator

The comparator circuit in figure (3.14) compares the voltage across the current sensing resistor with a preset d.c. reference voltage. When the sensed current exceeds the preset current limit, given by the reference d.c. voltage, the comparator output changes polarity and reverts to it's stable state as soon as the sensed current falls below the preset current limit.

In it's stable state, the differential input of the amplifier is positive with respect to the zero volt common rail and the comparator output is therefore negative at  $-V_s$ , neglecting collector-emitter saturation voltages in the amplifier. As the signal across the current sensing resistor exceed the preset d.c. reference



voltage, the differential input becomes positive and comparator output switches to  $+V_s$ . When the current sensing signal falls to below the preset d.c. reference, the comparator will revert to it's stable state and the cycle may be repeated.

#### (1.4.2) The Monostable Multivibrator

The output signal from the comparator is differentiated by the combination  $R_5 C_1$  in figure (3.14), producing a series of positive and negative pulses, assuming a comparator output signal of more than one cycle. The diode  $D_1$  will only allow the negative trigger pulses to go through the noninverting input of the amplifier.

The circuit remains in it's stable state until the triggering signal causes a transition to the quasistable state. Then after a time  $T_m$ , the circuit returns to it's stable state. In its stable state, the output of the circuit,  $V_o$ , is at  $+V_s$  and the capacitor is clamped by diode  $D_2$  at  $V_d$  say (where  $V_d$  is the forward voltage drop across  $D_2$ ): the output and capacitor voltage waveforms are shown in figure (A1.3). If the trigger amplitude is greater than  $\beta V_s - V_d$ , where  $\beta = \frac{R_7}{R_6 + R_7}$ , then it will cause the comparator to

switch to an output of  $-V$ . The capacitor will now charge through  $R_5$  toward  $-V$  because  $D_2$  becomes reverse biased. When the capacitor voltage  $V_o$  becomes more negative than  $-\beta V_s$ , the comparator output swings back to  $+V_s$ . The capacitor now starts charging toward  $+V_s$  through  $R_5$  until  $V_c$  reaches  $V_d$  and  $C$  becomes clamped again. The duration of the monostable output pulse,  $T_m$ , is given by

$$T_m = C_2 R_5 \text{ LOGe } \frac{1 + \frac{V_d}{V_s}}{1 - \beta}$$

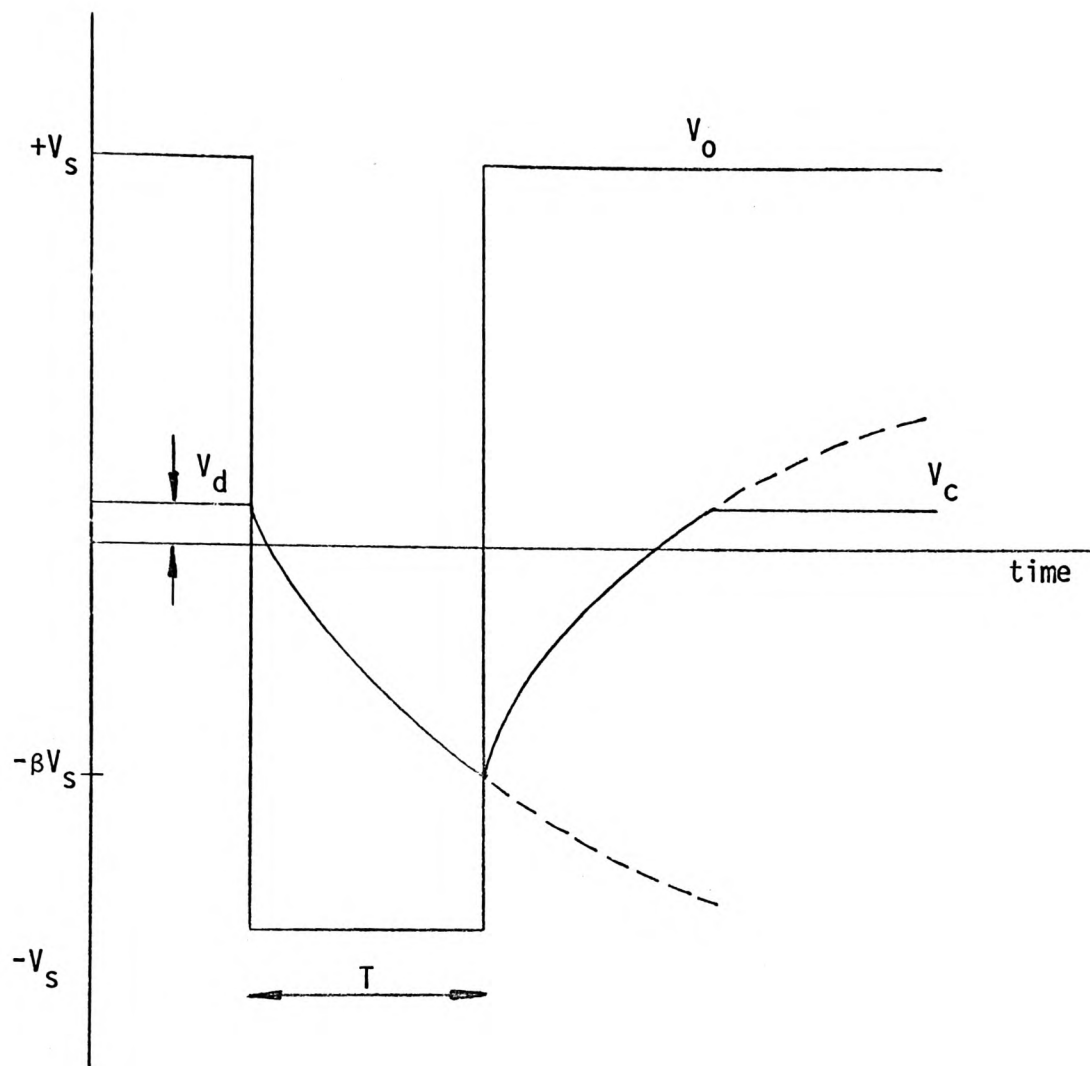


Figure A1.3 - Monostable multivibrator output and capacitor voltage waveforms.

Since  $V_s$  is much larger than  $V_d$ , and  $R_6$  is 1 M ohm and  $R_7$  is 100 k ohm, the above equation reduces to

$$T_m = C_2 R_5 \text{ LOGe} \quad (1.1)$$

therefore  $T_m = 0.1 C_2 R_5$

The values chosen for  $C_2$  and  $R_5$  will give a pulse duration of 0.015 seconds, a duration long enough to allow the current through the chopper regulator to fall below the preset current limit..

## Appendix (2.0) Chopper Circuit Voltage and Current Waveforms

The behaviour of the chopper circuit when used with an inductive load is better explained by examining a number of current and voltage waveforms in the circuit. The plates in figure (A2.1) show the voltage waveforms across the power circuit output devices and the motor load; while the plates in figure (A2.2) show the shape of battery, transistor, and load current waveforms.

The voltage waveform across the output transistors, shown in plate 1 of figure (A2.1), has a fast 'turn-on' edge and a 'turn-off' edge made up of two distinct portions: the fast portion is due to the delay in the recovery of the diode D in the load line tailoring circuit, once the diode has recovered, the capacitor will start charging and the voltage across the switching devices will fall relatively slowly towards the negative supply voltage. The small overshoot in the 'turn-off' edge is the result of the combined effects of the freewheeling diode and the switching 'off' load line tailoring circuit, C and D in figure (3.15), in suppressing the large voltage transients that occur across the switching devices when 'switching off' inductive loads. the sketches given in figure (A2.3) clearly show the effect on voltage waveforms across the output transistors when either a slow freewheeling diode is used or the load line tailoring circuit is excluded.

The voltage waveform across the load, shown in plate 2 of figure (A2.1), has a fast front (chopper 'turn-on') edge but, as in the case of the back (chopper turn-off) edge of the waveform across the output devices, the voltage across the motor rises to the zero reference voltage level in two distinct portions.

Plate 1

Voltage waveform across  
chopper output transistors.

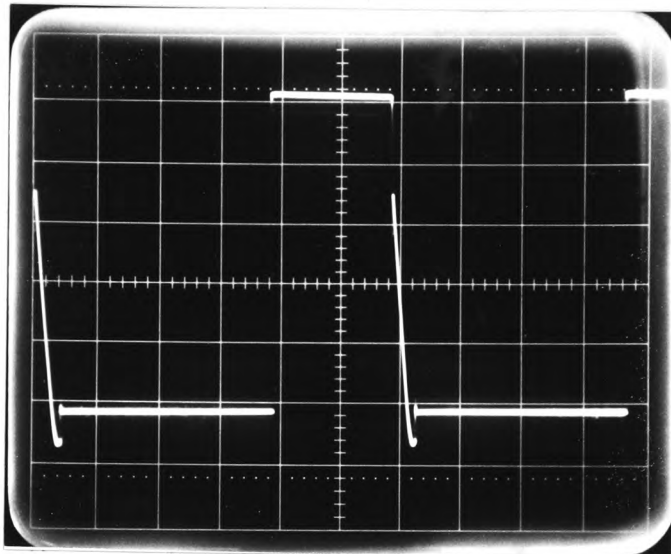


Plate 2

Voltage waveform across  
motor.

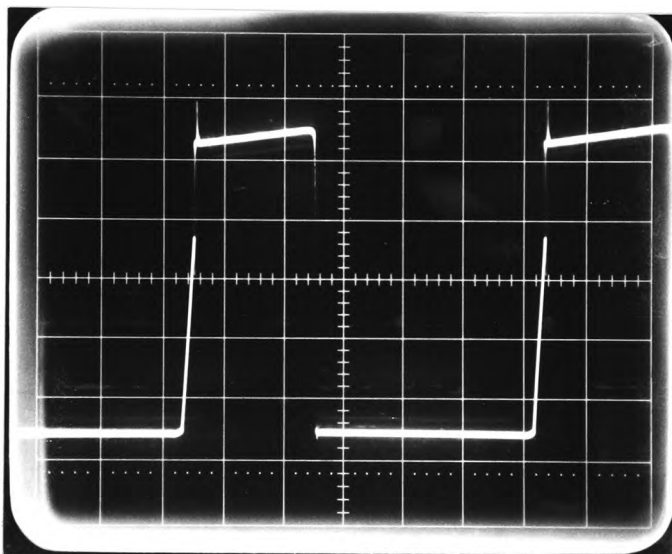


Figure A2.1 - Typical transistor chopper voltage waveforms.

Plate 1

Battery current waveform.

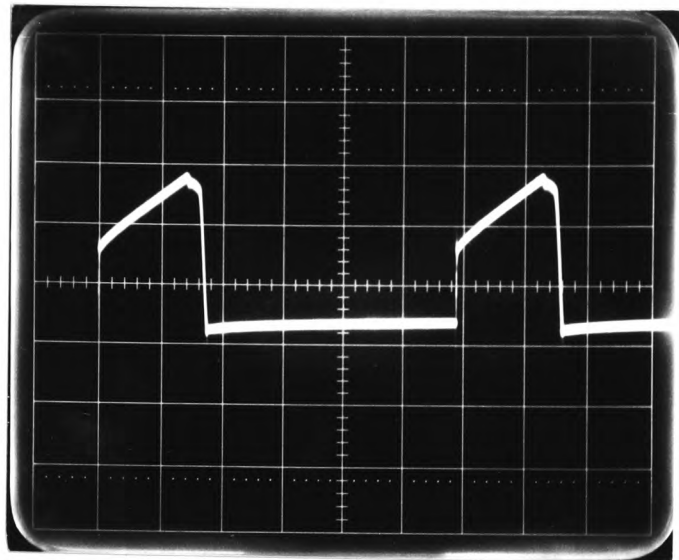


Plate 2

Output transistor current waveform.

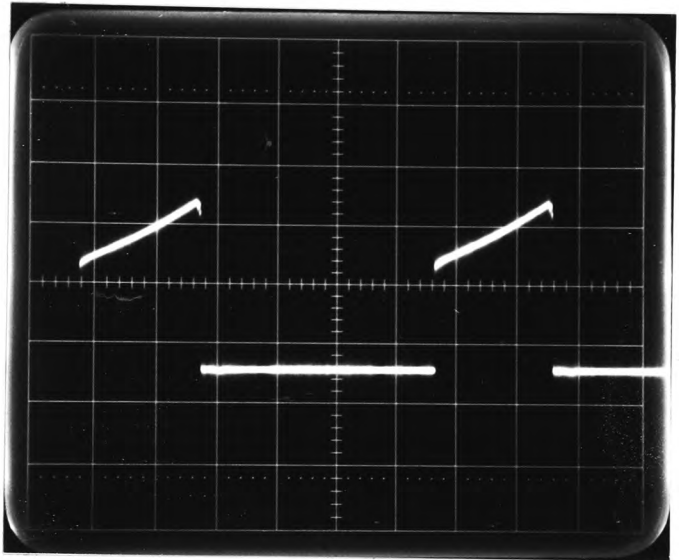


Plate 3

Motor current waveform.

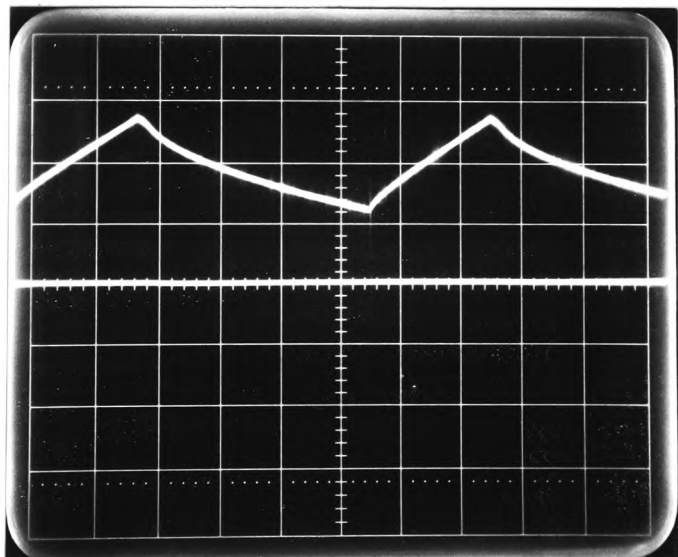
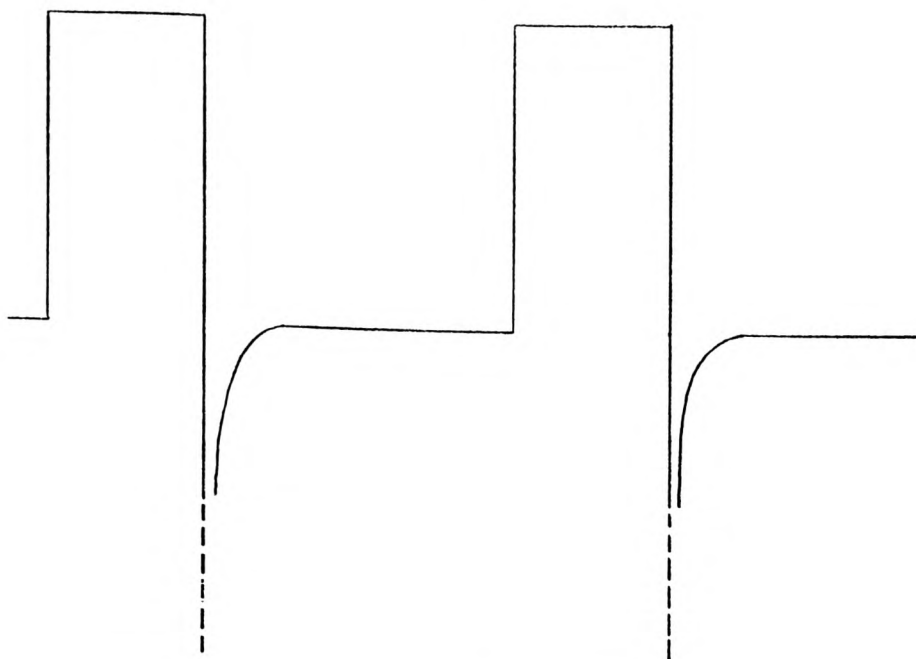
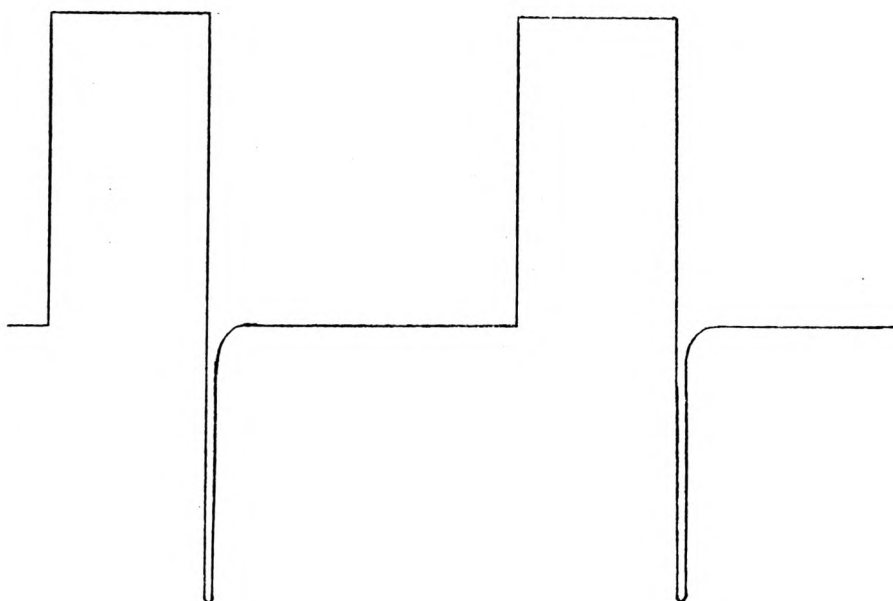


Figure A2.2 Typical transistor chopper current waveforms.



Transient conditions caused by the use of a slow recovery freewheeling diode.



Transient conditions caused by the absence of a loadline tailoring circuit.

Figure A2.3 - Typical voltage transients occurring across chopper output transistors.

The excellent clamping action of the fast recovery freewheeling diode used, can be observed by the complete absence of voltage transients in the waveform shown in plate 2 of figure (A2.1). The spike occurring just before the rise of the voltage across the motor (back edge of the waveform) is a characteristic of the circuit and is independent of the operational or load conditions of the circuit.

Plates 1 and 2 in figure (A2.2) show the battery and transistor current waveforms respectively: both waveforms contained very fast, high amplitude spikes in their front edges caused by the switching of a highly inductive load. Plate 3 of figure (A2.2) shows the motor current waveform: the straight horizontal line is the reference zero current level; when the chopper is 'on', the current through the motor will rise exponentially until the chopper turns 'off'. When the chopper is 'off', the energy stored in the motor inductance will cause an exponentially decaying current to flow through the motor via the freewheeling diode: this circulating current will decay until the chopper turns 'on' again and the cycle is repeated.



### Appendix (3.0) Calculation of Chopper Efficiency

Special Wattmeters, using the 'Hall' effect, have been developed to enable the measurement of chopped waveforms with accuracy, but these were not available for use in this work. An alternative way of measuring power is to photograph the current and voltage waveform simultaneously and 'multiply' the two point by point over a complete cycle. However, this is a very tedious process and measurements taken from oscilloscope traces are not very accurate.

A more commonly used method for calculating chopper efficiency is to estimate the power loss in the chopper: this process was tried and found to be laborious and inaccurate due to the many elements in the chopper contributing to the total power loss in the circuit. It was decided to calculate the efficiency by measuring the mean input and output power of the chopper circuit and using the expression

$$\text{efficiency} = \frac{\text{output power}}{\text{input power}} \times 100\%$$

Although a simple method to use, some error would exist in results taken at M-S-R of less than infinity due to the fact that the chopper current and voltage waveforms are not perfectly rectangular.

#### (3.1) Estimating Power Loss in the Chopper

With the chopper circuit, figure (3.15), the total power loss is made mainly of contributions from the following circuit parts:

1. Control oscillator.
2. Drive transistors  $Q_1 - Q_6$ .
3. First Darlington drive stage resistor  $R_3$ .

4. Output transistors during:
  - (a) turning 'on'.
  - (b) turning 'off'.
  - (c) saturation.
5. Emitter sharing resistors  $R_e$  (in the case of the initial chopper circuit employing Ge output transistors).
6. Output stage saturation resistors  $R_s$ .
7. Load line tailoring circuit.

The losses due to each of the above circuit parts can be calculated by estimating the current flowing in each component at certain load conditions: for example, if  $R_3$  has a current  $I$  flowing through it, then the power dissipated in  $R_3$  is

$$P_1 = M (I^2 R_3) \text{ watts} \quad (1)$$

where,

$$M = \frac{T_{\text{on}}}{T_{\text{on}} + T_{\text{off}}}$$

and where,

$T_{\text{on}}$  = time during which the output transistors are saturated.

$T_{\text{off}}$  = time during which the output transistors are cut off.

Equation (1) may be used to calculate the power dissipated in any resistor in the chopper circuit at any M-S-R. The power dissipated in transistors during saturation is given by

$$P_2 = M (V_{CEsat} I_c) \text{ watts}$$

while power dissipated in transistors during switching is given by

$$P_3 = \frac{1}{2} V_{cc} I_c \frac{t_{\text{on}}(\text{or } t_{\text{off}})}{T} \text{ watts}$$

where,

t on = turn 'on' time of transistor

t off = turn 'off' time of transistor

$T = \frac{1}{f}$  = period of a complete cycle.

As can be seen from above, calculation of chopper efficiency by estimating losses in the circuit can become tedious; in practice, great difficulty was found in estimating the relatively high losses incurred in the load line tailoring circuit, hence the low accuracy of the results obtained using such a method.

### (3.2) Measurement of Chopper Input and Output Power

The efficiency of the chopper, E, is given by

$$\begin{aligned} E &= \frac{\text{mean output power}}{\text{mean input power}} \times 100\% \\ &= \frac{I_m V_m}{I_B V_B} \times 100\% \end{aligned}$$

The currents  $I_B$  and  $I_m$  were measured using precision high current d.c. ammeters, whilst the voltages  $V_B$  and  $V_m$  were measured using a high precision electronic d.c. voltmeter. A schematic diagram of the test circuit is shown in figure (A3.1).

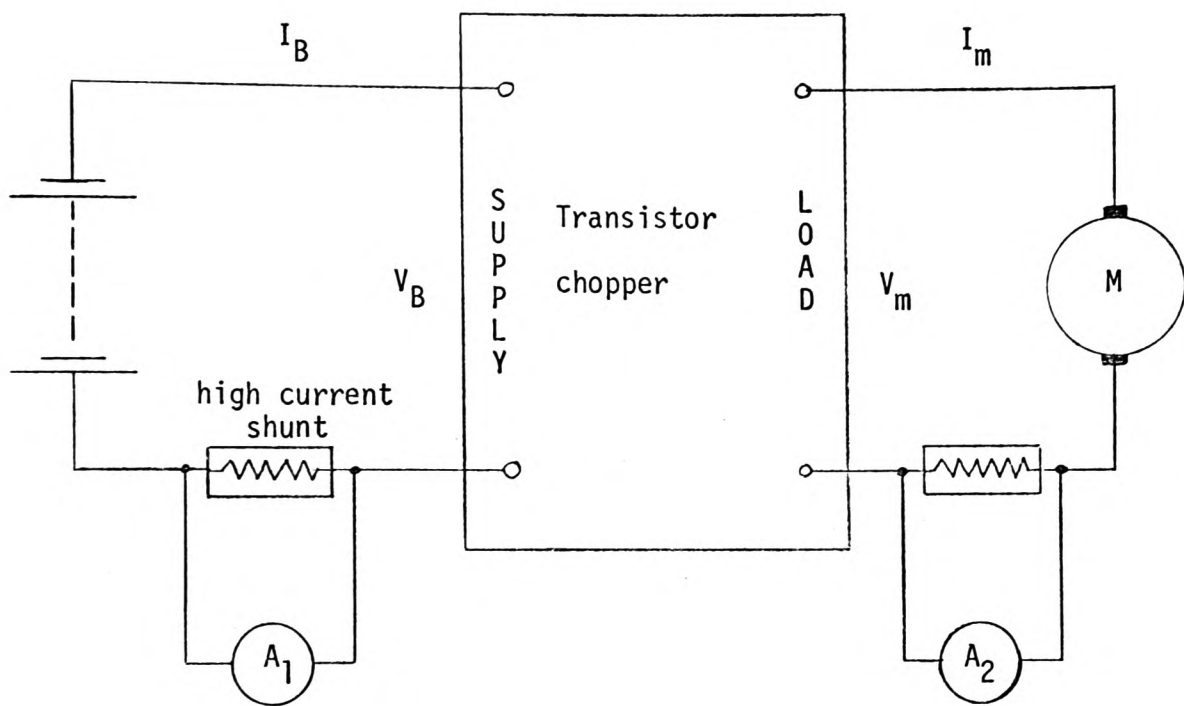


Figure A3.1 - Schematic diagram of chopper efficiency test circuit.